

**A MOLECULAR DESCRIPTION OF  
OXYGEN BINDING TO HEMOGLOBIN**

**Thesis by**

**Barry Duane Olafson**

**In Partial Fulfillment of the Requirements  
For the Degree of  
Doctor of Philosophy**

**California Institute of Technology**

**Pasadena, California**

**1979**

**(Submitted July 14, 1978)**

## ACKNOWLEDGMENTS

I am grateful for my association with the people and facilities of the California Institute of Technology. I feel my years working with Professor William A. Goddard III and the members of the MQM group have been pleasant and rewarding. Bill's tireless drive for greater understanding in all areas of chemistry will always be a constant source of inspiration to me.

I would like to express my appreciation to all members of the MQM group, especially Bill Wadt, for stimulating discussions, questions and viewpoints.

I thank Adria McMillan for giving much of her time to type this thesis. Financial support from the National Science Foundation, the National Institutes of Health, and the California Institute of Technology is gratefully acknowledged.

I dedicate this thesis to my parents; my hopes and dreams have been their hopes and dreams. And finally, I wish to thank Bonnie for her constant and warm companionship during the writing of this thesis.

## ABSTRACT

We discuss the bonding of  $O_2$  to hemoglobin (Hb) at the molecular level. The ideas presented here are the results of ab initio calculations on idealized portions of the Hb molecule.

The bond between Fe and  $O_2$  is formed by coupling a triplet state of Fe to the triplet ground state of  $O_2$ . The electronic structure of the  $FeO_2$  moiety is analogous to that of ozone. We show how the ozone model is in agreement with the EPR data for  $MnO_2$  and  $CoO_2$ , predicting unpaired spin density on the Mn for the former molecule, and unpaired spin density on the  $O_2$  ligand in  $CoO_2$ . Our calculations lead to a bound molecule with very little transfer of electron density onto the  $O_2$  ligand. Valence bond ideas also indicate the similarity between  $HbO_2$  and the formal Fe(III) complexes of  $HbOH$  and  $HbCN$ .

The heme plane and axial imidazole ligand are seen to play a key role in promoting reversible  $O_2$  binding. The effective size of high-spin Fe is not found to play a major role in the  $O_2$  binding process. The Fe remains in the heme plane for four-coordinate molecules, regardless of the local spin state about the Fe. The Fe moves out of the heme plane for five-coordinate complexes in order to keep a strong dative bond to the axial ligand while reducing the nonbonded repulsions between the heme plane and the axial ligand. The spin state change on Fe is found to occur, not because the Fe moves into the plane of the porphyrin, but because the formation of the  $FeO_2$  bond reduces the number of local exchange interactions that stabilize the high-spin state. The role of the coordination sphere of Fe pertaining to the chemistry of the Hb molecule is to reduce the energy separation between the

atomic states. It makes an intermediate-spin state accessible for bond formation and thereby provides a mechanism by which an  $O_2$  molecule can easily and reversibly bind to Hb. Neither the diamagnetic ( $t_{2g}$ )<sup>6</sup> excited state of Fe nor the excited singlet state of  $O_2$  play a role in the formation of the  $FeO_2$  bond.

We show how movement of the proximal imidazole, long thought to initiate the change in quaternary structure of Hb, is also responsible for the reduced  $O_2$  affinity in the T quaternary form of Hb. Assuming that protein forces hinder the movement of the axial ligand leads to the calculation of protein forces in the T and R quaternary forms, and a prediction of the movement of Fe upon a change in the quaternary structure. This movement of the Fe center is found to be on the order of 0.05 Å. Based upon the structural studies of Perutz and co-workers we show how the different protein forces in the T and R quaternary forms can be traced to a small number of hydrogen bonds and salt bridges. This allows us to present a model that displays the molecular origin for the cooperative binding effect. Transferring these protein forces to the coboglobin molecule allows us to calculate the magnitude of the cooperative effect in this metal-substituted Hb. The predicted cooperative effect is found to be in excellent agreement with the experimentally determined value.

The ozone model of transition metal- $O_2$  binding leads to the prediction of a second metal- $O_2$  stretching band between 1000-1200  $cm^{-1}$ . It has also been used to tentatively assign the near-infrared and z-polarized ultraviolet-visible spectra of  $HbO_2$ ,  $HbCN$ , and  $HbCO$ .

# TABLE OF CONTENTS

	<u>Page</u>
I. Introduction.....	1
II The Ozone Model for the Bonding of O <sub>2</sub> to an Fe Site.....	4
A. Fe Atom.....	4
B. O <sub>2</sub> Molecule.....	6
C. Bonds to O <sub>2</sub> .....	10
1. H-O <sub>2</sub> .....	10
2. O-O <sub>2</sub> (Ozone).....	13
3. Fe-O <sub>2</sub> .....	18
III. The Nature of the FeO <sub>2</sub> Bond in Fe-Porphyrin Complexes....	23
IV. Energetics of the Fe-O <sub>2</sub> Bond in Fe-Porphyrin Complexes....	30
A. Four-Coordinate Fe.....	33
1. Relative Energies of the q, t, and s States.....	33
2. Position of Fe Relative to the Porphyrin Plane...	37
B. Five-Coordinate Fe.....	39
1. Relative Energies of the q, t, and s States.....	39
2. Position of Fe Relative to the Porphyrin Plane...	40
C. The Six-Coordinate FeO <sub>2</sub> Complex.....	44
1. Molecular Description of the O <sub>2</sub> Bond to Mb.....	44
2. Energetics of the O <sub>2</sub> Bond to Mb.....	47
V. The CO Bond to the Fe-Porphyrin Complexes.....	52
VI. Cooperative Ligand Binding in Hb.....	55
A. Effects of the Protein Forces on the Position of Fe....	56
B. Origin of the Protein Forces.....	63
C. Molecular Description of Cooperativity.....	71
D. Other Models of Cooperative Binding.....	73

	<u>Page</u>
E. Qualifying Remarks.....	76
VII. Previous Models of the Electronic Structure of Oxyhemoglobin.....	79
VIII. Bonding of O <sub>2</sub> to Other Transition Metal Complexes.....	85
A. CoO <sub>2</sub> Complexes.....	85
B. EPR Experiments on O <sub>2</sub> Complexes.....	89
C. Geometry and Magnetic Properties of O <sub>2</sub> Complexes.....	91
D. Vibrational Transitions.....	93
E. Energetics of High-Spin O <sub>2</sub> Complexes.....	97
IX. Bonding of Other Ligands to Fe-Porphyrin Complexes.....	102
X. Properties Involving the Electronic States of Fe.....	108
A. Electronic Spectra of Hb Complexes.....	108
B. Mössbauer Experiments on Fe-Porphyrin Complexes...	112
XI. Summary.....	119
XII. Conclusions.....	121
XIII. References.....	123
Propositions.....	132

## I. Introduction

The hemoglobin molecule has often served as the first biological molecule to be subjected to newly evolving experimental techniques. It was one of the first molecules to be associated with a biological function.<sup>1</sup> Much of what is known about enzyme kinetics and allostery had its foundation in the study of the cooperative ligand binding of this protein.<sup>2-4</sup> The understanding of hemoglobin increased dramatically when the first results of globular protein crystallography began to reveal its three-dimensional structure.<sup>5,6</sup> It is thought to be the most extensively characterized molecule of biological importance.<sup>7</sup>

Hemoglobin is an extremely interesting molecule, both from a structural and dynamical point of view. Its structure is such that it has the ability to bind oxygen, transport it throughout the body, and then release it unaltered to the tissue for use in respiration. The kinetics of this reaction are quite complicated due to the fact that the four oxygen binding sites in hemoglobin are aware of each other's state of oxygenation. These sites work together to bind or release oxygen and, as a result, the molecule becomes a very efficient oxygen carrier. The driving force of oxygen transport is entropical in nature, and no external energy is required to facilitate it. Because of its central position in the application of new techniques directed towards understanding biological chemistry, and its unusual chemical properties, hemoglobin appeared to be an appropriate starting point for this group's venture into the area of theoretical biochemistry.

We have attempted to understand that part of the chemistry of hemoglobin which arises from its structural properties. Essentially

we are concerned with the energy separations of different electronic states of hemoglobin, the change in their relative energies as a function of geometry, and the associated electron densities for these various low-lying electronic states. We attempt, as much as is possible, to give a qualitative, conceptual picture of the electronic structure of hemoglobin. For the most part, these qualitative ideas have been gained from more rigorous studies of the electronic structure of simpler molecules. Where these qualitative ideas do not effectively define the structural properties of hemoglobin, we have performed ab initio theoretical calculations on idealized portions of the hemoglobin molecule. Throughout this study we have been guided by the vast amount of experimental data obtained for hemoglobin and related systems. Even though it is extensively characterized experimentally, a sound electronic description of this molecule is still lacking. To this end we have applied the techniques of modern theoretical chemistry. Using these techniques, we hope to demonstrate the ability to gain additional insight into the chemistry of hemoglobin and to show how similar studies could usefully be applied to other biologically interesting molecules.

To begin with, we will divide the hemoglobin molecule (Hb) [or myoglobin (Mb)] into three parts; the Fe-O<sub>2</sub> moiety, the rest of the iron coordination sphere, and the remainder of the hemoglobin molecule. We have studied extensively the interaction between iron and dioxygen. In Section II of this paper we describe the electronic structure of the FeO<sub>2</sub> moiety and define the possible dioxygen bonding modes available. In Secs. III and IV we then examine what effects the

coordination sphere of iron has on the intrinsic chemistry of  $\text{FeO}_2$ . It has been shown from experimental studies on model oxygen carriers<sup>8,9</sup> that the chemistry of hemoglobin is fairly well determined by the chemistry of the coordination sphere of iron, and it is the understanding of the electronic structure of this part of the molecule that we approach directly. Apparently the role of the protein is to hinder any undesirable, competing reactions, and to fine-tune the thermodynamics and kinetics of the basic reactions of the iron coordination sphere to be more optimal for biological functions. In a subsequent section we examine ways in which the protein could perturb the coordination sphere of iron and thereby lead to the known cooperative ligand binding in hemoglobin. As the conceptual ideas for iron-dioxygen complexes are being developed, we will apply them to other transition metal-dioxygen complexes, and also to other iron-ligand complexes. These applications will serve as further tests of the qualitative predictions generated by the ideas given here, and indicate how these concepts can be extended to related molecules.

## II. The Ozone Model of the Bonding of O<sub>2</sub> to an Fe Site

To understand how iron (Fe) and dioxygen (O<sub>2</sub>) can interact favorably, we must first review the electronic structure of the separated species.

### A. Fe Atom

There are a large number of low-lying atomic states of Fe atom. The ground state of Fe has the electronic configuration of  $3d^6 4s^2$ . This configuration leads to quintet ( $S = 2$ ), triplet ( $S = 1$ ), and singlet ( $S = 0$ )<sup>†</sup> states with the quintet state lowest in energy. This state has four singly-occupied d orbitals and one doubly-occupied d orbital. There are 100 different possible arrangements of six electrons in five orbitals. In atomic Fe, 73 of the  $s^2 d^6$  states have been assigned with the total separation being only  $\sim 100$  kcal<sup>10</sup> (the order of the energy of a covalent bond), so we see that there is the possibility of a large number of low-lying excited states for molecules containing Fe atoms. The energy separation in the atom between the lowest quintet, triplet, and singlet is shown in Table I. Because of the antisymmetric nature of electronic wavefunctions (the Pauli principle), aligning two electron spins (high-spin coupling) leads to an interaction between the two that decreases the energy of the system. This is generally referred to as an exchange interaction,  $K_{12}$ .  $K_{12}$  is always positive, and in the case of high-spin coupling, it enters the energy expression with a negative sign. The total exchange energy for an atom can be found by counting the number of interactions between all electrons of the same spin. For N spin-

---

<sup>†</sup> S is the electron-spin quantum number.

TABLE I. Relative energies (kcal) of the lowest state of each spin for the Fe (4s)<sup>2</sup>(3d)<sup>6</sup> and Fe<sup>++</sup> (3d)<sup>6</sup> configurations.

State	Experimental Energy <sup>a</sup>		Number of Exchange Terms	Predicted Energy <sup>b</sup>
	Fe	Fe <sup>++</sup>		
quintet ( <sup>5</sup> D)	0	0	10	0
triplet ( <sup>3</sup> P)	53	56	7	66
singlet ( <sup>1</sup> I)	83	86	6	88

<sup>a</sup> Reference 10

<sup>b</sup> Using K<sub>12</sub> = 22 kcal (see text).

aligned electrons there are N(N - 1)/2 exchange interactions. It is these exchange interactions that lead to the high-spin state of an atom being the lowest energy state (Hund's rule). For quintet Fe there are ten favorable exchange terms. Seven favorable exchange terms exist for the triplet states of Fe, and there are only six favorable exchange terms for the singlet states. Each exchange term between Fe d electrons is worth about 22 kcal.<sup>‡</sup> Taking only exchange terms into account would lead to excitation energies of 66 and 88 kcal to the lowest triplet and singlet states, respectively. Thus the exchange terms dominate the energy separations between the atomic states of the same electronic configuration. Slight differences in the coulomb interaction energy, orbital size changes in the triplet and singlet states, and electron correlation effects are neglected in this simple analysis. They lead to

<sup>‡</sup> We will use kcal as an abbreviation for kcal/mole.

corrections in the predicted energies as shown in Table I.

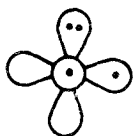
There are also many low-lying atomic states of Fe which are  $s^1d^7$  in character, but as shown later, these states are not important in considering the electronic structure of hemoglobin.

We also see from comparing the doubly-ionized  $3d^6$  states of iron to the states of  $s^2d^6$  iron neutral (Table I) that the relative energies of the various d configurations are not dependent on the presence of the Fe 4s electrons or their effective radius. The corresponding states have the same ordering and the corresponding energy separations differ at the most by 4 kcal.

#### B. $O_2$ Molecule

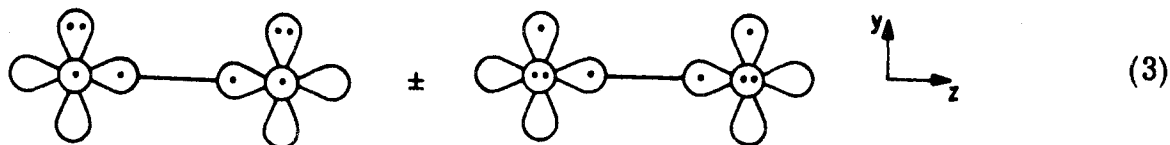
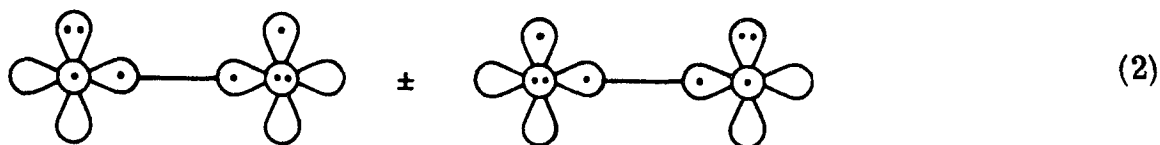
The structure of the  $O_2$  molecule and its interaction with  $H$ ,<sup>11</sup>  $O$ ,<sup>12,13</sup>  $CH_2$ ,<sup>14,15</sup> and  $CHO$ <sup>16</sup> has been studied by Goddard and co-workers. We summarize here the description of the electronic structure of  $O_2$  and the basic nature of its interaction with other chemical species that has resulted from these studies.

Consider first the formation of the oxygen molecule. It can be formed by joining two ground-state oxygen atoms with a sigma bond. We will depict the various idealized electronic states of a molecule through the use of diagrams emphasizing their atomic character. An oxygen atom is shown in (1).



(1)

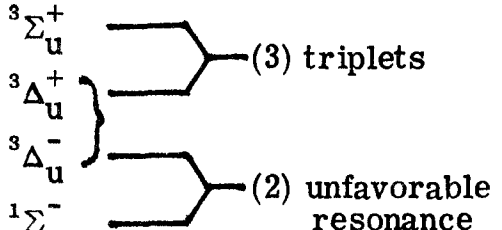
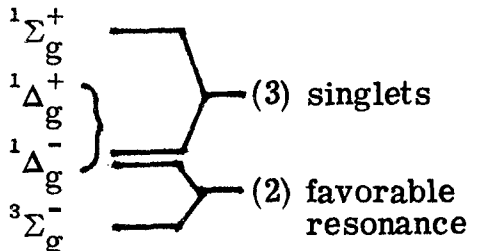
Its ground state configuration is  $(1s)^2(2s)^2(2p)^4$ . The  $(1s)$  and  $(2s)$  orbitals are not shown since they do not affect the qualitative description of the bonding. The lobes drawn in the  $z$  direction represent a  $2p_z$  orbital and the dot in one of these lobes represents a single electron occupying the  $2p_z$  orbital. The  $2p_x$  orbital is represented as a circle centered on the  $x$ -axis, and in this particular diagram it is singly-occupied. The diagram in (1) indicates an orbital occupation of  $(2p_x)^1(2p_y)^2(2p_z)^1$ . Aligning the spins of the electrons in the two singly-occupied orbitals leads to a favorable exchange interaction (similar to those discussed for Fe) and therefore the ground state of oxygen is a triplet. In order to form a dioxygen molecule, we must make a covalent bond between two ground state oxygen atoms. There are two possibilities as shown in (2) and (3).



In configuration (3), the singly-occupied  $p\pi$  orbitals on different centers overlap, and the lowest energy state for this configuration is a singlet state. The proper symmetry for the  $O_2$  wavefunction is obtained by mixing the two possible resonance forms for this configuration, leading to a  ${}^1\Delta_g^+$  state and a higher lying  ${}^1\Sigma_g^+$  state. In (2) the singly-occupied orbitals do not overlap, and there are low-lying singlet and triplet states for this configuration. As in Fe and O, high-spin coupling

leads to favorable exchange interactions and the triplet state ( $^3\Sigma_g^-$ ) is lowest in energy. The lowest singlet state ( $^1\Delta_g^-$ ) for configuration (2) is separated from the  $^3\Sigma_g^-$  state by approximately twice the exchange integral between the singly-occupied orbitals on the different oxygen centers. This singlet state is the other component of the lowest-lying singlet state ( $^1\Delta_g^+$ ) of configuration (3). Therefore, the lowest-lying state of  $O_2$  is the triplet state ( $^3\Sigma_g^-$ ) of configuration (2). The resonance interaction in configuration (2) is large, leading to high-lying  $^1\Sigma_u^-$  and  $^3\Delta_u^-$  states. The energy orderings of the states of  $O_2$  are shown in Table II.

TABLE II. The low-lying states of  $O_2$ .

Excitation Energy (kcal)		State
Theory <sup>a</sup>	Experiment <sup>b</sup>	
98.0	101.2	$^3\Sigma_u^+$ $^3\Delta_u^+$ $^3\Delta_u^-$ $^1\Sigma_u^-$ 
96.2	99.3	
90.8	94.5	
39.0	37.7	
25.1	22.6	$^1\Sigma_g^+$ $^1\Delta_g^+$ $^1\Delta_g^-$ $^3\Sigma_g^-$ 
0.0	0.0	

<sup>a</sup> Reference 17.

<sup>b</sup> Reference 18, including corrections for zero-point energies.

The essential thing to note about the electronic structure of  $O_2$  is that the ground state of the molecule is a triplet state with biradical character. For our purposes it will generally be adequate to think of the ground state of  $O_2$  as



(which we will refer to as  $^3O_2$ ) where the motions of the electrons in the two singly-occupied orbitals are correlated such that they are on different centers and in different planes. The lowest lying singlet state (which we call  $^1O_2$ ) is 22.5 kcal above  $^3O_2$  and can be thought of as



This singlet state of  $O_2$  is isoelectronic with the ground state of ethylene.

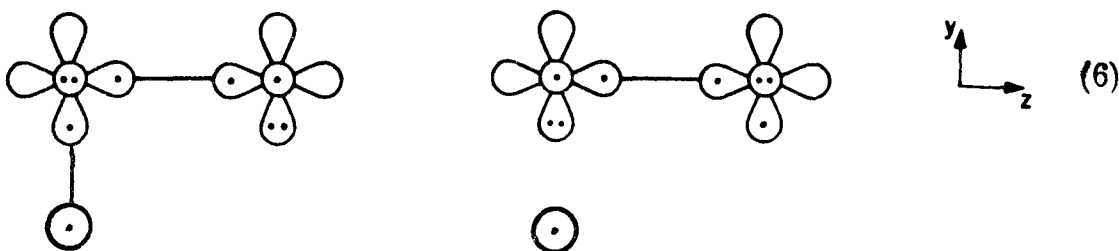
The stability of  $^3O_2$  is enhanced by the formation of two three-electron  $\pi$  bonds. The singly-occupied  $2p\pi$  orbital does not effectively shield its nucleus from the doubly-occupied orbital in the same direction on the other center. This allows the doubly-occupied  $2p\pi$  orbital to delocalize onto the other oxygen center, leading to a decrease in the total energy of the molecule. This delocalization is possible because it moves electron charge in opposite directions in the different  $\pi$  planes and thus preserves overall charge neutrality. This delocalization does cause the singly-occupied orbitals to mix in

antibonding character, but the net effect is that the three-electron pi system leads to bonding interactions between the two oxygen centers.

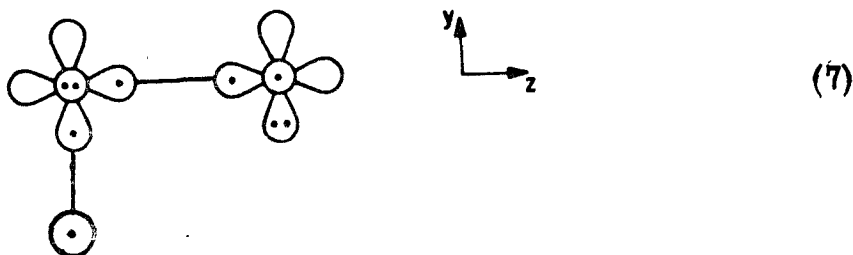
### C. Bonds to O<sub>2</sub>

In order to provide a semi-quantitative understanding of the bonding of O<sub>2</sub> to various species, the bonding of first hydrogen and then oxygen atom to O<sub>2</sub> will be discussed. These ideas are then easily extended to give a simple description of the electronic structure of O<sub>2</sub> bonding to Fe.

1. H-O<sub>2</sub>. The total bond energy of <sup>3</sup>O<sub>2</sub> is 118 kcal, of which 47 kcal are involved in the sigma bond and 71 kcal involve the pi bonding.<sup>19</sup> A covalent bond between a hydrogen atom and <sup>3</sup>O<sub>2</sub> is formed when the hydrogen orbital begins to overlap a singly-occupied orbital of <sup>3</sup>O<sub>2</sub>, as in (6).



The problem here is that this overlap is favorable only for the resonance form on the left. As a result, the bonding of H to <sup>3</sup>O<sub>2</sub> leads to configuration (7)



where most of the resonance energy of  $^3\text{O}_2$  is lost. The result is an H-O bond energy 57 kcal smaller than a normal H-O bond [ $D(\text{H}-\text{OCH}_3) = 104 \text{ kcal}^{20}$ ],

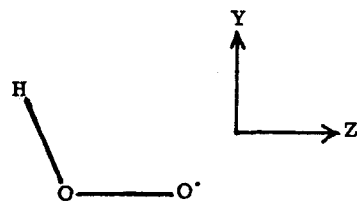
$$D(\text{H}-\text{O}_2) = 104 - 57 = 47 \text{ kcal.}$$

The orbitals obtained from the calculation are shown in Fig. 1. These figures depict the amplitude of a wavefunction in a particular plane. The contour lines connect points of equal amplitude. Solid lines are used for positive amplitudes and broken lines are used for negative amplitudes. Points of zero amplitude (nodal planes) are shown with a line of long dashes. The difference in amplitude between successive contours is 0.05 a.u. Regions of high electron density are indicated by closely grouped contours, and regions of diffuse electron density appear as widely separated contour lines. The equilibrium  $\text{HO}_2$  bond angle of  $103^\circ$  was used in these orbital plots. In (7) the radical electron is depicted as a  $\pi$  orbital localized on the right O atom. In fact, there is some bonding delocalization of the doubly-occupied  $\pi_x$  orbital onto the right O atom, and a concomitant antibonding delocalization of the radical orbital onto the left O atom, as shown in Fig. 1c. The result is a three-electron  $\pi$  bond worth  $\sim 14 \text{ kcal}$ .

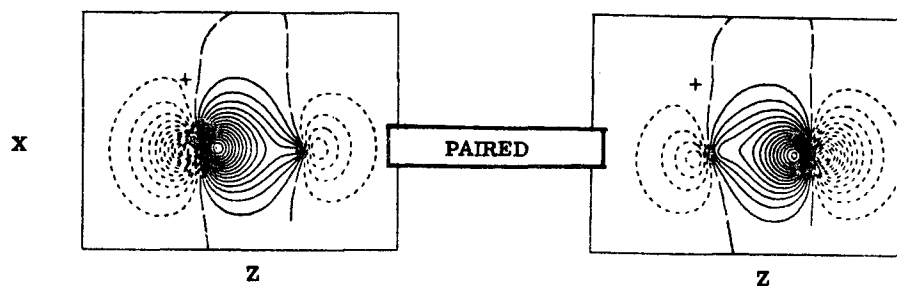
Bonding an H atom to  $\text{HO}_2$  leads to a localization of the radical orbital on the right O atom which forms a covalent bond with the H atom. Only the remaining 14 kcal of  $\text{O}_2$   $\pi$  bonding is lost when this bond is formed, leading to a bond energy of 90 kcal,

$$D(\text{H}-\text{O}_2\text{H}) = 104 - 14 = 90 \text{ kcal.}$$

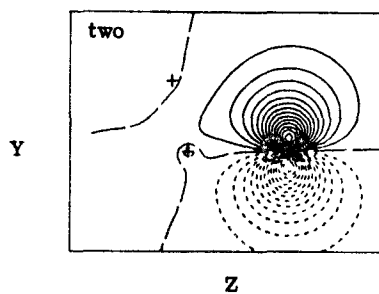
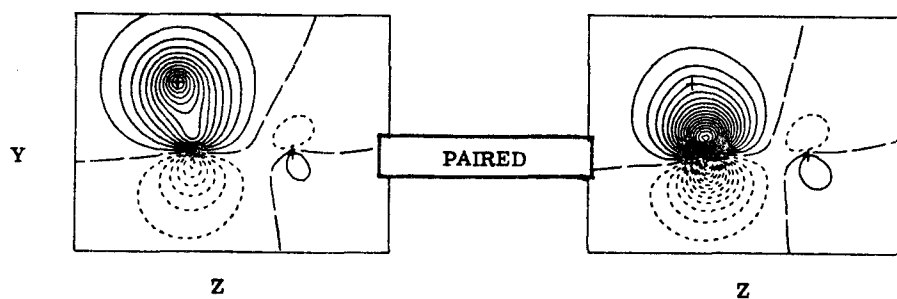
The resonance energy of  $^3\text{O}_2$  leads to a very special bonding situation.  $^3\text{O}_2$  is a biradical, but the radical orbitals are intimately involved



a) O-O  $\sigma$  pair



b) O-H  $\sigma$  pair and  $\sigma$  nonbonding orbital (YZ plane)



c) The  $\pi$  orbitals (XZ plane)

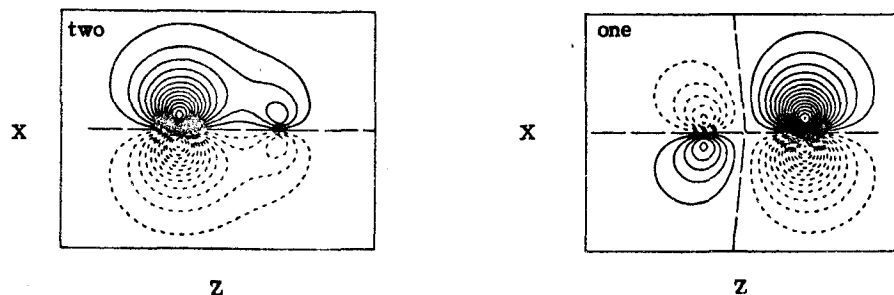
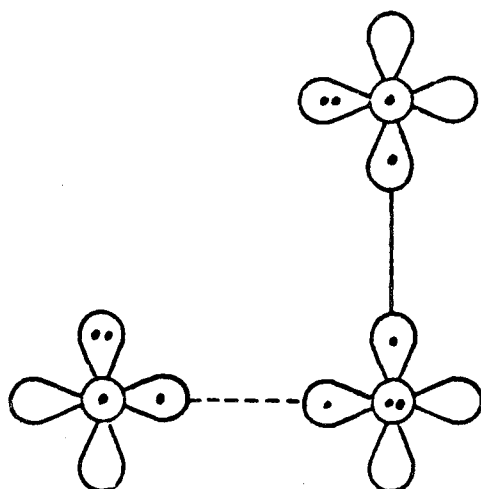


Figure 1. GVB orbitals for peroxy radical.

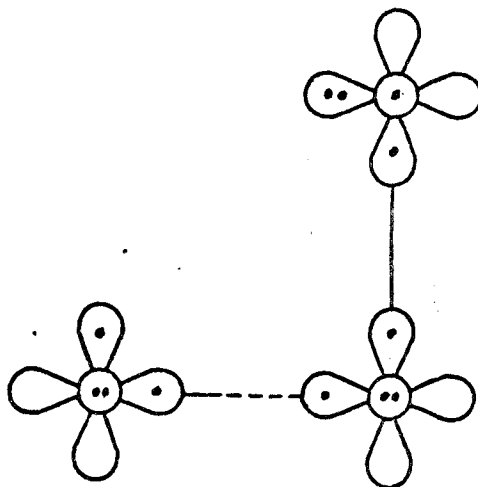
in  $\pi$  bonding, mainly through the interaction of the two resonance forms. Forming a single covalent bond to  $^3\text{O}_2$  destroys this resonance, and the bond is much weaker than would have been obtained by bonding to an O atom or OH radical. Once the first bond to  $^3\text{O}_2$  is made, the  $\text{O}_2$  molecule has been activated such that a second strong bond can then be formed.

2.  $\text{O}-\text{O}_2$  (Ozone). Forming a covalent bond between a singly-occupied orbital on ground state  $^3\text{O}_2$  and ground state  $^3\text{O}$  atom leads to two possible configurations,



(8)

and



(9)

Configuration (8) is the lowest state of  $O_3$  because the central doubly-occupied  $\pi$  orbital can delocalize in both the y and z directions, forming three-electron  $\pi$  bonds similar to the ones occurring in  $^3O_2$  and  $HO_2$ . In fact, the local electronic structure of the two oxygen atoms in either the y or z directions for configuration (8) is identical to  $^3O_2$ . For configuration (9) the two oxygen centers in the z direction correspond locally to the excited singlet state of  $O_2$ , leading to an excited state of  $O_3$ .

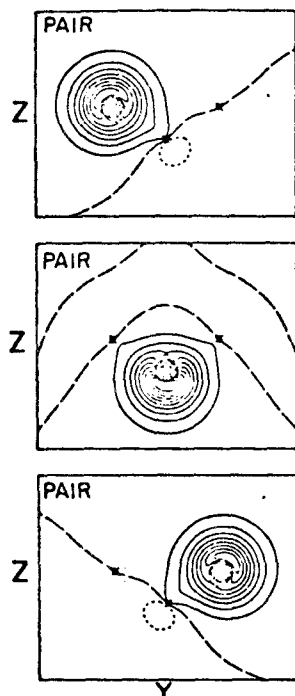
Configuration (8) has its two singly-occupied  $\pi$  orbitals low spin-coupled, corresponding to a 1-3 biradical-like singlet ground state of  $O_3$ .<sup>\*</sup> The bonding interactions between these two singlet-coupled radical orbitals and the doubly-occupied central  $\pi$  orbital is essential to the stability of the molecule, as is indicated by considering the energetics of O- $O_2$  bond. The formation of the O-O  $\sigma$  bond results in  $\sim 47$  kcal decrease in the energy of the system. But, as we saw in  $HO_2$ , the formation of a bond to one of the oxygen centers of  $^3O_2$  destroys the resonance and decreases the  $\pi$  bonding of  $^3O_2$  by 57 kcal. The net result of forming the O-O  $\sigma$  bond is an increase of 10 kcal in the energy

---

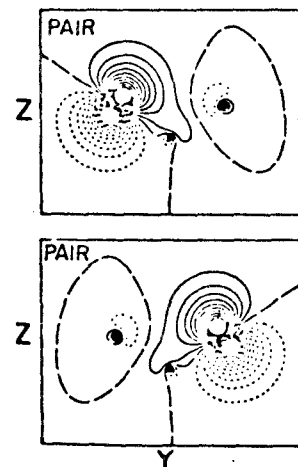
<sup>\*</sup> The ground state of  $O_3$  is a singlet state rather than the triplet state that would have been obtained by high-spin coupling the radical orbitals. Only if the singly-occupied orbitals had zero overlap, as in  $^3O_2$ , would we expect the triplet state to be lowest in energy. The overlap between these two orbitals is large because both radical orbitals build up anti-bonding character on the central oxygen atom. The overlap between these two orbitals is 0.3 a.u., leading to a stabilization of the singlet state by  $\sim 21$  kcal. The overlap between these two orbitals can be seen in Fig. 2d.

# OZONE ( ${}^1A_1$ )

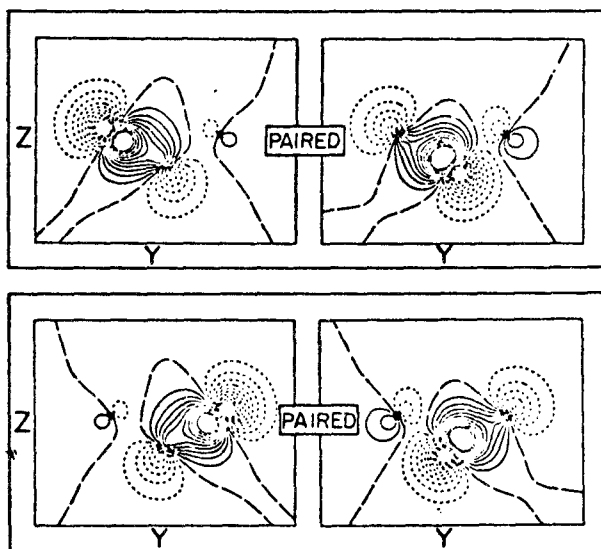
(a) the 2s  
non-bonding orbitals



(b) the 2p $\sigma$   
non-bonding orbitals



(c) the  $\sigma$  bonding orbitals



(d) the  $\pi$  orbitals

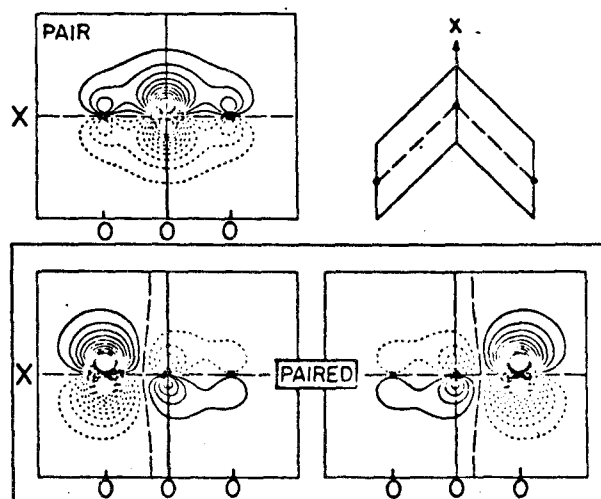


Figure 2. The GVB orbitals for ozone.

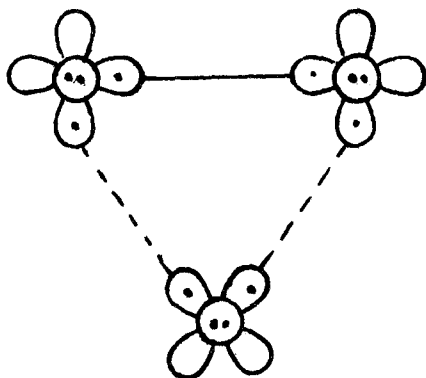
of the reacting species,

$$D_{\sigma} = 47 - 57 = -10 \text{ kcal.}$$

If these were the only bonding interactions,  $O_3$  would not be energetically stable. Besides the O-O  $\sigma$  bond, an additional three-electron  $\pi$  bond is formed in the z direction (this was worth  $\sim 14$  kcal in  $HO_2$ ) and the singlet pairing of the radical orbitals contributes  $21 \text{ kcal}^{\ddagger}$  to the bond strength of O- $O_2$ , resulting in an overall bond of

$$D(O-O_2) = -10 + 14 + 21 = 25 \text{ kcal.}$$

Another possible state of  $O_3$  can be formed by bonding a ground state triplet oxygen atom to the excited singlet state of  $O_2$  as in (10).



(10)

The optimum geometry for this state is a ring structure, where two strained O-O  $\sigma$  bonds have been formed at the expense of the  $^1O_2$   $\pi$  bond. This state lies 27 kcal above the ground state of ozone and is slightly unbound with respect to  $^3O_2$  and  $^3O$  atom.<sup>13</sup>

The orbitals for the valence electrons of the ground state of  $O_3$  are shown in Fig. 2. Note the small distance between the two nonbonding

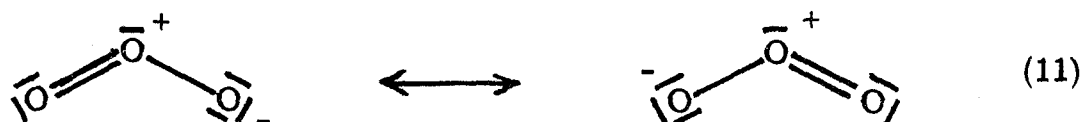
---

<sup>‡</sup> See footnote on page 14.

2p $\sigma$  orbitals (Fig. 2b). There is a repulsive interaction between these two orbitals that tends to open up the bond angle in ozone from the 90° we indicated in our idealized description. The delocalization occurring in the  $\pi$  system is shown in Fig. 2d.

In summary, the bond of O to O<sub>2</sub> leads to a bound molecule of O<sub>3</sub> in which the configurations of the reactant ground state <sup>3</sup>O atom and ground state <sup>3</sup>O<sub>2</sub> are left intact. A singly-occupied orbital of O<sub>2</sub> pairs with the O atom to form a localized covalent  $\sigma$  bond, and the three-electron  $\pi$  system of O<sub>2</sub> pairs with the remaining singly-occupied orbital on O atom to form a three-center, four-electron  $\pi$  bond. Although all four electrons play an essential role in the  $\pi$  bonding interaction, for simplicity we will often say that the singly-occupied  $\pi$  orbital of O<sub>2</sub> is singlet-paired to the p $\pi$  orbital of O atom.

The bonding in the  $\pi$  system is unusual. The singly-occupied orbitals that are paired up are not on adjacent centers, as in a normal  $\pi$  bond. It is impossible to form two  $\sigma$  O-O bonds and a normal O-O  $\pi$  bond in O<sub>2</sub> without introducing a buildup of positive charge on the central oxygen, as in (11).



The description of O<sub>3</sub> presented here corresponds to the neutral biradical resonance structure of (12),

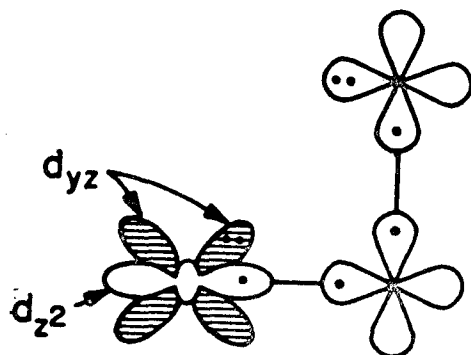


For  $O_3$ , as in most molecules made up of atoms of similar electronegativity, preserving charge neutrality is the overriding factor in properly describing the electronic structure of the molecule. Strong covalent bonds will not form unless atomic charge neutrality can be highly preserved. This principle of electroneutrality was first stated by Pauling in 1948.<sup>21</sup>

3. Fe-O<sub>2</sub>. The bond between Fe and O<sub>2</sub> can be formed in a manner analogous to the bond made between O and O<sub>2</sub>. A singly-occupied Fe d<sub>z<sup>2</sup></sub> orbital can form a covalent  $\sigma$  bond with one of the singly-occupied ground state triplet O<sub>2</sub> orbitals. The remaining three-electron  $\pi$  system of <sup>3</sup>O<sub>2</sub> can pair up with an Fe d $\pi$  orbital to form a three-center, four-electron  $\pi$  bond. This bonding situation requires singly-occupied Fe d<sub>z<sup>2</sup></sub> and Fe d $\pi$  orbitals. The idealized bonding situation is shown in (13). Since the O<sub>2</sub> complex of Mb and Hb is diamagnetic, the remaining four d electrons of Fe must be paired up in two of the remaining three Fe d orbitals. As we will show in Sec. III, one of the Fe d orbitals is highly antibonding, and it is reasonable to assume that this orbital is not populated. Therefore, we can describe the bond between Fe and O<sub>2</sub> as resulting from a pairing up of the singly-occupied orbitals of a triplet state of Fe with the singly-occupied orbitals of ground state <sup>3</sup>O<sub>2</sub>. The bond forms, leaving the basic character of the <sup>3</sup>O<sub>2</sub> intact, which is consistent with the reversibility of the Fe-O<sub>2</sub> bond. The  $\pi$  system has biradical character, which is necessary to preserve charge neutrality in the Fe-O<sub>2</sub> moiety.

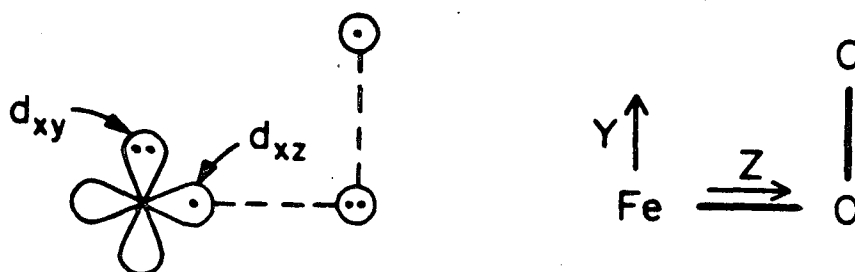
We carried out calculations<sup>\*\*</sup> on the Fe-O<sub>2</sub> moiety with the restriction that one of the Fe d orbitals was always unoccupied.<sup>§</sup> This restriction was removed when the coordination sphere of iron was included

## SYMMETRIC ORBITALS



(13)

## ANTISYMMETRIC ORBITALS



more explicitly in a model calculation for oxyhemoglobin (see Secs. III and IV). As we will show later, the electronic structure of the Fe-O<sub>2</sub> moiety in this simple calculation agrees quite well with the electronic structure of the corresponding atoms in the larger oxyhemoglobin model system.

The lowest energy state of this model Fe-O<sub>2</sub> system does indeed correspond to the idealized description given in (13). The GVB orbitals for the Fe-O<sub>2</sub> molecule are shown in Fig. 3. The major difference between these orbitals and the ones previously shown for peroxy radical and ozone is that the doubly-occupied outer oxygen nonbonding  $\sigma$  orbital is more delocalized onto the central oxygen in Fe-O<sub>2</sub>, as compared with

HO<sub>2</sub> or O<sub>3</sub>, indicating that the <sup>3</sup>O<sub>2</sub> resonance may be retained to a greater extent in FeO<sub>2</sub> than in HO<sub>2</sub> or O<sub>3</sub>.

The lowest-lying state of the ring geometry lies at 1.45 eV above the ground state of FeO<sub>2</sub>. It has a configuration corresponding to (10) where the <sup>3</sup>O atom has been replaced with <sup>3</sup>Fe (d<sub>z<sup>2</sup></sub> and d<sub>xz</sub> singly-occupied).

---

\*\* (a) GVB calculations were carried out for the singlet 4π, triplet 5π, and triplet 6π states of the open geometry, and the singlet 4π, triplet 5π, and singlet 6π states for the ring geometry. An extensive CI was carried out for each set of GVB orbitals (for example, 120 spin eigenfunctions or 285 determinants for the 4π singlets, 150 spin eigenfunctions or 180 determinants for the 5π triplets). (b) The geometry used was R<sub>FeO</sub> = 1.75 Å, R<sub>OO</sub> = 1.26 Å, ∠ FeOO = 136° for the open structure; and R<sub>FeO</sub> = 1.92 Å, and R<sub>OO</sub> = 1.43 Å for the ring structure (bond length changes between the open and ring forms were based on the differences in the corresponding states of ozone, Ref. 12). (c) The basis used was the (14s9p5d) Gaussian basis of Wachter [J. Chem. Phys. 52, 1033 (1970)] contracted to [4s2p1d] and the Pople STO-4G basis on each oxygen [J. Chem. Phys. 51, 2657 (1969)].

§ The calculations were performed first excluding the Fe d<sub>x<sup>2</sup>-y<sup>2</sup></sub> and then excluding the Fe d<sub>xy</sub>, corresponding to the O<sub>2</sub> eclipsing the pyrrole nitrogen of porphyrin, on bisecting them, respectively. The results were essentially independent of the orbital being excluded. The numerical results quoted here are from the calculation where the Fe d<sub>xy</sub> orbital was excluded.

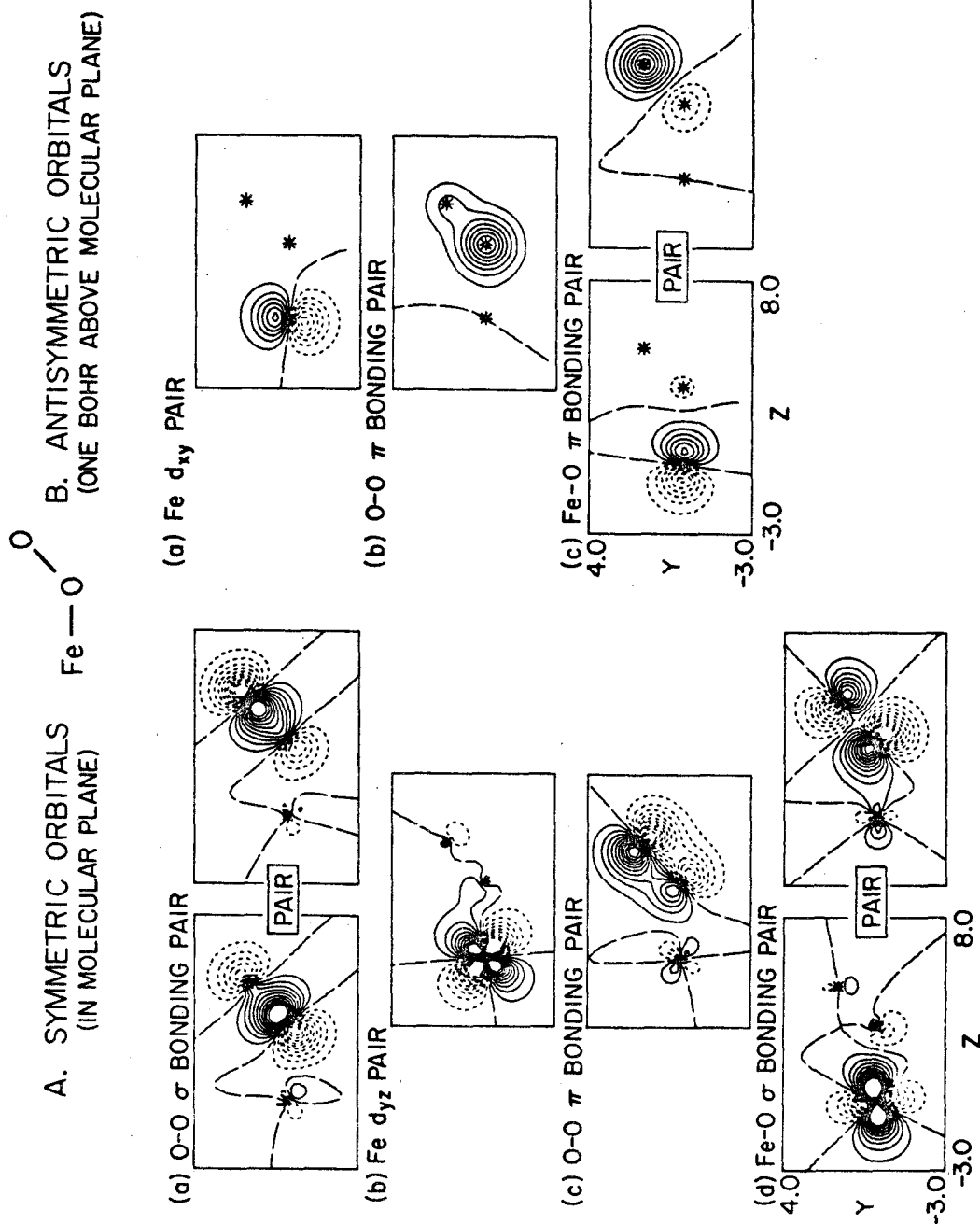


Figure 3. GVB orbitals of  $\text{FeO}_2$ .

A Mulliken population analysis was carried out on the CI wave-functions for the low-lying singlet states of the bent geometry. The ground state showed almost no charge transfer, with resultant electronic charges of Fe = +0.09, central oxygen = -0.09, and outer oxygen = 0.00. None of the 20 lowest singlet states (up to  $\sim 10$  eV) showed a degree of charge transfer that was significantly different from that found for the ground state of FeO<sub>2</sub>.

In summary,

1. Ground state triplet O<sub>2</sub> and <sup>3</sup>Fe react to form a diamagnetic Fe-O<sub>2</sub> moiety in a bent, end-on geometry.
2. The ground state character of <sup>3</sup>O<sub>2</sub> is left intact, consistent with reversible oxygen binding.
3. There is very little charge transfer upon bond formation.
4. The  $\pi$  system of FeO<sub>2</sub> has biradical character, with the singly-occupied  $\pi$  orbitals on Fe and O<sub>2</sub> singlet-coupled.
5. The lowest state of the ring geometry is 1.45 eV higher than the ground state.

### III. The Nature of the FeO<sub>2</sub> Bond in Fe-Porphyrin Complexes

In order to determine the nature of the Fe-O<sub>2</sub> bond in metalloporphyrins, Mb and Hb, we modeled the coordination sphere of Fe with five nitrogen ligands to simulate the porphyrin ring and the axial imidazole ligand of Mb and Hb.<sup>†</sup> In this section we are concerned mainly with the properties of the Fe-O<sub>2</sub> unit in the presence of the coordination sphere of Fe. We will discuss the interaction of the nitrogen ligands with the Fe center in more detail in Sec. IV.

The presence of the coordination sphere of Fe does not greatly affect the interaction between <sup>3</sup>Fe and <sup>3</sup>O<sub>2</sub>. All the conclusions we reached in the previous section carry over to the six-coordinate Fe-O<sub>2</sub> complex. The ground state of the O<sub>2</sub> complex<sup>‡</sup> is a singlet (S = 0) with an electronic configuration on the Fe of

$$(d_{xy})^2(d_{yz})^2(d_{xz})^1(d_{z^2})^1, \quad (14)$$

where the d<sub>z<sup>2</sup></sub> orbital is paired with the pσ orbital of <sup>3</sup>O<sub>2</sub> and the d<sub>xz</sub> orbital pairs with the π system of <sup>3</sup>O<sub>2</sub>. This calculated result confirms the ozone model of FeO<sub>2</sub> bonding for the coordinated Fe complex. The

---

<sup>†</sup> Four NH<sub>2</sub> groups taken with C<sub>4v</sub> geometry were used to model the porphyrin nitrogens. In these calculations the N-H bond length was 1.014 Å and the HNH bond angle was 120°. An NH<sub>3</sub> molecule was used to represent the fifth axial nitrogen ligand. The N-H bond length was also 1.014 Å and the HNH bond angle was 107°.

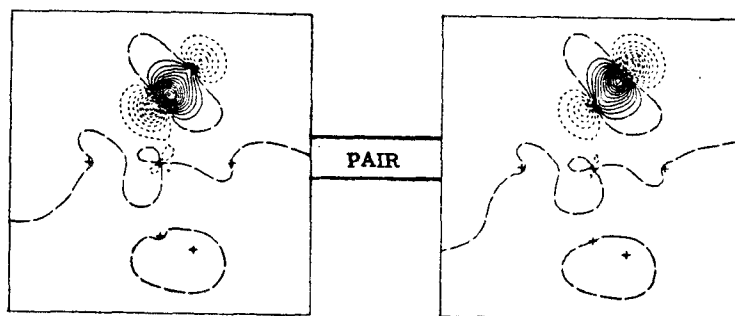
<sup>‡</sup> The Fe-O<sub>2</sub> plane has been chosen to eclipse the pyrrole nitrogens of porphyrin lying in the y direction. In this coordinate system, the x direction has π symmetry with respect to the FeO<sub>2</sub> plane.

GVB orbitals for the  $\text{FeO}_2$  moiety in the six-coordinate complex are shown in Figs. 4 and 5. In comparing these orbital plots with the previous  $\text{Fe-O}_2$  plots in Sec. II, we see that there are at most only small changes in the amplitude of the orbitals involved in the  $\text{Fe-O}_2$  moiety. These orbital plots clearly indicate that the coordination sphere has little effect on the nature of the  $\text{Fe-O}_2$  bond. The  $\text{Fe-O}_2$   $\pi$  system and the  $\text{O-O}$   $\sigma$  bonds are essentially unchanged for the two systems. There appear to be small differences in the  $\text{Fe-O}$   $\sigma$  bonding orbitals and the  $\text{O}_2$  doubly-occupied  $\sigma$  orbital between the two molecules. The latter orbital is slightly more localized on the outer oxygen in the six-coordinate complex, and the  $\text{Fe-O}$   $\sigma$  bonding orbitals appear to have slightly more character on the central oxygen for the coordinated Fe system. This is probably due to a destabilization of the  $\text{Fe } d_{z^2}$  orbital by the axial fifth ligand causing the  $\text{O}_2$   $\sigma$  doubly-occupied pair to build in less  $\text{Fe } d_{z^2}$  and central oxygen 2p character, resulting in an orbital more strongly localized on the outer oxygen.

The Mulliken populations indicate a charge transfer of  $\sim 0.1$  a.u. to the  $\text{O}_2$  for the ground state of the six-coordinate complex. Since this amount of charge transfer is the same as in the uncomplexed  $\text{FeO}_2$  molecule, any changes in the  $\sigma$  orbitals between the two molecules indicates only a localization of the  $\text{O}_2$  orbitals in the six-coordinate complex. No net charge transfer from Fe to  $\text{O}_2$  is induced by the coordination sphere of Fe.

There are a number of ground state properties known for  $\text{HbO}_2$  and model Fe oxygen carriers that allow us to compare our qualitative predictions from the ozone model of the  $\text{FeO}_2$  bond to the experimentally determined

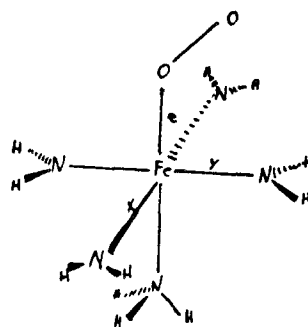
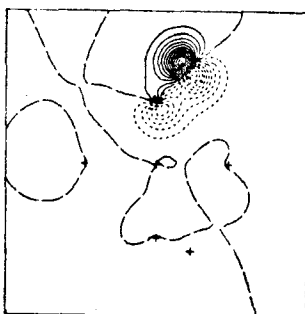
a) O-O  $\sigma$  bonding pair



b) Fe  $d_{yz}$  pair



c) O-O  $\pi$  bonding pair



d) Fe-O  $\sigma$  bonding pair

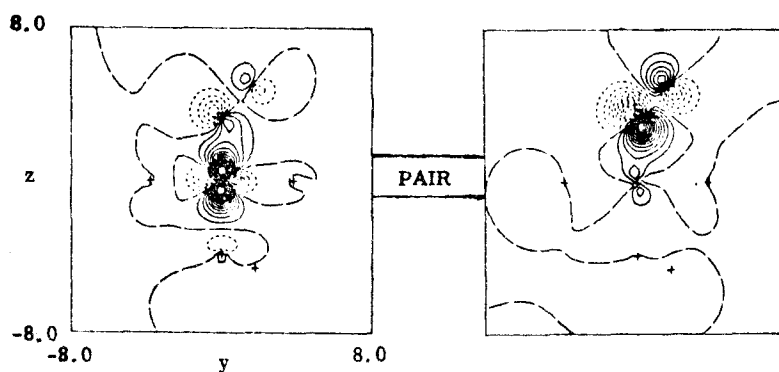
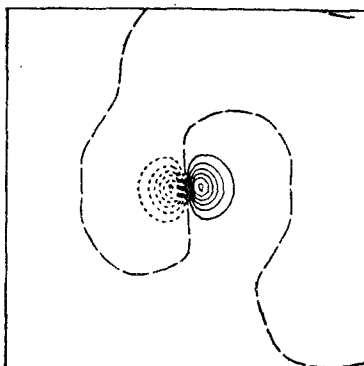
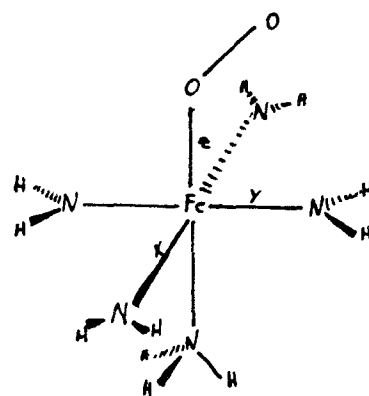
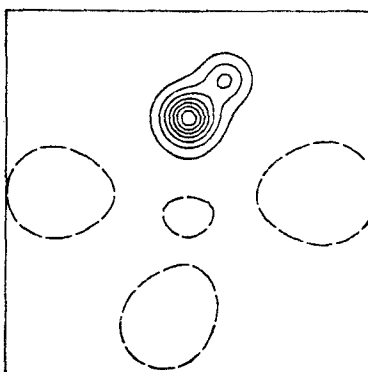


Figure 4. Fe-O<sub>2</sub> GVB  $\sigma$  orbitals for six-coordinate complex ( $\sigma$  plane).

a) Fe  $d_{xy}$  pair



b) O-O  $\pi$  bonding pair



c) Fe-O  $\pi$  bonding pair

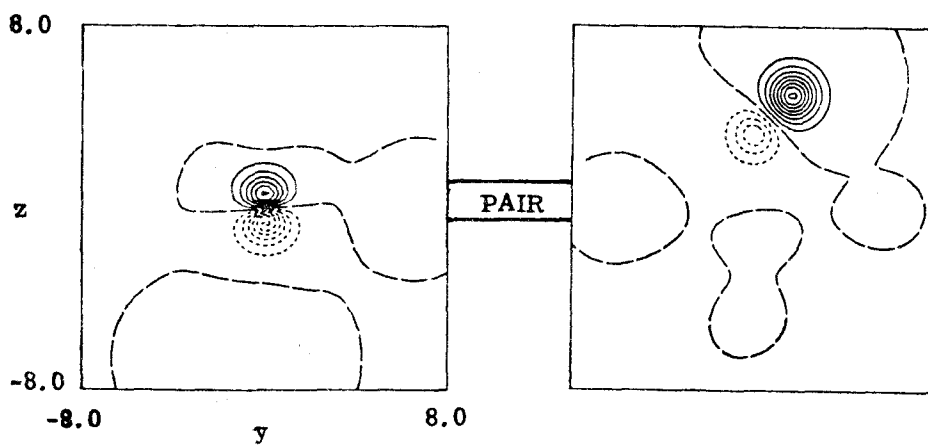


Figure 5. Fe-O<sub>2</sub> GVB  $\pi$  orbitals for six-coordinate complex (1 bohr above  $\sigma$  plane),

parameters. We calculate an FeOO bond angle of  $119^\circ$  for the six-coordinate  $\text{FeO}_2$  complex. The corresponding bond angle is  $116^\circ$ <sup>22</sup> in  $\text{O}_3$  and  $117^\circ$ <sup>22</sup> for peroxymethylene (15),



The experimental geometry for the Fe "picket-fence"  $\text{O}_2$  complex is  $136^\circ$ ,<sup>23</sup> and 1:1 cobalt (Co) oxygen carriers have bond angles ranging from  $117^\circ$ <sup>24</sup> to  $126^\circ$ .<sup>25</sup>

The O-O vibrational frequency of peroxy radical systems are  $1101 \text{ cm}^{-1}$  for  $\text{HO}_2$ <sup>26</sup> and  $1042$  and  $1103 \text{ cm}^{-1}$  for  $\text{O}_3$ .<sup>27</sup> The ozone model would predict two stretching frequencies for  $\text{FeO}_2$  in this region of the spectrum. We expect to see two bands since the intrinsic Fe-O<sub>2</sub> bond strength is similar to the O-O<sub>2</sub> bond strength, as discussed in Sec. IV.

The  $^{16}\text{O}$ - $^{18}\text{O}$  difference infrared spectra of the oxygenated "picket fence" compounds have been taken in benzene solution, where 1-tritylimidazole was the axial base. These spectra were also taken in the solid state in the form of nujol mulls between KBr plates, where 1-methylimidazole was the axial ligand.<sup>28</sup> From the solution spectra the band at  $1163 \text{ cm}^{-1}$  was assigned to the  $^{16}\text{O}_2$  stretch and the band at  $1080 \text{ cm}^{-1}$  was assigned to the  $^{18}\text{O}_2$  stretch. An unassigned feature was found at  $\sim 1100 \text{ cm}^{-1}$ .

Since the Fe-O and O-O bond strengths are similar in  $\text{FeO}_2$ , we expect two bands corresponding to the symmetric and asymmetric stretches of this triatomic unit. Therefore, we assign the band at  $\sim 1100 \text{ cm}^{-1}$  as the second stretching frequency of the  $\text{Fe}(^{16}\text{O}_2)$  moiety, noting that the separation of the two  $^{16}\text{O}_2$  bands of  $\sim 63 \text{ cm}^{-1}$  is close to

the separation of  $61\text{ cm}^{-1}$  between the two stretching frequencies of  $\text{O}_3$ . The  $^{18}\text{O}_2$  isotope shift of  $83\text{ cm}^{-1}$  would place the second band of the  $\text{Fe}(^{18}\text{O}_2)$  moiety at  $\sim 1020\text{ cm}^{-1}$ . Benzene absorbs strongly in this region and obscures the presence of any  $\text{FeO}_2$  bands in the solution spectra. This problem is not encountered in the nujol mull preparations, and the expected band shows up very prominently at  $\sim 1015\text{ cm}^{-1}$ .<sup>29</sup> There are previous assignments which indicate that the Fe-O stretch in porphyrin compounds should occur in this region of the spectrum. Bands ranging between  $840$  and  $903\text{ cm}^{-1}$  have been found for Fe-porphyrin  $\mu$ -oxo dimers, with  $^{18}\text{O}$  isotope shifts from  $45$  to  $80\text{ cm}^{-1}$ .<sup>30</sup>

The O-O stretch has been reported at  $1103$  and  $1107\text{ cm}^{-1}$  for  $\text{MbO}_2$ <sup>31</sup> and  $\text{HbO}_2$ ,<sup>32</sup> respectively. In our assignment, this band would correspond to the lower  $\text{FeO}_2$  stretch found in the oxygenated "picket-fence" model oxygen carrier. The previous assignments led to an anomalously large difference between the O-O stretch in the model oxygen carrier and the protein systems. The verification of our assignment lies in locating the expected higher band (at  $\sim 1163\text{ cm}^{-1}$ ) in  $\text{MbO}_2$  and  $\text{HbO}_2$ .

It is well established that the ground state of  $\text{HbO}_2$  is diamagnetic.<sup>33</sup> Recent high-temperature experiments indicate a low-lying paramagnetic excited state.<sup>34</sup> Our calculations predict a low-lying triplet state  $\sim 8\text{ kcal}$  above the singlet ground state for the six-coordinate complex.

The calculated electronic configuration of the Fe for the ground state of the six-coordinate complex, given in (14), is highly asymmetric. The large quadrupole splittings found in the Mössbauer studies of  $\text{HbO}_2$ <sup>35</sup> are consistent with high asymmetry of the electronic charge

distribution about the Fe. The Mössbauer studies are discussed in more detail in Sec. VIII.B.

A low-lying transition (1.3 eV) has been observed in  $\text{HbO}_2$ .<sup>36</sup> A similar transition also occurs in ferric hemoglobin,<sup>37</sup> and has been assigned as a porphyrin  $\rightarrow \text{Fe } t_{2g}$  transition. In the ozone model,  $^3\text{O}_2$  binds to a triplet state of Fe in which one of the  $t_{2g}$  orbitals is singly-occupied. This hole in the  $t_{2g}$  space is needed in order for the assigned transition to occur, and the observed "ferric" transition in  $\text{HbO}_2$  is easily explained by the ozone model.

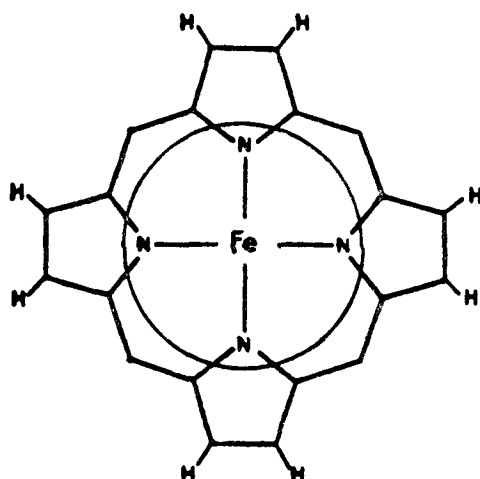
As we mentioned earlier, the calculations indicate only a slight charge transfer ( $\sim 0.1$  electrons) onto the  $\text{O}_2$  in the six-coordinate complex. Chang has recently synthesized a capped porphyrin that can hold a univalent metal, such as potassium, approximately 6 Å above the Fe-porphyrin plane.<sup>38</sup> He has investigated the binding constant of  $\text{O}_2$  to this molecule both in the presence and absence of potassium ion.<sup>39</sup> He finds that the binding constant of  $\text{O}_2$  to the capped Fe-porphyrin is only slightly affected by the presence of  $\text{K}^+$ . These studies support our result of minimal charge transfer in the  $\text{FeO}_2$  band.

From the above discussion, we see that the qualitative predictions of the ozone model are in agreement with the known ground state properties of  $\text{HbO}_2$ .

#### IV. Energetics of the $\text{FeO}_2$ Bond in Fe-Porphyrin Complexes

In this section we will examine in more detail the interactions between Fe and the porphyrin and imidazole ligands, and how these interactions pertain to the bonding of an  $\text{O}_2$  to a coordinated Fe center. In the previous section we saw that the coordination sphere did not change the nature of the  $\text{FeO}_2$  bond. However, we will show in this section that the porphyrin and imidazole ligands play a crucial role in the energetics of the  $\text{FeO}_2$  bond, leading to a weakly (reversibly) bound  $\text{O}_2$  adduct.

In performing the calculations in which the coordination sphere of Fe is taken into account, we have modeled the system by including the Fe atom and all the other atoms that are directly complexed to it. For Fe-porphyrin, the atoms inside the circle of (16) are the centers



(16)

that have been explicitly included in the calculations. Charge neutrality is preserved by making covalent bonds to hydrogens whenever the circle in (16) intersects a covalent  $\sigma$  bond. This model is meant to

reproduce the environment of the Fe in Fe-porphyrin. This model does not include any strain effects caused by the porphyrin macrocycle. For free-base porphyrin, the optimal porphyrin hole radius is estimated to be 2.05 Å.<sup>40</sup> Therefore, for any geometry of our model porphyrin system in which the hole radius is smaller than 2.05 Å, we should include an additional strain energy due to the porphyrin macrocycle which increases as we move to shorter hole radii. We estimate that if porphyrin strain were correctly included in our model, it would lead to optimum hole radii which are  $\leq 0.03$  Å longer than those calculated in our model system. None of the potential surfaces that we present here have been corrected for this effect.

The axial imidazole ligand complexes as a nitrogenous base, making a dative bond to the Fe with a doubly-occupied lone pair. We have modeled the axial ligand with the smallest nitrogenous base,  $\text{NH}_3$ .

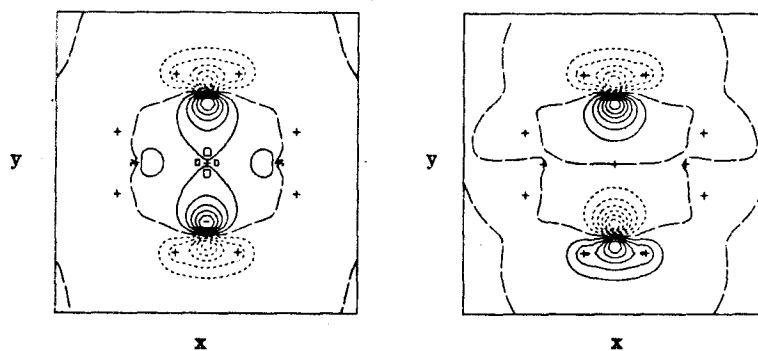
The Fe 4s electrons become localized in the plane of the porphyrin, effectively giving four nitrogen lone pairs pointing towards a formally  $\text{Fe}^{++}$  center. The nitrogen orbitals in the porphyrin plane are depicted in (17).

The GVB orbitals corresponding to the nitrogen lone pairs are shown in Figure 6.<sup>†</sup> The Fe  $d_{xy}$  and  $d_{x^2-y^2}$  orbitals are also shown in order to compare the relative spatial extents of the two types of orbitals.

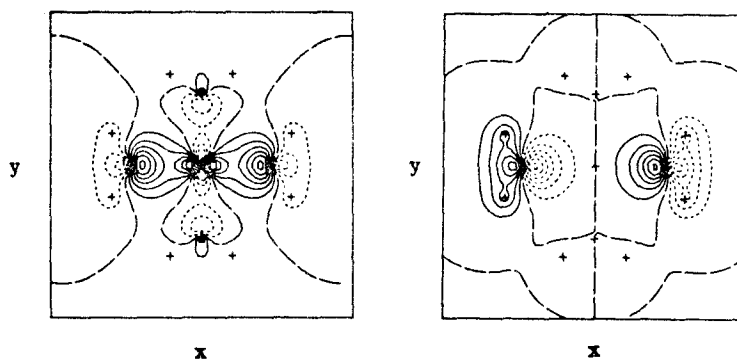
---

<sup>†</sup> The nitrogen orbitals and the Fe  $d_{xy}$  orbital are taken from the ground state wavefunction for the six-coordinate oxyhemoglobin model complex. There is asymmetry between the x and y directions due to the position of the  $\text{O}_2$ . The Fe  $d_{x^2-y^2}$  is taken from an excited quintet state of the six-coordinate complex.

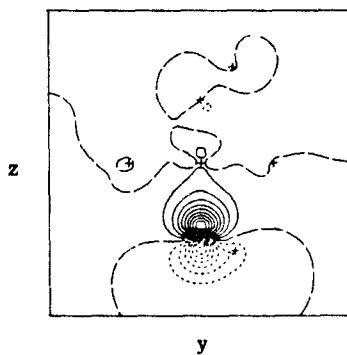
a)  $N_y$  lone pairs (symmetric and antisymmetric combinations)



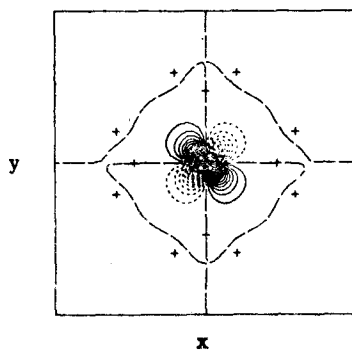
b)  $N_x$  lone pairs (symmetric and antisymmetric combinations)



c) Axial nitrogen lone pair



d)  $Fe\ d_{xy}$



e)  $Fe\ d_{x^2-y^2}$

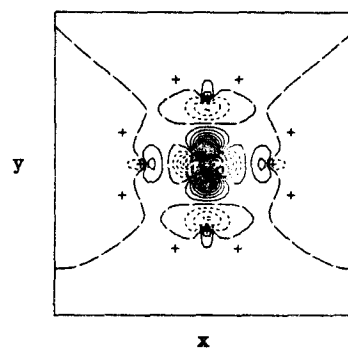
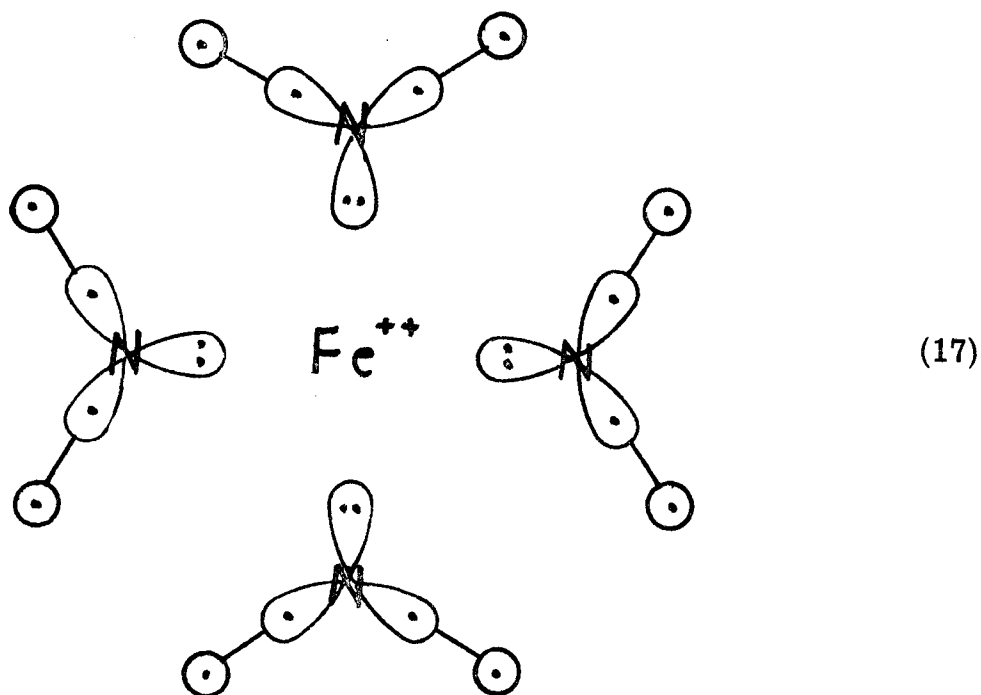


Figure 6. Selected orbitals from model oxyhemoglobin complex.



#### A. Four-Coordinate Fe

1. Relative Energies of the q, t and s States. First we will consider the lower states of Fe in a porphyrin environment. In Sec. II. A we found that for the atomic  $s^2d^6$  states of iron, the energy difference between the quintet ground state and the lowest triplet state is 53 kcal/mole. We also saw that most of the energy difference could be attributed to the loss of three favorable exchange terms in going from the quintet to the triplet state. In Fe-porphyrin there exists a similar situation. In exciting from a quintet state of Fe-porphyrin to a triplet state, three favorable exchange terms are lost. However, for Fe-porphyrin this loss of energy is partially compensated if an electron is removed from the (highly antibonding)  $d_{x^2-y^2}$  orbital in exciting to the triplet state. The bond length of the metal-pyrrole nitrogen bonds

(the radius of the porphyrin hole when the metal is centered in the porphyrin plane) determines the degree of antibonding interactions between the porphyrin  $\sigma$  orbitals and the  $d_{x^2-y^2}$  orbital, and thereby the separation between the triplet and quintet states. As the metal-nitrogen bond length is decreased, the  $d_{x^2-y^2}$  orbital becomes more antibonding, favoring the triplet state with respect to the quintet state. Our calculations indicate that for a porphyrin hole radius of 1.95 Å the exchange terms (favoring the quintet state) balance the  $d_{x^2-y^2}$  antibonding term (favoring the triplet state) leading to quintet and triplet states of Fe-prophyrin with equal energies. For porphyrin radii larger than 1.95 Å, the antibonding energy of the  $d_{x^2-y^2}$  orbital decreases, leading to a quintet ground state. For porphyrin radii less than 1.95 Å, the antibonding effects dominate the exchange terms, leading to a triplet ground state.

In the above description we discussed only the lowest quintet and triplet states. There are actually four low-lying quintet states (corresponding to either  $d_{xy}$ ,  $d_{xz}$ ,  $d_{yz}$ , or  $d_{z^2}$  doubly-occupied) and six low-lying triplet states. Here we will be concerned with the one particular quintet state denoted as q and the one particular triplet state denoted as t, which play a role in bonding of  $O_2$ . These states have the following configurations,

$$q: (d_{yz})^2(d_{xy})^1(d_{xz})^1(d_{z^2})^1(d_{x^2-y^2})^1 \quad (18)$$

$$t: (d_{yz})^2(d_{xy})^2(d_{xz})^1(d_{z^2})^1. \quad (19)$$

Thus, to form t from q we excite an electron out of the  $d_{x^2-y^2}$  antibonding orbital and place it in the  $d_{xy}$  orbital (also in the porphyrin plane).

An additional state of some interest is the low-spin ferrous state denoted here as s,

$$s: (d_{xy})^2(d_{xz})^2(d_{yz})^2. \quad (20)$$

In octahedral symmetry, this configuration gives a completely filled Fe  $d(t_{2g})$  shell and is often referred to as the  $(t_{2g})^6$  state of Fe.

The dominant effect of porphyrin on atomic Fe is to raise the energy of the antibonding  $d_{x^2-y^2}$  orbital. Since this orbital is not occupied in either the t state or the s state of Fe-porphyrin, we would expect their energy separation to remain approximately the same as in atomic Fe ( $\sim 30$  kcal) for all porphyrin hole radii. This result has been verified by our calculations.

The energy separations between the q and the t state as a function of porphyrin hole radius is shown in Fig. 7. Optimizing the Fe-N bond

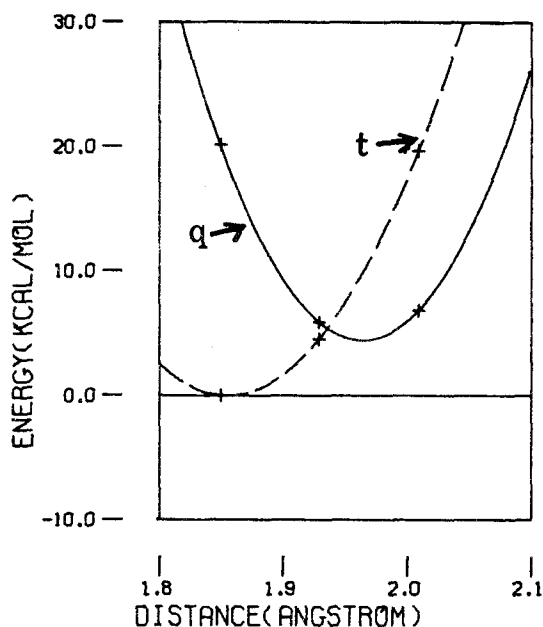


**Figure 7.** The energy separation of the q and t states as a function of porphyrin hole radius.

length of the four-coordinate complex, we find the optimal bond length of the q state to be 1.96 Å, which is 0.11 Å longer than the optimal bond length, 1.85 Å, found for the t state. This difference is due to the q state containing an electron in the antibonding  $d_{x^2-y^2}$  orbital; however, our calculated optimal Fe-N bond distance for the q state of Fe of 1.95 Å is far shorter than the value (approximately 2.2 Å) previously estimated.<sup>41, 42</sup> The reason for this discrepancy is that previous estimates were based on Fe and Co complexes consisting of saturated nitrogen ligands (possessing a coordinate bond to the Fe), whereas the ligands of our complex (and porphyrin) should be viewed as partially unsaturated (two of the four Fe-N complexing bonds have significant covalent character.)

The effect of the porphyrin on the atomic states of Fe is summarized in Fig. 8. The major effect of porphyrin ligand is to destabilize

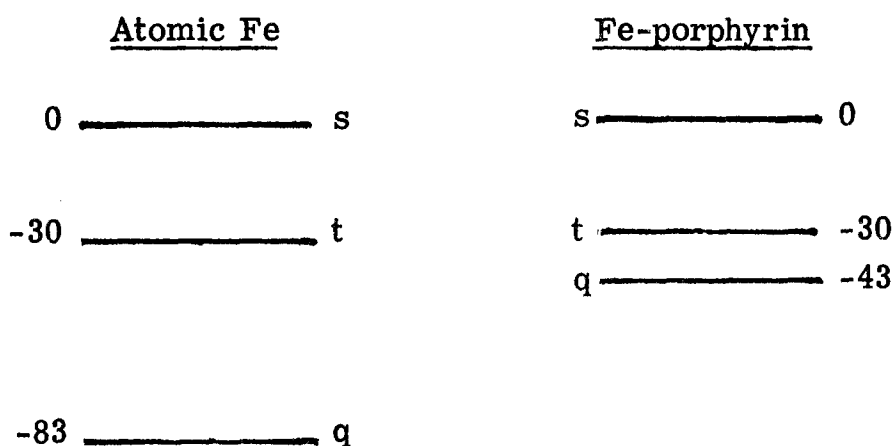


Figure 8. Energy separations between the q, t, and s states of atomic Fe and Fe porphyrin (porphyrin radius of 2.01 Å).

the quintet state of Fe, making the excited triplet and singlet states of

atomic Fe more accessible for bond formation. The fact that the q state crosses the t state at porphyrin hole radii accessible to Fe-porphyrin indicates the possibility of using the porphyrin hole radius as a means of modifying the energetics of reactions that involve bonding to the q and t states of Fe-porphyrin.

Baldwin and Huff have synthesized an Fe macrocyclic compound<sup>43</sup> that has a coordination sphere about Fe which is very similar to the coordination sphere in Fe-porphyrin, except that the unconstrained ring size is close to 1.85 Å.<sup>44</sup> Our calculations indicate that at this geometry only the t state is accessible to biological reactions with the q state lying about 20 kcal higher in energy. Indeed, the magnetic properties of the Baldwin-Huff compound ( $\mu_{\text{eff}} = 2.94 \mu_{\beta}$  at 300°K)<sup>45</sup> suggest a triplet ground state. For Fe-porphyrin, the magnetic properties have not yet been explained in detail. The fact that our calculated crossing point for the q and t states occurs close to the experimentally determined Fe-N bond length in Fe-porphyrin<sup>46</sup> indicates that the magnetic properties may be determined by an interaction between these two states.

2. Position of Fe Relative to the Porphyrin Plane. A common argument for the origin of why the Fe is significantly out of the porphyrin plane in both deoxy Mb and deoxy Hb is that the high-spin Fe is too large to fit in the porphyrin hole. However, as shown in Fig. 9, we find that the planar geometry is the optimum geometry for both the q and t states in Fe-porphyrin. That is, even in the q state the bonding interactions of the Fe with the N  $\sigma$  lone pairs hold the Fe in the plane. However, comparing the q state, with its singly-occupied  $d_{x^2-y^2}$  antibonding orbital,

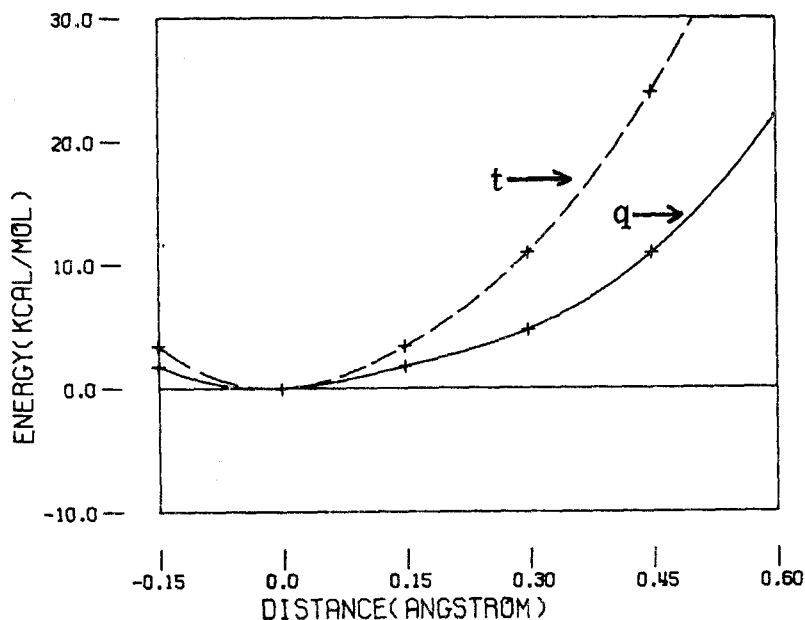


**Figure 9.** Relative energies of the q and t states of Fe-porphyrin at different Fe out-of-plane displacements (porphyrin ring radius of 1.93 Å).

and the t state, with no such occupied orbital, we find that the restraining forces holding the Fe in the plane are much smaller for the q state than for the t state. These restraining forces lead to a small force constant for the out-of-plane displacement of Fe in the q state. As the porphyrin hole radius is decreased, the force constant for Fe out-of-plane displacement in the q state also decreases, due to the greater degree of antibonding character in the  $d_{x^2-y^2}$  orbital. The energy required to pull Fe out of the porphyrin plane for different porphyrin hole radii is shown in Fig. 10.

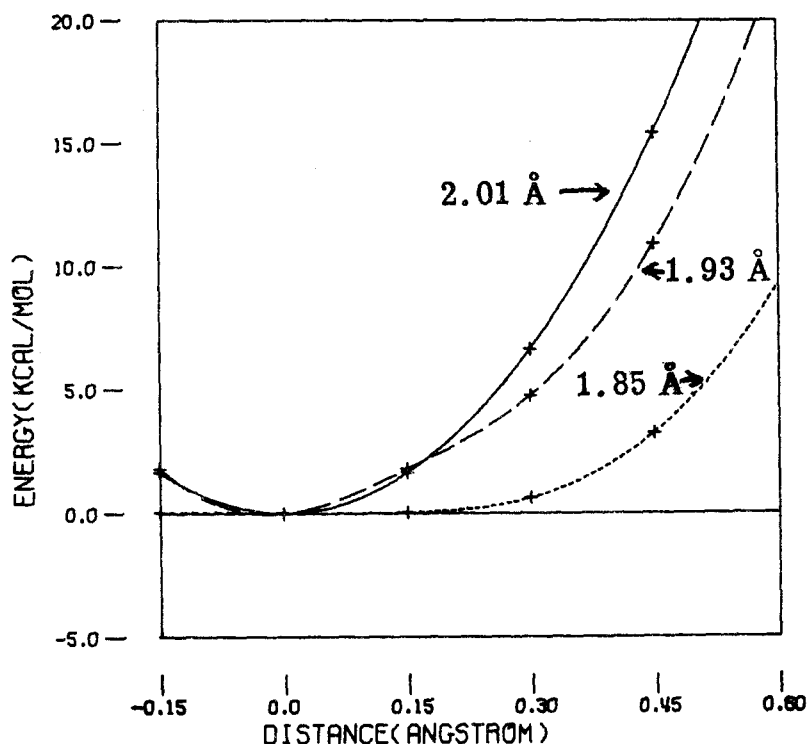


**Figure 10.** Relative energies of the q state of Fe-porphyrin at different Fe out-of-plane displacements as a function of porphyrin hole radius.

## B. Five-Coordinate Fe<sup>†</sup>

1. Relative Energies of q, t, and s States. In deoxyhemoglobin, the fifth Fe coordination site is filled by an imidazole molecule of a histidine amino acid side chain. The imidazole acts as a nitrogenous base, with its doubly-occupied nitrogen lone-pair orbital making a dative bond to the Fe (see Fig. 6c). In our coordinate system, this dative bond is formed along the z axis, having its largest electronic effect on the Fe  $d_{z^2}$  orbital. We saw from our analysis of Fe-porphyrin that the interaction of the porphyrin ligand destabilizes the  $d_{x^2-y^2}$  orbital by  $\sim 40$  kcal. To a first approximation, we might then expect the single nitrogen lone-

<sup>†</sup> Five-coordinate Fe refers to the five-coordinate Fe-porphyrin, deoxy Mb and deoxy Hb. Only in Sec. VI will a distinction be made between these molecules.

pair orbital of imidazole to destabilize the  $d_{z^2}$  orbital by  $\sim 20$  kcal.<sup>†</sup> In our model five-coordinate calculation we find that the quintet state having a doubly-occupied  $d_{z^2}$  orbital is destabilized by 18 kcal with respect to the states with  $d_{z^2}$  singly-occupied. However, this effect leaves the relative energies of the q and t states nearly unchanged (the s state drops by 18 kcal relative to the q and t states).

2. Position of Fe Relative to the Porphyrin Plane. The ordering of the states of deoxyhemoglobin given above was for the geometry of the five-coordinate complex where Fe was centered in the porphyrin plane. This particular geometry of the five-coordinate complex was chosen because it corresponds to the geometry of deoxyhemoglobin achieved upon bonding dioxygen or other axial ligands in the sixth coordination site.

We also carried out calculations in which the Fe (and the fifth ligand,  $NH_3$ ) was allowed to move relative to the porphyrin plane. Modelling the porphyrin system as before (with four  $NH_2$  units) we optimized both the Fe out-of-plane distance and the Fe- $NH_3$  bond length simultaneously. Fixing these parameters at their optimum values, we also optimized the tilt of the four  $NH_2$  groups to account for the doming of the porphyrin plane that is found to occur in high-spin five-coordinate Fe complexes. The calculated equilibrium geometry (q state) has the Fe 0.28 Å out of the plane of the porphyrin nitrogens, with an Fe- $NH_3$  distance of 2.1 Å, a porphyrin hole radius of 1.98 Å, and the  $NH_2$  groups

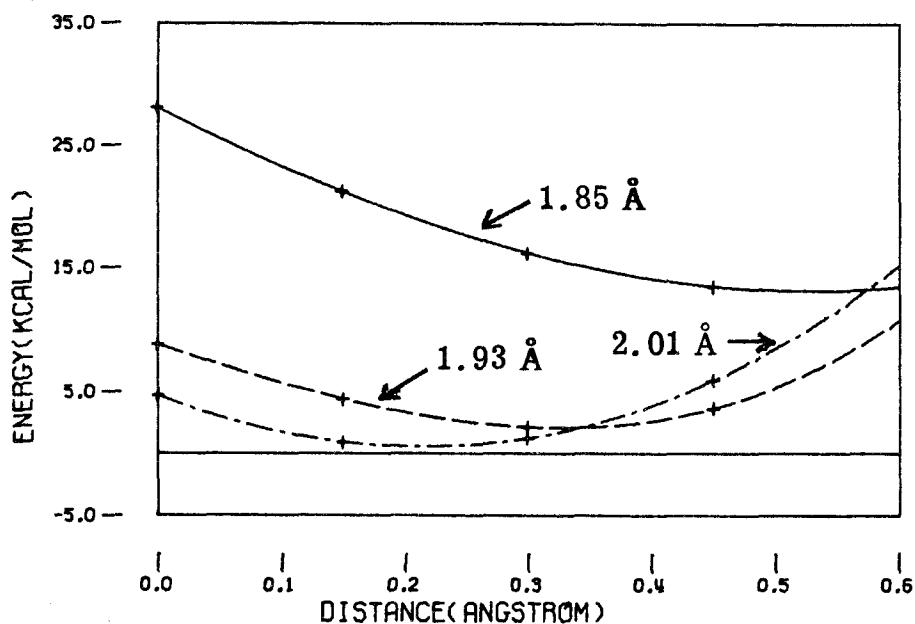
---

<sup>†</sup> Two axial imidazoles should destabilize the  $d_{z^2}$  by  $\sim 40$  kcal, since in this case there is pseudo-octahedral symmetry and the two  $e_g$  orbitals ( $d_{z^2}$  and  $d_{x^2-y^2}$ ) should be degenerate.

domed by  $\sim 9^\circ$ . Comparisons with experiment are difficult because no published crystal structure analysis has led to a reliable value for the distance of the Fe from the porphyrin on an analogous system. Radonovich and Hoard examined the 2-methyl imidazole complex of Fe (tetraphenylporphyrin) and found that the Fe is  $0.42 \text{ \AA}$  out of the N plane and  $0.55 \text{ \AA}$  out of the mean porphyrin plane.<sup>47</sup> The methyl group leads to a short contact with the porphyrin and probably the unsubstituted imidazole would have the Fe closer to the N plane. Recent high-resolution ( $2 \text{ \AA}$ ) x-ray diffraction studies on Mb lead to Fe  $0.55 \text{ \AA}$  from the mean porphyrin plane with the Fe about  $0.42 \text{ \AA}$  from the porphyrin N plane,<sup>48</sup> suggesting that the protein causes at most only a slight increase in the Fe-porphyrin separation.

The potential surfaces for the q and t states of the deoxy Hb model are shown in Fig. 11. This potential surface illustrates the relative energies of the two states as the porphyrin hole radius and Fe out-of-plane displacement are varied. For these potential surfaces the Fe-NH<sub>3</sub> bond has been fixed at  $2.06 \text{ \AA}$  and the four NH<sub>2</sub> groups have been kept planar. The energy changes occurring as a function of Fe out-of-plane displacement for a fixed porphyrin ring size are shown. From this figure we see that as the porphyrin hole radius gets larger the Fe moves closer to the porphyrin plane, with the effect being much larger in the q state than in the t state. Although the minima of the various curves shift markedly, the shapes of the curves remain very similar, resulting in only small changes in the force constants for the q and t states as the porphyrin hole radius is changed.

a) q state



b) t state

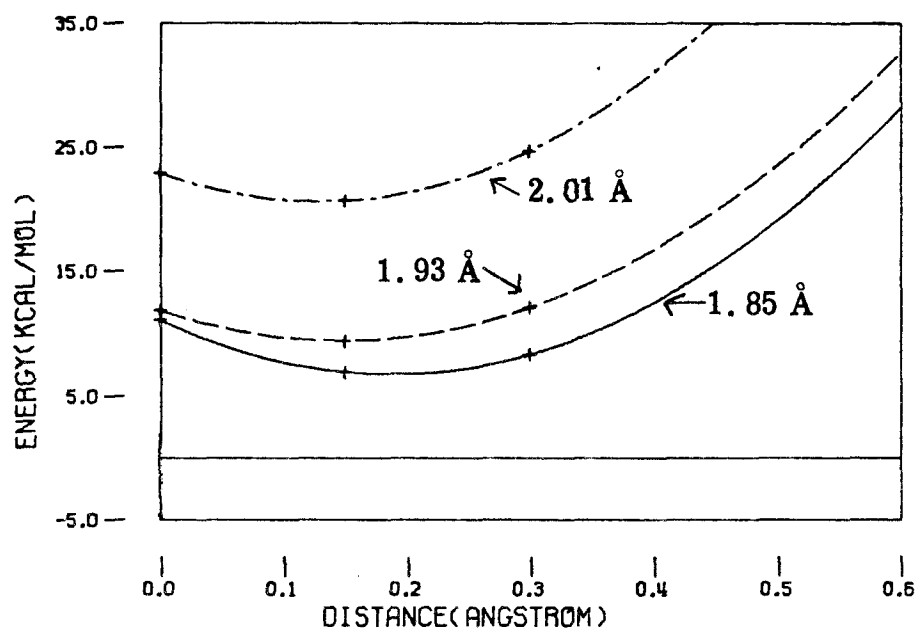


**Figure 11.** The relative energies for the q and t states of the deoxy-hemoglobin model porphyrin as a function of Fe out-of-plane displacement for fixed porphyrin hole radii.

Since in the q state of Fe-porphyrin, Fe lies in the porphyrin plane, one might wonder why the Fe moves out of the plane for the five-coordinate complex. The answer is nonbonded repulsions. With the Fe in the plane and the  $\text{NH}_3$  at its optimum position, nonbonded interactions between the  $\text{NH}_3$  orbitals and the porphyrin orbitals are large. We repeated the calculations of the five-coordinate complex but with the Fe atom deleted. Moving the axial ligand from infinite separation to a position 2.1 Å from the porphyrin-N plane (appropriate for a five-coordinate complex with Fe in the plane) led to an increase of 15 kcal in the energy of the system.

Since model calculations lead to a proper geometry for the five-coordinate model deoxyhemoglobin complex, our result that the quintet high-spin state of Fe-porphyrin is planar appears valid. From these results, we see that the role of the Fe is to oppose nonplanarity, even for the five-coordinate complex. Acting against this are the nonbonding repulsions between the axial ligand and the porphyrin nitrogen atoms. Thus, the porphyrin pulls on the Fe and Fe pulls on the ammonia, but ammonia pushes against the porphyrin nitrogen atoms. The pull of the porphyrin on Fe is weaker than the nonbonding repulsive effects incurred by the axial ligand. All these effects balance when Fe is  $\sim 0.28$  Å out of the porphyrin plane.<sup>†</sup> Because there are opposing effects, only  $\sim 5$  kcal

---

<sup>†</sup> The effects of covalent bonding interactions between the Fe and the porphyrin ligand are also illustrated in Fig. 11. For large Fe out-of-plane displacements where nonbonded repulsions are minimized, the lowest energy results for the geometries where the Fe-N distance is smallest. In these instances, retaining strong Fe-porphyrin covalent bonds is more important than reducing the nonbonded repulsion between

of energy is required to pull the Fe-NH<sub>3</sub> group back into the porphyrin plane.

The relative energies of the q and t states of model deoxyhemo-globin as a function of Fe out-of-plane displacement are shown in Fig. 12.

Similar effects operate for the excited t state. However, the force constant for pulling the Fe out of the plane is much larger and consequently the nonbonded repulsions of the five-coordinate complex pull the Fe only 0.13 Å out of the porphyrin plane.

### C. The Six-Coordinate FeO<sub>2</sub> Complex

1. Molecular Description of the O<sub>2</sub> Bond to Mb. Both the q and t states of the model deoxymyoglobin complex have singly-occupied d<sub>z<sup>2</sup></sub> and d<sub>xz</sub> orbitals that can pair with the pσ and pπ orbitals of the ground state <sup>3</sup>O<sub>2</sub> to form an ozone-like Fe-O<sub>2</sub> complex as described in Sec. II. Since two orbitals of the Fe are paired with the two unpaired orbitals of <sup>3</sup>O<sub>2</sub>, the q state of deoxy Mb leads to MbO<sub>2</sub> with two remaining unpaired electrons on the Fe, while the t state leads to a final state of MbO<sub>2</sub> with no unpaired electrons. Thus the q state of MbO<sub>2</sub> is paramagnetic (S = 1) and the t state is diamagnetic (S = 0).

Our calculated energy separation between the q and t states of MbO<sub>2</sub> is ~8 kcal with the diamagnetic t state being the ground state.

---

the axial nitrogen and porphyrin ligands. At small Fe out-of-plane displacements, the Fe-N bond lengths are only slightly affected by movement of the Fe, and nonbonded repulsions dominate the various interactions that influence the geometry of the molecule.

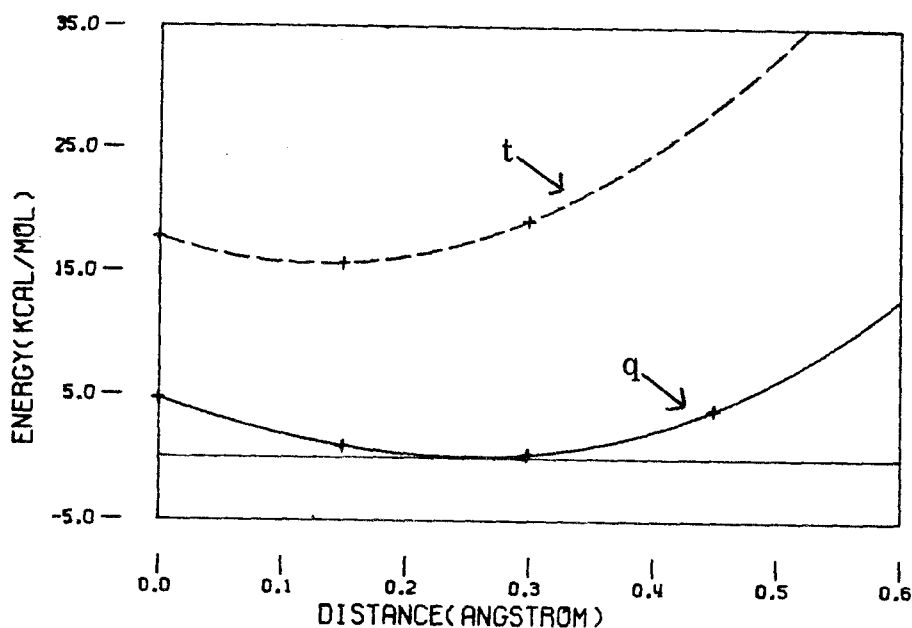


**Figure 12.** Relative energies of the q and t states of model deoxyhemoglobin as a function of Fe out-of-plane displacement (porphyrin hole radius of 1.98 Å).

The role of the q and t states in the formation of the  $\text{FeO}_2$  bond is depicted in Fig. 13.

In the ozone model of the  $\text{FeO}_2$  bond, the Fe d orbitals and the  $^3\text{O}_2$  singly-occupied orbitals interact in the same manner for both the q and t states, and therefore should lead to the same intrinsic  $\text{FeO}_2$  bond strength. In order to understand why the q and t states reverse in energy upon bonding  $\text{O}_2$ , we must again consider the exchange terms between the singly-occupied Fe d orbitals.

As we discussed earlier in this section, the  $d_{x^2-y^2}$  is  $\sim 40$  kcal antibonding, and at least two additional exchange terms have to be

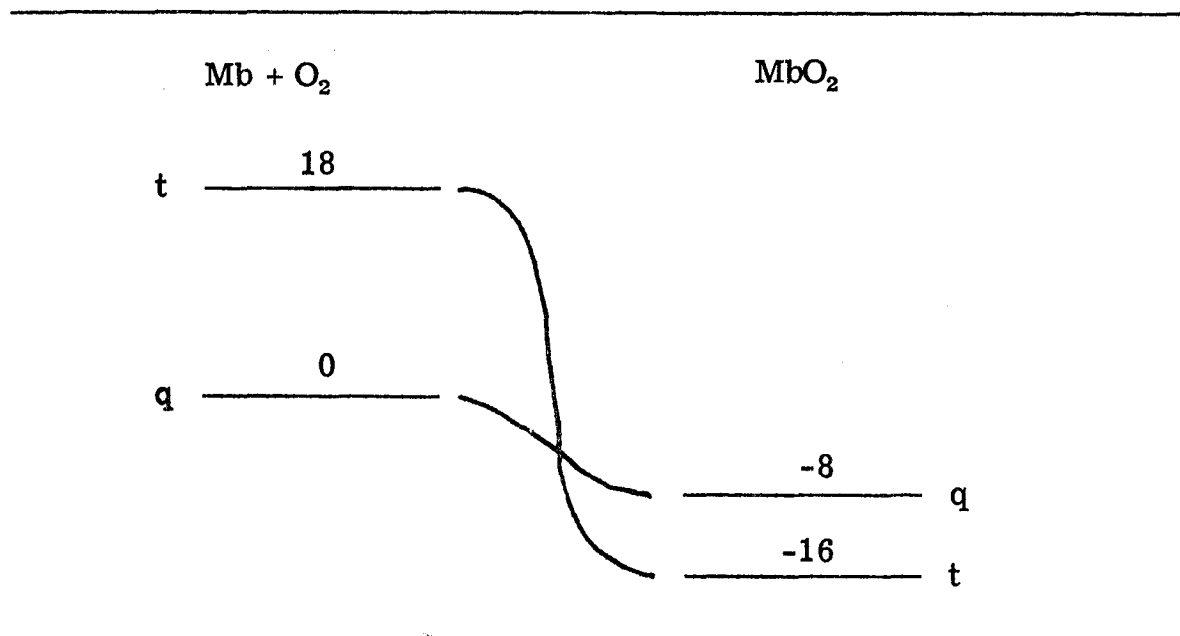


Figure 13.

gained if singly-occupying this orbital is going to be favorable energetically. This is the case for Fe-porphyrin and deoxy Mb, where three exchanged terms are gained by occupying the  $d_{x^2-y^2}$  orbital. This is not the case for  $MbO_2$ . By spin-pairing two of the q state's singly-occupied Fe d orbitals with singly-occupied orbitals of  $O_2$  we are left with only two singly-occupied orbitals, which give rise to one exchange term between them. Pairing these electrons up in the  $d_{xy}$  orbital leads to the t state which has no exchange terms between these electrons. Because two of the Fe d singly-occupied orbitals are spin-paired with the  $O_2$ , we gain only one additional exchange term by occupying the  $d_{x^2-y^2}$  orbital in  $MbO_2$ . The  $d_{x^2-y^2}$  antibonding effects are much larger than the energy gained from one exchange, and, as a result, the t state becomes the ground state for the oxygenated molecule. These antibonding effects are larger than the energy of a single exchange term for all accessible

porphyrin hole radii, and the t state will be the ground state of MbO<sub>2</sub> for all accessible porphyrin hole radii.

The picture of bonding of O<sub>2</sub> to Mb presented here departs markedly from the usual description. First we note that there are at least two electronic states of Fe involved, q and t. The process of bonding an O<sub>2</sub> to Mb probably involves coupling of the <sup>3</sup>O<sub>2</sub> with the q state of Mb (qMb) to form the triplet state of qMbO<sub>2</sub>, which would be followed by a spin conversion to the singlet state tMbO<sub>2</sub>. Thus a bound intermediate and a spin conversion are probably involved in the bond formation and dissociation of O<sub>2</sub> to Mb and Hb.

Our mechanism indicates how the bonding process proceeds smoothly from ground state reactants to product. We expect little or no energy of activation for dioxygen binding in deoxy Mb. The only source of an activation energy that could occur would result from moving Fe back towards the porphyrin plane. Since our calculation indicates that to move the Fe completely back into the porphyrin plane for the five-coordinate complex requires only 5 kcal of energy, this amount would be an upper limit to the activation energy. Our mechanism never involves bonding to an excited state of either deoxy Mb or O<sub>2</sub>, and therefore no energy source is needed to activate the reactant species. These ideas also indicate that it is formation of the Fe-O<sub>2</sub> bond that causes the spin change on Fe to occur. This spin change will occur independently of any movement of the Fe towards the porphyrin plane.

2. Energetics of the O<sub>2</sub> Bond to Mb. The changes in the energy separations between the q, t, and s states that occur as porphyrin and imidazole complex to Fe are summarized in Fig. 14. The end result

Atomic Fe	Planar		Equilibrium Five-Coordinate Fe
	Four-Coordinate Fe	Five-Coordinate Fe	
30 — s	30 — s	30 — s	30 — s
		18 — t	18 — t
0 — t	0 — t	5 — q	0 — q
	-13 — q		
-53 — q			

Figure 14. The effect of the coordination sphere of iron on the energy separations (kcal) of the q, t, and s states.

of complexing a porphyrin and an imidazole ligand to Fe is to reduce the energy separations between the q, t, and s states to about 1/3 of their value in atomic Fe.

In MbO<sub>2</sub> the configuration of the Fe corresponds to a planar t state. In order to reach this configuration about the Fe, the q state of the deoxy Mb must first move back into the porphyrin plane, at a cost of ~ 5 kcal of energy, and then be excited to the t state lying 13 kcal above the planar q state. Thus bonding an O<sub>2</sub> to Mb reduces the intrinsic FeO<sub>2</sub> bond strength by the 18 kcal of energy required to carry out these two processes.

From these calculations we find that the coordination sphere of Fe plays a crucial role in determining the bond strength of O<sub>2</sub> to Mb. It brings about the proper energy separation between the q and t states in deoxy Mb such that the t state is accessible to <sup>3</sup>O<sub>2</sub>. If the t state were inaccessible, <sup>3</sup>O<sub>2</sub> would have to bind to the q state of deoxy Mb, resulting in a weak MbO<sub>2</sub> bond strength of only 8 kcal. If the t state were actually lower than the q state, a very strong Fe-O<sub>2</sub> bond would form. From our calculations we estimate the bond strength of planar t state deoxy Mb to <sup>3</sup>O<sub>2</sub> to be ~ 34 kcal.\* For a bond strength this large, extreme conditions would be needed to promote reversible oxygenation.

---

\* Since triplet oxygen atom bonds to <sup>3</sup>O<sub>2</sub> (ozone) with a bond strength of ~ 25 kcal, our estimate of the Fe-O<sub>2</sub> bond strength may be too large. The exchange interaction for the singly-occupied orbitals of oxygen atom is 3 kcal larger than the exchange interaction for Fe d orbitals, and this difference would result in a 3 kcal larger bond strength for Fe-O<sub>2</sub> as opposed to ozone. The amount of energy required to move Fe back into

For the model oxygen carrier synthesized by Baldwin and Huff,<sup>43</sup> this latter situation actually occurs. Because of the small macrocyclic ring size, the t state is the ground state for the unoxygenated system. For this molecule, the energy of the Fe-O<sub>2</sub> bond is reduced by two factors from its intrinsic bond strength. From Fig. 11b we see that ~5 kcal are needed to pull the t state of Fe back into the plane for the short macrocyclic hole radius of 1.85 Å. An additional factor that tends to reduce the Fe-O<sub>2</sub> bond strength in the oxygenated Baldwin-Huff compound as compared with the porphyrin-based compounds is the extra nonbonded repulsions between the O<sub>2</sub> ligand and the macrocycle. Taking into consideration the difference in the van der Waals radius of N and O,<sup>41</sup> we estimate an increase in the nonbonded repulsions between the O<sub>2</sub> ligand and the macrocycle of ~7 kcal for the Baldwin-Huff compound as compared with the porphyrin-based FeO<sub>2</sub> complex. These corrections give an estimate of  $\Delta H = 22$  kcal for the O<sub>2</sub> bond strength to the Baldwin-Huff compound. For Collman's picket-fence model oxygen carrier, the bound O<sub>2</sub> can be removed by simply bubbling nitrogen through the solution.<sup>49</sup> For the Baldwin-Huff oxygenated compound, three freeze-thaw

---

the porphyrin plane and to excite it from the q state to the t state is very sensitive to the porphyrin ring size, and a shift of only 0.03 Å to a smaller ring size could decrease the sum of these two effects by ~9 kcal, which would lead to an intrinsic Fe-O<sub>2</sub> bond strength of 25 kcal, the same as in ozone. Our calculations do not use a basis set of sufficient flexibility to calculate the intrinsic Fe-O<sub>2</sub> bond strength accurately. The additional computational effort has not yet been done to determine this quantity.

cycles have to be performed in order to remove most of the complexed  $O_2$ ,<sup>43</sup> an indication that in the latter compound the  $O_2$  ligand is bound more securely. An experimental verification of a larger Fe- $O_2$  bond strength for the Baldwin-Huff model oxygen carrier would be convincing evidence in support of the idea that two electronic states are involved in the  $O_2$  bonding process in Mb and Hb.

Based upon our demonstration of the importance of nonbonded steric interactions (between the imidazole axial ligand and the porphyrin plane) in the energetics of ligand binding to five-coordinate porphyrin complexes, Warshel<sup>128</sup> has carried out semi-empirical calculations indicating that "a change in spin state should be considered more a consequence of ligand binding than the major factor in control of oxygen affinity." As indicated herein, it is the electronic configuration of the Fe (q or t) that is fundamental (rather than the spin itself), and the change in electronic configuration goes hand-in-hand with the ligand binding rather than one implying the other.

## V. The CO Bond to Fe-Porphyrin Complexes

After  $O_2$ , the next most widely studied adduct of hemoglobin is carbon monoxide (CO), often referred to as carbonyl hemoglobin. CO binds to Fe in a manner very similar to  $NH_3$ , making a dative bond through the doubly-occupied lone pair on carbon. The bond is basically electrostatic in nature, involving very few shape changes in the doubly-occupied ligand orbital (shown for  $NH_3$  in Fig. 6c).

X-ray studies indicate that CO binds to a five-coordinate Fe-porphyrin complex in a linear arrangement perpendicular to the porphyrin plane with an Fe-C distance of 1.77 Å.<sup>50</sup> In myoglobin CO binds in a noticeably bent geometry<sup>51</sup> in order to reduce its nonbonded interactions with amino acid residues situated close to the Fe binding site. Because of these interactions the bond strength of CO to myoglobin is significantly smaller than that found for the unconstrained Fe-porphyrin complexes. The bond strength for the former molecule has been estimated at 10.5 kcal,<sup>52</sup> whereas unconstrained porphyrin complexes have CO bond strengths ranging from 16-19 kcal.<sup>53</sup>

In bonding CO to planar five-coordinate Fe-porphyrin, the presence of the doubly-occupied lone pair further destabilizes the  $d_{z^2}$  orbital and drops the s state relative to the q and t states. This destabilization is expected to be larger than the 18 kcal destabilization of the  $d_{z^2}$  orbital by the axial nitrogen ligand for two reasons. First, the open coordination site in the five-coordinate complex allows the  $d_{z^2}$  electron to hybridize in a manner such that it localizes more of its electron density towards the open coordination site, reducing its antibonding interactions with the axial nitrogen ligand. Secondly, CO forms very short dative bonds to

metal centers, resulting in large amounts of metal d orbital destabilization. For these reasons it is not unreasonable to expect that CO destabilizes the  $d_{z^2}$  orbital by more than 25 kcal, causing the s state to drop below the q and t states (Fig. 15).

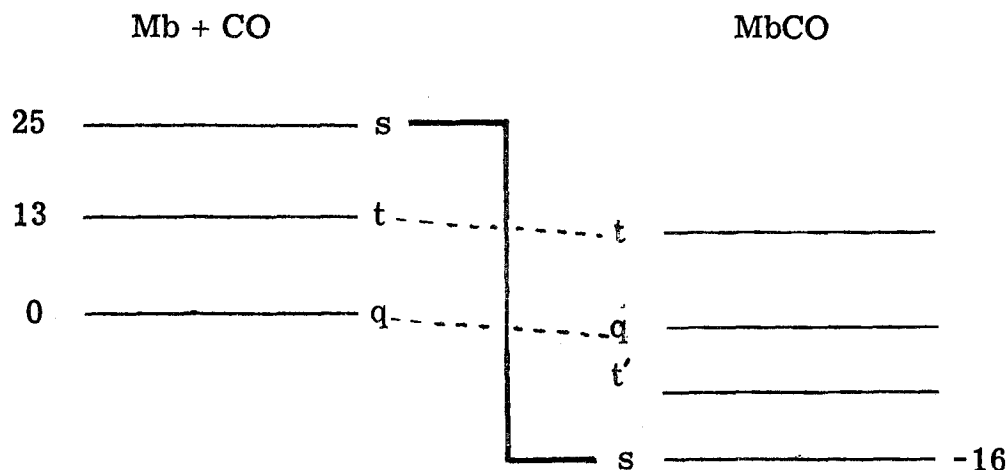


**Figure 15.** Role of the q, t, and s states in CO bond formation of planar five-coordinate Fe-porphyrin. The  $t'$  state is a triplet ( $S = 1$ ) state of Fe in which the  $d_{z^2}$  orbital is unoccupied. The positions of the q, t, and  $t'$  states are uncertain for MbCO.

CO bound to the s state  $[(t_{2g})^6]$  of Mb gives rise to a diamagnetic complex with very little asymmetry of charge distribution about the Fe nucleus, in agreement with the magnetic properties<sup>33</sup> and Mössbauer data for HbCO.<sup>54</sup>

The formation of the CO bond will involve two intermediate electronic states and two spin-conversion processes. The fact that CO has a slower on rate than  $O_2$ <sup>9</sup> indicates a larger energy of activation than in  $O_2$ , or a longer period of time needed for the spin-conversion process

to take place. Frauenfelder and co-workers have carried out detailed kinetic experiments that indicate the possibility of a large number of intermediate states in the bonding and dissociation of CO from myoglobin.<sup>55</sup>

There exists the possibility of a low-lying quintet ( $S = 2$ ) excited state of MbCO obtained by binding CO to the q state of Mb. For ligands that do not form dative bonds as strong as CO, the q state may actually be the ground state. This may be the case for  $\text{Fe(OTBP)THF}_2$  (OTBP = octamethyltetrabenzporphyrin), which has a magnetic moment  $\mu_{\text{eff}} = 5.5$  BM at  $23^\circ$ .<sup>42</sup> It is not yet known whether both THF molecules act as ligands, or whether one of the molecules is trapped as a solvent molecule in the crystal structure of the five-coordinate molecule. The stronger field pyridine ligand gives rise to a diamagnetic complex of  $\text{Fe(OTBP)}$ , which strongly indicates six-coordination for this axial ligand.

In this model it is clear why intermediate-spin six-coordinate complexes of Fe are rare. If the ligand field is strong enough to destabilize an orbital to the extent that it is energetically favorable to unoccupy an orbital at the expense of three exchange terms, in almost every case the ligand field in the other direction should be strong enough to push the configuration on the Fe all the way to the s state, since only one more exchange interaction need be overcome. Only complexes that have a very weak ligand field in one direction, such as planar four-coordinate complexes, will give rise to intermediate-spin ( $S = 1$ ) complexes.

## VI. Cooperative Ligand Binding in Hb

The thermodynamics of O<sub>2</sub> binding to Hb is basically defined by the chemistry of the coordination sphere of Fe. The cooperative mechanism arises because the protein can exert small forces on the Fe coordination sphere and thereby change the thermodynamic equilibrium between O<sub>2</sub> and Hb. The basis for understanding the cooperative mechanism of ligand binding is in determining how the small forces exerted on the coordination sphere of Fe by the protein are modified by ligand binding at other Fe sites.

It is now well accepted that Hb has two stable quaternary structures.<sup>56†</sup> One state is referred to as the tense state, or T state, and is the stable quaternary state for deoxy Hb. It has a reduced affinity for binding O<sub>2</sub>. The other quaternary form is the stable form for completely oxygenated Hb, referred to as the relaxed or R form. In the R quaternary form, the  $\Delta G$  for O<sub>2</sub> binding is 3.4 kcal larger than the  $\Delta G$  for O<sub>2</sub> binding in the T quaternary form.<sup>57</sup> This energy difference corresponds to an O<sub>2</sub> affinity for the R form that is  $\sim 400$  times greater than the O<sub>2</sub> affinity for the T form.

The tertiary (three-dimensional) structure of the Hb subunits affects the thermodynamic equilibrium between the R and T forms, and the tertiary structure of the subunits is obviously affected by ligand binding. Using x-ray diffraction studies, Perutz has given a detailed description of the stereochemical changes that take place upon ligand

---

<sup>†</sup> The quaternary structure of Hb is the arrangement of the four amino acid chains, each of which contains an Fe prosthetic group, to form a tetramer of ligand binding sites.

binding.<sup>58</sup> He found, as Hoard had earlier predicted,<sup>59</sup> that a large movement of the Fe atom occurs upon ligand binding and that this movement, coupled through the axial fifth ligand (proximal imidazole) to the protein, could lead to changes in the subunit that would disrupt salt bridges at the subunit interfaces. He then suggested that it is the presence of these salt bridges that stabilizes the T quaternary form of deoxy Hb. Despite this very significant piece of work, there still remains much to learn concerning the microscopic details of the difference in the O<sub>2</sub> affinity for the two quaternary forms.

#### A. Effect of the Protein Forces on the Position of Fe

In the following discussion we will examine the different contributions to the FeO<sub>2</sub> bond energy for Fe in the environment of the porphyrin macrocycle and the axial imidazole ligand. We will then investigate various ways in which the protein environment could perturb one or more of these bonding interactions to determine a rationale for the decreased O<sub>2</sub> affinity of the perturbed Fe environment. We will then consider which structural changes in the protein could lead to such a perturbation.

In order to facilitate the discussion of the energetics of the bonding process, we will separate the process of bonding O<sub>2</sub> to a five-coordinate Fe-porphyrin complex into three distinct steps.

1. Starting with Fe in its optimal geometry for the q state (Fe displaced from the porphyrin plane) and moving the Fe-imidazole group to the point where Fe is in the porphyrin plane will change the energy of the system by

$$\Delta E_q = E_q (\text{Fe in the plane}) - E_q (\text{Fe at equilibrium}). \quad (21)$$

2. With Fe in the plane, the energy difference between the q and t

states is

$$\Delta E_{tq} = E_t (\text{Fe in the plane}) - E_q (\text{Fe in the plane}). \quad (22)$$

3. Given Fe in the t state and in the porphyrin plane, the bond energy for bonding  $^3\text{O}_2$  to the t state of Fe is

$$D_t = E_t (\text{t state of Fe in the plane and } ^3\text{O}_2 \text{ at infinite separation}) \\ - E_t (\text{FeO}_2, \text{ Fe in the plane}). \quad (23)$$

Therefore, the net bond energy for bonding  $^3\text{O}_2$  to the five-coordinate Fe-porphyrin complex is

$$\bar{D} = D_t - \Delta E_{tq} - \Delta E_q. \quad (24)$$

That is, the net bond energy is equal to the Fe (t state) -  $^3\text{O}_2$  bond energy minus the energy necessary to form the planar t state of Fe in the five-coordinate complex.

The difference in the oxygen affinity for structurally distinct states of the hemoglobin molecule must result from one or more of the three energy contributions in (24) being dependent upon the protein structure. These dependencies could arise in a number of ways. For example, these could be steric repulsions between  $\text{O}_2$  and the amino acid side chains lining the cavity on the accessible side of the porphyrin plane. If these groups move into the way of the  $\text{O}_2$  upon a change in the quaternary structure from R to T, the result would be a decrease in  $D_t$  for the T form. There is no strong evidence to indicate that this is true, and we will assume that modification in  $D_t$  is not responsible for the change in  $\text{O}_2$  affinity.

Several effects could cause an increase in  $\Delta E_{tq}$  as the quaternary structure is changed from R to T. For example, an increase in the effective porphyrin hole radius would increase  $\Delta E_{tq}$ . It is also possible that the conjugation of the  $\pi$  system could be modified (i) by changes in the doming of the porphyrin, (ii) by rotation of the propionic or vinyl groups attached to the heme into or out of the porphyrin plane, or (iii) by steric interactions between the porphyrin pi system and amino acid side chains, resulting in a different  $\Delta E_{tq}$ . Nuclear magnetic resonance evidence by Shulman and co-workers argues against significant changes in the porphyrin conjugation<sup>60</sup> and against  $\Delta E_{tq}$  being responsible for different oxygen affinities in structurally distinct forms of Hb.

This leaves changes in  $\Delta E_q$  as the most likely source of decreased  $O_2$  affinity in deoxy Hb. If the protein were to hinder the motion of the proximal imidazole by exerting a force that opposes motion towards the porphyrin plane, a weaker net  $FeO_2$  bond would result. Our calculated potential energy surfaces for movement of the Fe imidazole group in the model five-coordinate Fe-porphyrin complex allows us to estimate the differences in the Fe displacement between the unliganded T and R forms of deoxy Hb. The analysis that follows is similar to one given by Hopfield.<sup>61</sup>

The  $FeO_2$  bond energy reported for Collman's porphyrin-based model oxygen carrier is 15.6 kcal.<sup>62</sup> The corresponding  $\Delta H$  ranges from 13.1-16.4 kcal for various forms of myoglobin obtained from a number of different species.<sup>63</sup> The  $\Delta H$  for human myoglobin is 13.5 kcal, and we will use this value as a typical bond energy for myoglobin. At high partial pressures of  $O_2$ , the oxygen equilibrium curve for Mb

and Hb coincide,<sup>64</sup> indicating an  $O_2$  bond strength for the R quaternary form of deoxy Hb that is identical to deoxy Mb. The difference in the free energy of bonding  $O_2$  to the T and R forms of deoxy Hb is 3.4 kcal.<sup>57</sup> We assume this difference reflects the difference in  $\Delta H$  for the two quaternary forms, and take 10.1 kcal as the bond strength of  $O_2$  to the T state of deoxy Hb.

It is clear that the protein in the T quaternary form acts to hinder the formation of the  $Fe-O_2$  bond. Due to the range of values for the bond strength of  $O_2$  to deoxy Mb, it cannot be said with certainty that the protein also hinders  $FeO_2$  bond formation in deoxy Mb. In the following discussion, we will use the value of 13.5 kcal for the  $MbO_2$  bond strength and view the difference between this bond strength and the value found for the unconstrained model compound to indicate that protein forces also act on the coordination sphere of Fe in deoxy Mb.

Therefore, we assume that there is a constant protein force pulling on the axial fifth ligand for both the R and T forms of Hb. In forming the  $Fe-O_2$  bond, these protein forces must be overcome at the expense of the  $Fe-O_2$  bond strength. In order to explain cooperative ligand binding, either (i) the protein forces acting on the axial ligand must be greater in the T form than in the R form, or (ii) the Fe must move significantly further distances in the T form than in the R form upon ligand binding. Early x-ray evidence obtained by Perutz indicated that (ii) was the more correct explanation for the reduced  $O_2$  affinity of the T form of Hb.<sup>58</sup>

Knowledge of the force constant for movement of the Fe relative to the porphyrin plane for the unconstrained system allows us to calculate the changes in the position of the Fe due to the force exerted on the Fe by the protein through the axial ligand. We find a relatively small distortion occurs in the equilibrium position of the Fe when the quaternary structure changes from the R to the T form, and therefore we believe that larger protein forces are acting on the axial ligand in the T form, reducing its O<sub>2</sub> affinity. Recent higher resolution x-ray data support the idea of small changes in the position of the Fe upon a change in the quaternary structure of Hb,<sup>48, 65</sup> and therefore also support (i) as the better description of the origin of cooperative ligand binding.

The difference in bond energies, together with the equilibrium Fe position for the unconstrained molecule, and the force constant for movement of the Fe perpendicular to the porphyrin plane in the unconstrained molecule determine the shift in the position of the Fe atom due to protein forces. The relationship between these quantities is

$$\Delta(\Delta H) = \frac{1}{2} k[(\chi^p)^2 - (\chi^u)^2] , \quad (25)$$

where  $\chi^p$  is the out-of-plane distance of Fe in the protein and  $\chi^u$  is the corresponding distance for the unconstrained molecule.

From our calculations we find the optimal Fe out-of-plane distance for the five-coordinate q state to be 0.28 Å with  $\Delta E_q = 4.7$  kcal. We calculate a force constant for moving the Fe-imidazole unit toward the porphyrin plane of  $k = 120$  kcal/Å<sup>2</sup>:

$$\begin{aligned}\Delta E_q &= 4.7 \text{ kcal} \\ x &= 0.28 \text{ \AA} \\ k &= 120 \text{ kcal/\AA}^2.\end{aligned}\tag{26}$$

Using these parameters, the difference in  $O_2$  bond energies of 2.1 kcal between the unconstrained molecule and the R state of Hb gives

$$\chi^R = 0.32 \text{ \AA}.$$

Thus the protein pulls Fe 0.04  $\text{\AA}$  further away from the porphyrin plane. This movement is brought about by a protein force ( $F_p$ ) of

$$F_p^R = 4.9 \text{ kcal/\AA}.$$

A protein force of this size moving through 0.45  $\text{\AA}$ \* accounts for the 2.1 kcal of reduced  $FeO_2$  bond strength in the R form of Hb.

In a similar manner we can account for the energy of cooperativity, 3.4 kcal, by having a protein force in the T state of Hb of

$$F_p^T = 12.0 \text{ kcal/\AA},$$

which distorts the Fe out-of-plane distance in the T form of Hb to

$$\chi^T = 0.38 \text{ \AA}.$$

---

\* In this analysis we have also taken into account that the porphyrin plane undomes upon binding the  $O_2$  ligand, resulting in a movement of the Fe of an additional 0.13  $\text{\AA}$ . This is the distance from the plane of the porphyrin nitrogen to the mean heme plane.<sup>48</sup> Ignoring this additional movement of Fe upon  $O_2$  binding would lead to  $\chi^R = 0.34 \text{ \AA}$ ,  $F_p^R = 6.8 \text{ kcal/\AA}$ ,  $\chi^T = 0.41 \text{ \AA}$  and  $F_p^T = 15.9 \text{ kcal/\AA}$ .

The key quantities derived from this model are the protein forces acting on the axial ligand in the T and R forms of Hb. These forces are much smaller than the forces exerted on the Fe by the porphyrin ligand, and as a result, they cause only small distortions in the position of the Fe. These small protein forces have significant effects on  $\text{FeO}_2$  bond energies because they are amplified by the normal movement of the Fe upon  $\text{O}_2$  binding. Operating through distances of 0.4 - 0.5 Å, they give rise to the necessary reductions in  $\text{O}_2$  affinity observed in the protein systems.

This model predicts that a small movement of the Fe takes place upon incorporating the five-coordinate Fe-porphyrin complex in a globular protein, and a further small displacement of Fe takes place when four globular proteins are bound together to form Hb. Our model predicts Fe out-of-plane displacements of 0.28, 0.34, and 0.38 Å for five-coordinate Fe-porphyrin, the R form of deoxy Hb, and the T form of deoxy Hb, respectively. If the full porphyrin had been included in the calculations, we would expect slightly larger nonbonded repulsions due to the pyrrole carbons; and therefore we expect that our predicted Fe out-of-plane positions will be systematically too small. 2.0 Å resolution x-ray studies of deoxymyoglobin indicate an Fe out-of-plane distance of 0.42 Å.<sup>48</sup> For deoxy Hb, 2.5 Å resolution x-ray studies give an Fe displacement of 0.42 Å for the  $\alpha$  subunit, and 0.49 Å for the  $\beta$  subunit.<sup>65</sup> These distances are measured relative to the plane formed by the four pyrrole nitrogens of the porphyrin ring. From these studies we see that experiment and theory both indicate a very small movement of the Fe upon a change in quaternary structure. The estimated

positional error for Fe in the deoxy Hb structure is 0.1 Å, and our theoretical value lies within this range of Fe out-of-plane distances. As mentioned before in Sec. IV, the structural parameters for an unconstrained Fe-porphyrin complex of imidazole have not yet been obtained. The 2-methylimidazole complex leads to an Fe out-of-plane displacement of 0.42 Å, but this molecule has short contacts between the methyl group and the porphyrin ligand that could lead to an Fe out-of-plane displacement larger than that expected for an unhindered imidazole ligand.

#### B. Origin of the Protein Forces

The obvious extension of these ideas is to determine the origin of the protein forces acting on the axial ligand, and to discover how changes in quaternary structure can modify these protein forces. From our calculations we find the protein force increases from  $\sim 5$  kcal/Å in the R form to  $\sim 12$  kcal/Å in the T form. Thus, in order to prove the model for the cooperative ligand binding effect given here, interactions in the protein that cause an increased pull on the proximal imidazole equal to a force of  $\sim 7$  kcal/Å must be located for the T form of Hb.

The structure of a hemoglobin subunit is shown in Fig. 16.<sup>66</sup> This diagram emphasizes the arrangement of the helical regions of the molecule in relation to the heme plane. The heme plane is shown lying between the E and F helices and the proximal imidazole (axial fifth ligand) is labeled F8. The interactions that restrict the movement of the F, FG, and upper G regions of the molecule will most directly affect the movement of the proximal imidazole. In this subsection we will review the structures of the R and T forms for both the  $\alpha$  and  $\beta$

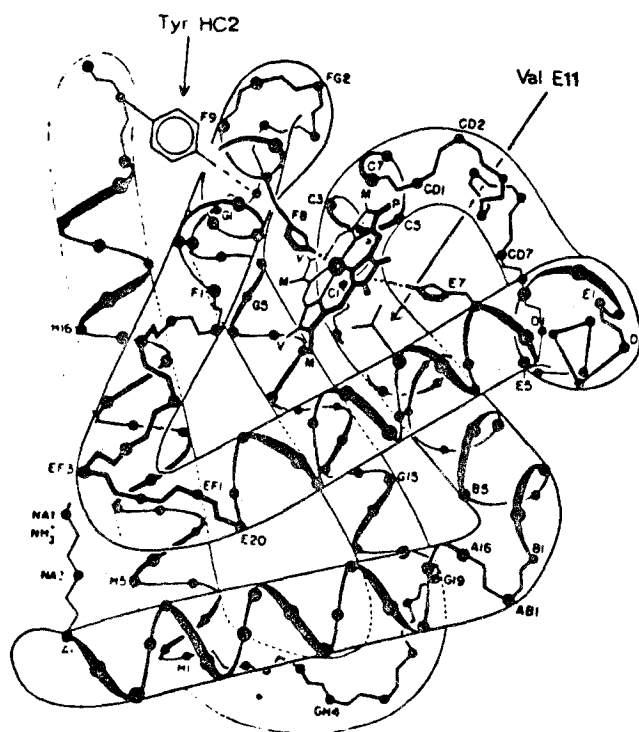


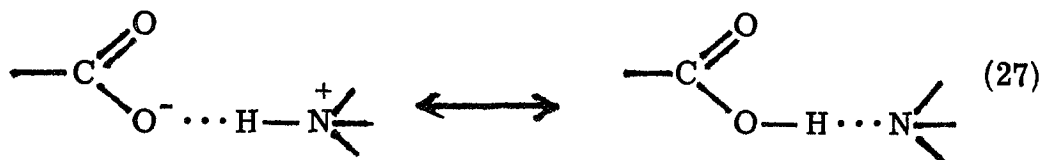
**Figure 16.** The helical structure of the  $\beta$  subunit of Hb.

subunits in these regions of the molecule to determine what interactions might affect the motion of the proximal imidazole.

Three types of interactions occur between the amino acid units of a protein; hydrogen bonds, salt bridges, and van der Waals interactions. Van der Waals interactions are weak and directionally nonspecific and in most circumstances cannot give rise to protein forces of the magnitude and specificity necessary to explain allosteric effects. Therefore we do not consider them here.

The bonding interaction of a hydrogen bond and a salt bridge are similar in nature. A salt bridge is formed by two oppositely charged molecular groups through electrostatic interactions. These charged groups can either be amino acid side chains or the charged terminal group of main polypeptide chains. There is some ambiguity in the

position of the hydrogen atom in a salt bridge.



In the case where the proton is forced to remain attached to the acidic group [the right side of (27)], the bonding interaction of the salt bridge corresponds to a hydrogen bond. Since relaxing the position of the proton can only lead to a stronger interaction, the bond strength of a salt bridge is seen to be at least as large as the bond strength of a hydrogen bond. As a typical example, the bond strength of a linear hydrogen bond in water is shown as a function of the O-O separation<sup>67</sup> in Fig. 17. From this potential energy surface we see that if the

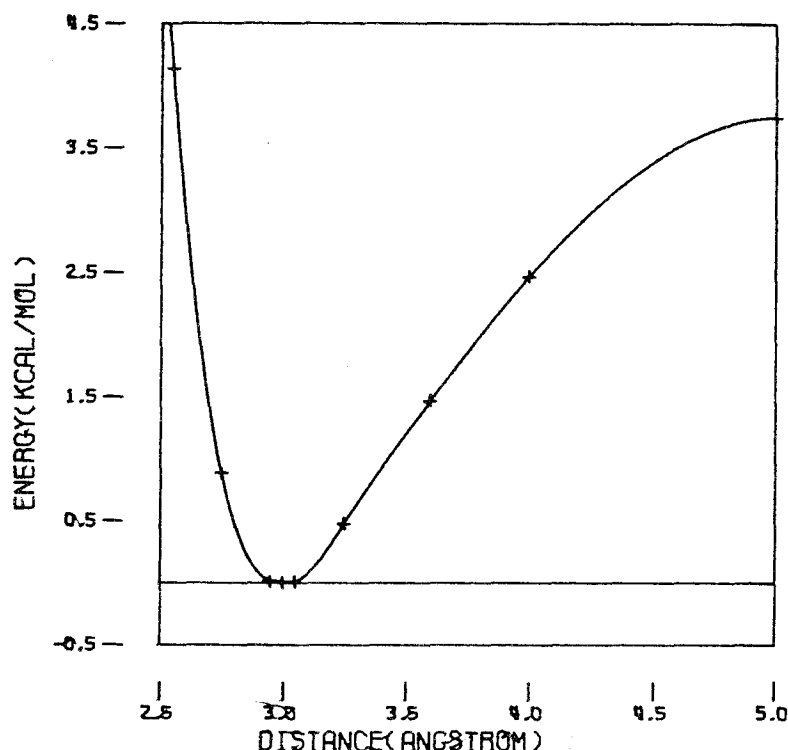


Figure 17. The bond strength of a linear hydrogen bond in water as a function of the O-O separation.

hydrogen bond is stretched  $\sim 0.55 \text{ \AA}$  at its steepest point, the hydrogen bond strength will be reduced by  $\sim 1.5 \text{ kcal}$ .

Perutz and co-workers have given a stereochemical description of the differences in the structure between the R and T forms of Hb. In the T form of Hb there is an intra subunit hydrogen bond between the penultimate tyrosine (HC2) and the main chain carbonyl group of valine FG(5). In the  $\beta$  subunits, a salt bridge between the imidazole of histidine HC3 (146) and aspartate FG1 (94) is seen to occur. Neither of these interactions is found in the R form, where both HC2 and HC3 are accessible to the solvent.<sup>58</sup> Both of these interactions cause a link between the H helix and the FG region of the  $\alpha$  and  $\beta$  subunits. If the main chain of the subunits is rigid in the F and FG regions, movement of the proximal imidazole by  $0.55 \text{ \AA}$  would stretch this hydrogen bond and this salt bridge by a similar amount.\*

This movement would require  $\sim 3 \text{ kcal}$  loss of energy in these two interactions, and thus this movement can account for most of the reduction of the  $\text{O}_2$  bond strength in the  $\beta$  subunits. In the  $\alpha$  subunit, where the corresponding salt bridge does not form, an  $\text{O}_2$  bond energy  $\sim 1.5 \text{ kcal}$  larger would be expected to result from hindered motion of the proximal imidazole due to interactions between residues of the H helix and the FG region.

In Hb there is a large number of intermolecular contacts at the  $\alpha_1\beta_1$  and  $\alpha_2\beta_2$  interfaces that remain essentially unchanged as the Hb molecule changes quaternary forms. However, at the  $\alpha_1\beta_2$  interface, large

---

\* The H helix appears to be securely anchored by other salt bridges.<sup>58</sup>

changes in structure do occur upon a change in the quaternary structure, with relative shifts of up to 7 Å between the two subunits.<sup>58</sup>

The structure of the  $\alpha_1\beta_2$  interface is shown in Fig. 18.<sup>68</sup> The

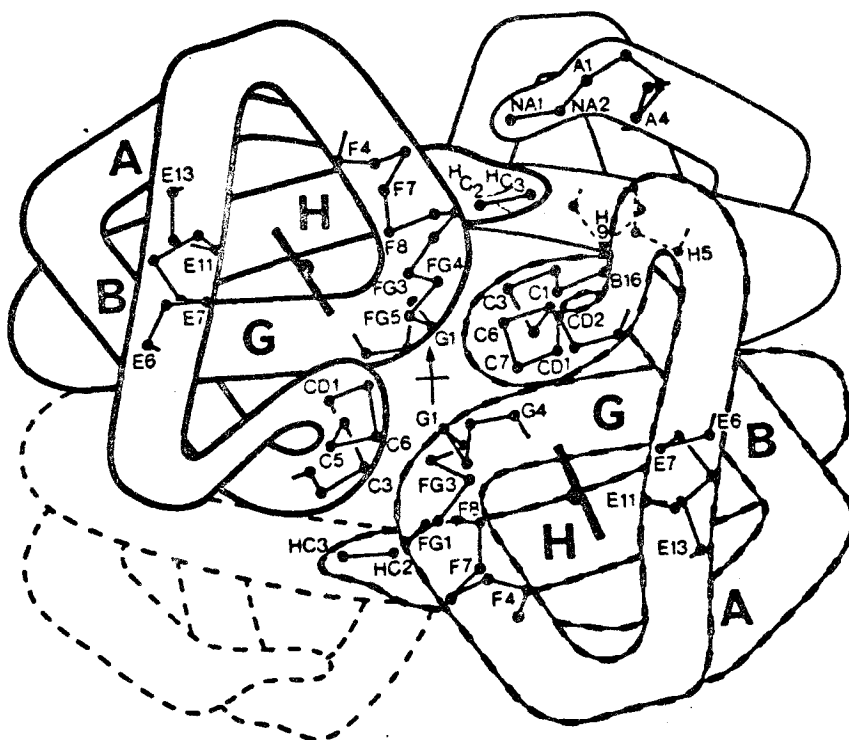


**Figure 18.** The structure of the  $\alpha_1\beta_2$  interface in Hb. The heavy solid line shows the folding of the  $\alpha$  chain, and the heavy broken line shows the folding of the  $\beta$  chain.

FG and G regions of the subunits are involved in the contacts at the  $\alpha_1\beta_2$  interface, and this suggests the possibility that the structure at this interface could affect the movement of the proximal imidazole. X-ray studies indicate that the number of hydrogen bonds (two) at this interface remains the same upon a change in quaternary structure of Hb, although the hydrogen bonds are broken and reformed between different amino acid side chains.<sup>69</sup> It appears that only one of these four different

hydrogen bonds could affect the movement of the proximal imidazole to any substantial degree. In the R form, a hydrogen bond between G1 (94)  $\alpha_1$  and G4 (102)  $\beta_2$  is formed, which tends to pull the FG region closer to the heme plane in both the  $\alpha$  and  $\beta$  subunits, thus making the Fe-O<sub>2</sub> bond easier to form. No large change in the strength of this hydrogen bond is needed upon O<sub>2</sub> bond formation, since it is not present in the T quaternary form. Its presence merely has to modify the protein forces tending to pull the F helix away from the heme plane to the extent that it decreases the energy required to pull the proximal imidazole towards the heme plane upon O<sub>2</sub> binding by  $\sim 1$  kcal.

Summarizing the effects of the different quaternary structures on the movement of the proximal imidazole, we find that for the  $\alpha$  subunit the tyrosine hydrogen bond present in the T form and the different hydrogen bonding present at the subunit interface in the R form can account for a difference in  $\Delta E_q$  of 2.5 kcal between the two quaternary forms, the energy being greater for the T form. In the  $\beta$  subunit,  $\Delta E_q$  is further increased to 4 kcal by the presence of the intrasubunit salt bridge.

This model predicts different O<sub>2</sub> bond strengths for the  $\alpha$  and  $\beta$  subunits of Hb. Gibson has given evidence obtained from kinetic studies of O<sub>2</sub> binding that the  $\alpha$  and  $\beta$  chains do not interact identically with O<sub>2</sub>.<sup>70</sup> He has found that O<sub>2</sub> dissociates from the  $\beta$  subunit in HbO<sub>4</sub> 16 times faster than from the  $\alpha$  subunit. Since we do not expect any activation barrier upon O<sub>2</sub> bond formation, this difference corresponds to an FeO<sub>2</sub> bond strength that is 1.7 kcal weaker for the  $\beta$  subunit, a value very similar to the difference predicted by our model.

This model also leads to a prediction of a larger Fe out-of-plane displacement for the  $\beta$  subunit as compared with the  $\alpha$  subunit in deoxy Hb, due to the increased pull on the proximal imidazole caused by the intrasubunit salt bridge. X-ray studies at 2.5 Å resolution indicate that the Fe lies 0.07 Å farther away from the porphyrin nitrogen plane in the  $\beta$  subunit as compared with the  $\alpha$  subunit, although this separation is within the possible errors of the Fe position.<sup>65</sup> A similar situation is found in the x-ray structure of horse Met Hb.<sup>71</sup> Here the Fe out-of-plane distances are 0.07 Å for the  $\alpha$  subunit and 0.21 Å for the  $\beta$  subunit. Neutron diffraction studies of COMb also support the idea that protein forces exist in the R form of Hb. In COMb the Fe is found to lie 0.1 Å out-of-plane towards the proximal imidazole.<sup>51</sup> In a model five-coordinate Fe-porphyrin CO complex, the CO lies 0.02 Å out-of-plane towards the CO side.<sup>50</sup>

In deriving the results of this model, we made two key assumptions; that of a constant protein force, and that of rigid F and FG regions of the protein molecule. The first assumption appears to a very good approximation to the real protein forces encountered. We see from Fig. 17 that the shape of the potential energy surface for stretching a hydrogen bond is nearly linear throughout most of the hydrogen bond separation distances. The second assumption is more critical, but x-ray studies indicate that the F helix and the FG region move as rigid units.<sup>48</sup> In comparing the relative positions of the F helix and the heme plane for met Mb and deoxy Mb, a movement of the F helix away from the heme plane and towards the EF corner is seen to occur as the molecule changes from the met to the deoxy form. The

entire F helix moves and pulls the FG region closer to the heme plane. The shift is absorbed at the junction with helix G and fades out after the first few residues. The shift of the proximal imidazole was estimated to be  $0.1 \text{ \AA}$ , and the overall shift of the main chain and  $C(\beta)$  atoms of the F helix was estimated to be  $0.15 \text{ \AA}$ . Thus, at least for small movements of the proximal imidazole, the F helix and FG regions appear to move as rigid units.

In our model we assumed the F helix and the FG region were rigid, resulting in an increased separation of  $0.55 \text{ \AA}$  between the F and H helices due to  $O_2$  bond formation. This result cannot be tested directly because of the difficulty of doing the crystal structure of  $HbO_2$ . However, similar movements between the F and H helices should occur on CO bond formation to Hb. This crystal structure has been carried out at 2.8 resolution,<sup>72</sup> but a comparison of the distances between the F and H helices for different Hb molecules has not yet been done.

The movement of the F helix upon going from met Mb to deoxy Mb has also been compared with the corresponding movements in met Hb and deoxy Hb.<sup>48</sup> These comparisons show that the movement of the F helix is in the same direction in both Mb and Hb, but that the movements are larger in Hb. This is another experimental indication of stronger protein forces pulling on the proximal imidazole in the T form of Hb. The movements are about twice as large in the  $\beta$  subunit as in the  $\alpha$  subunit, correlating with the increased protein force our model predicts for the  $\beta$  subunit.

### C. Molecular Description of Cooperativity

From the above ideas, we propose a molecular description of the cooperative binding of O<sub>2</sub> to Hb that is similar in many respects to the description given by Perutz.<sup>58</sup>

When a ligand binds to deoxy Hb, movement of the proximal imidazole stretches the intrasubunit hydrogen bonds and salt bridges occurring between the H helix and the FG region of the subunits. In the  $\alpha$  subunit only one hydrogen bond is stretched, resulting in a stronger FeO<sub>2</sub> bond in this subunit. In the  $\beta$  subunit, both a hydrogen bond and a salt bridge connect the FG region and the H helix. The groups that form intrasubunit hydrogen bonds and salt bridges are closely coupled to the amino acids that form salt bridges between subunits. These charged groups are accessible to the solvent and an equilibrium exists between solvating these groups or making specific hydrogen bonds and salt bridges with other parts of the protein molecule. Upon liganded binding, the intrasubunit bonds are stretched to the point that the equilibrium now lies towards solvating these side chains, leading to the disruption of the intersubunit salt bridges. As the salt bridges between subunits are broken, the bonding interactions holding the  $\alpha_1\beta_2$  interface in an energetically metastable state are lessened, and at some point the  $\alpha_1\beta_2$  interface moves to its more stable configuration. Upon this change in quaternary structure from the T form to the R form, a different hydrogen bond is formed at the  $\alpha_1\beta_2$  interface that makes it  $\sim 1$  kcal easier to pull the proximal imidazole toward the heme plane upon ligand binding. Also, the change in quaternary structure disrupts the remaining salt bridges formed between subunits. This perturbs the equilibrium between the remaining

protein-bound intrasubunit hydrogen bonds and salt bridges and their solvated forms such that the intrasubunit interactions are broken and replaced by larger solvation energies. When this happens, the proximal imidazole is much less constrained by protein forces, and the O<sub>2</sub> binds more strongly to the remaining unbound subunits.

This model suggests that the Fe-O<sub>2</sub> bond strength in the R form of Hb and in deoxy Mb may not be the same. In the R form of Hb, a hydrogen bond at the  $\alpha_1\beta_2$  interface is promoting the O<sub>2</sub> bonding reaction. This could lead to an Fe-O<sub>2</sub> bond strength that is larger in the R form of Hb than in Mb. Since these two bond strengths do not appear to be greatly different, other contacts at the  $\alpha_1\beta_2$  interface must be working against FeO<sub>2</sub> bond formation, and the two interactions tend to balance each other in the R form of Hb.

There are ways that these ideas can be tested directly. Kinetic experiments similar to those performed by Gibson<sup>70</sup> on a mutant hemoglobin in which the histidine HC3 (146)  $\beta$  residue has been removed enzymatically should eliminate the heterogeneity observed between the  $\alpha$  and  $\beta$  subunits with respect to O<sub>2</sub> binding. Measurement of the changes in the distance between the F and H helices for a number of different Hb complexes would test one of the key predictions of this model. The O<sub>2</sub> binding reaction could be carried out in nonprotic solvents that would tend to disrupt the equilibrium between the intramolecular hydrogen bonds and salt bridges and the solvation of these groups. According to our model the Hb molecule should exhibit very little cooperativity in a nonprotic solvent.

#### D. Other Models of Cooperative Binding

Perutz has given a stereochemical model of cooperative ligand binding that is the basis for the model presented here. He was the first to suggest that salt bridges between subunits stabilized the T quaternary structure.<sup>58</sup> He proposed that these salt bridges are broken upon binding O<sub>2</sub>. When enough salt bridges have been broken, the Hb molecule undergoes a change in quaternary structure, severing the remaining salt bridges occurring between subunits, causing O<sub>2</sub> to bind more easily. In his model, the tertiary changes brought about by ligand binding cause a narrowing of the tyrosine pocket and subsequent expulsion of the penultimate tyrosine. As the tyrosine moves away from the FG region, it disrupts the intersubunit salt bridge formed by its neighboring amino acid and thereby destabilizes the T form. We have incorporated Perutz's description of the quaternary change in Hb with minor modifications in the number of intersubunit salt bridges being involved in the quaternary transition.<sup>†</sup> We have given a different interpretation to the tertiary structural changes in the F and FG regions upon O<sub>2</sub> binding, and have shown how these structural changes can be brought about by FeO<sub>2</sub> bond formation.

---

<sup>†</sup> Originally, Perutz believed that six salt bridges were formed between subunits,<sup>58</sup> but later high resolution studies indicate that the salt bridge between the alpha amino group of Val NA1 (1)  $\alpha_1$  and the alpha carboxyl group of Arg HC3 (141)  $\alpha_2$  does not form directly. It was suggested that this linkage is still preserved through solvent mediation.<sup>65</sup>

Hopfield has discussed a model in which the protein force is caused by small amounts of strain in a large number of bond lengths and bond angles, which he has termed the "distributed energy model".<sup>61</sup> This strain is due to forces occurring at subunit interfaces that are propagated throughout the protein chain. The key point of this model is that it predicts a linear relationship between the free energy stored in the protein and the displacement of the Fe. In our model, where the free energy is stored in a small number of bonds, the same relationship exists due to the nature of the interaction between hydrogen bonded species.

In the distributed energy model, small changes in structure should occur throughout the protein on changing quaternary forms. Since this is not the case, the distributed energy model does not appear to be the best extreme for describing the cooperative binding effect.

Another theory about the origin of the protein forces that modify the chemistry of the coordination sphere of Fe states that movement of the heme plane upon ligand binding initiates interactions between subunits. This theory has received support from many sources.<sup>73-76</sup> In this model of cooperative interactions, as the ligand binds, the porphyrin plane becomes noticeably more planar, with the peripheral heme atoms moving  $\sim 1 \text{ \AA}$ . This movement causes stress at the contacts between the heme plane and the protein, which is then transmitted to the  $\alpha_1\beta_2$  subunit interface. Gelin and Karplus have used empirical energy functions to calculate tertiary changes induced by strained heme-protein contacts upon ligand binding.<sup>76</sup> From their calculations, they find that the strained heme-protein interactions are initiated by the imidazole moving towards

the heme plane. As the  $O_2$  bond forms, the porphyrin plane undomes and the distance between the imidazole ligand and the porphyrin plane is decreased. Since the proximal imidazole is asymmetrically coordinated to the Fe-porphyrin, these two effects cause the axial imidazole to exert a torque on the porphyrin plane due to nonbonded repulsion with the porphyrin nitrogen atoms. As the porphyrin plane tilts, nonbonded interactions between the pyrrole groups of the porphyrin ring and amino acid side chains in close contact with the porphyrin plane cause a readjustment in the tertiary structure of the protein. These readjustments are localized mainly in the FG region of the protein. Also, some rearrangements of the residues in the C helix occur. They conclude that this change in the tertiary structure of a subunit remaining in the T quaternary form is a strained situation, and leads to a reduced oxygen affinity.

In order for the oxygen bond strength to be different between the T and the R forms in this model, the tilt of the porphyrin plane must be easier to accomplish in the R state. This could happen if the interunit salt bridges and hydrogen bonds occurring between the FG region and C helices are reduced in the R quaternary form. Gelin and Karplus have not yet discussed how these changes in the tertiary structure affect the equilibrium between the T and R quaternary forms. Our main reservation about the tertiary changes discussed in this model is that the rigidity of the heme plane does not appear strong enough to induce the tertiary structure changes found from the x-ray studies. Gelin and Karplus have calculated that only a very small amount of energy is lost upon undoming the heme plane in the five-coordinate complex. Because of this fact, it

seems reasonable to assume that only a small amount of energy is gained by keeping the porphyrin plane rigid in the six-coordinate complexes, and that strong nonbonded repulsive contacts between the porphyrin and the protein could be effectively absorbed by doming the heme plane. If this is the case, the structural changes that do indicate a tilting of the porphyrin plane can be explained if the tertiary structural changes that occur upon movement of the proximal imidazole allow the porphyrin plane to tilt. That is, the movement of the porphyrin plane follows the change in tertiary structure rather than forcing it.

The calculations performed by Gelin and Karplus concerning the motion of the penultimate tyrosine and the FG region of the molecule support our interpretation of the tertiary changes induced by ligand binding. They find that the FG region moves away from the penultimate tyrosine. Thus the change in tertiary structure tends to weaken the hydrogen bond between the penultimate tyrosine and valine FG5(73), rather than expelling the tyrosine by closing up the pocket between the F and H helices, as suggested by Perutz.<sup>58</sup> These calculations are in agreement with a similar motion deduced from an x-ray crystal structure of liganded Hb forced to remain in the T quaternary form.<sup>74</sup>

#### E. Qualifying Remarks

We have shown that much of what is known about the cooperative mechanism of ligand binding in Hb is consistent with the idea that protein forces restrict the movement of the proximal histidine. This analysis does not exclude the possibility that other forms of protein interactions may be important in controlling oxygen binding. In particular, Perutz has shown that the cavity above the heme plane is smaller in the

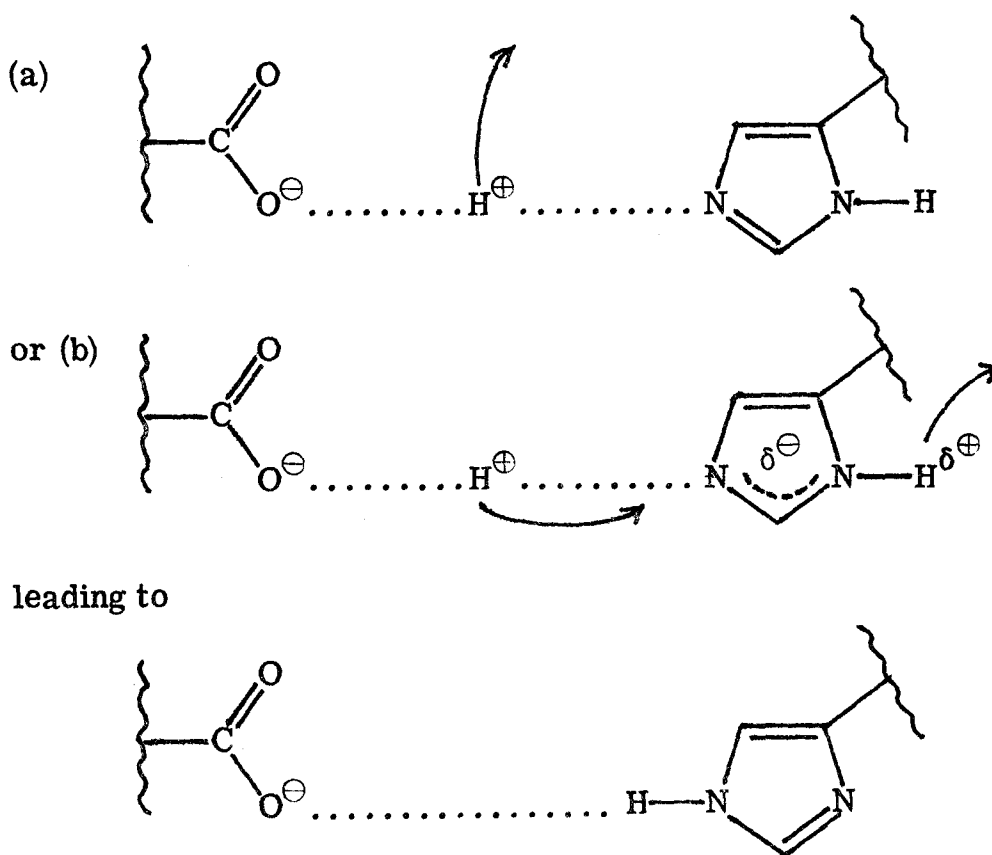
unliganded  $\beta$  subunits than in the unliganded  $\alpha$  subunits, and that upon a change in quaternary structure, the cavity widens in the  $\beta$  subunit.<sup>58</sup> Thus, steric interactions between the  $O_2$  ligand and the residues lining the heme cavity could reduce the  $O_2$  bond strength in the  $\beta$  subunit, and provide a means of cooperative interaction through changes in the quaternary structure of Hb. Contradictory evidence concerning the ability of  $\alpha$  subunits to bind ligands more readily than  $\beta$  subunits was presented by Gibson.<sup>129</sup> He found that n-butyl isocyanide, a much bulkier ligand than  $O_2$ , binds more readily to  $\beta$  subunits than to  $\alpha$  subunits.<sup>129</sup> Support for the idea that ligands have a preference for  $\alpha$  subunits was found by Huestis and Raftery from  $^{19}F$  NMR data on a fluorinated derivative of Hb.<sup>130</sup> The model presented above also indicates a thermodynamic preference for  $\alpha$  subunit ligation, but this preference is independent of any steric interactions between the  $O_2$  ligand and the protein residues.

Huestis and Raftery have also found a pH-dependent process in their fluorinated derivatives of deoxyHb which they attribute to deprotonation of histidine HC3(146) in the  $\beta$  subunit.<sup>131,132</sup> Since this residue is thought to form an intrasubunit salt bridge in deoxyHb that is broken upon a change in quaternary structure<sup>58</sup> (a result incorporated into our model), the invariance of the Hill coefficient through pH 6.0-9.0 has led to the suggestion that this salt bridge may not be a major factor in the stabilization of the deoxy form of Hb.<sup>132</sup>

We suggest two lines of experimental work that might further define the role of  $\beta$  histidine HC3. As discussed later with regard to CoHb, the Hill coefficient is not always sensitive to changes in the bond

strength of  $O_2$ . The scatter of the data for the Hill coefficient measured as a function of pH (2.7-3.4)<sup>132</sup> may be too large to exclude the possibility of a pH-dependence on the  $O_2$  bond energy. Determining the free energy of cooperativity as a function of pH would be a more sensitive test. Secondly, there is the possibility that the deprotonation observed by Huestis and Raftery may not lead to total disruption of the salt bridge involving histidine HC3 (146) $\beta$ . The two groups involved in the salt bridge have two possible titratable hydrogens. The interaction between these two groups must be considered in describing the titration process, as this interaction strongly affects the electronic structure of the titratable species.

Two possible ionization processes could be as depicted below:

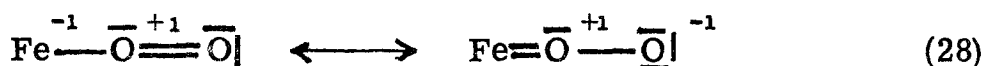


In process (b), an interaction still remains between the negative charge on the carboxyl group and the hydrogen now attached to the neutral imidazole group. Although this interaction is probably not as strong as that found in a normal salt bridge, the energy gained in solvating the end products of process (b) is also less than that gained in solvating a normal salt bridge, due to the neutral character of the imidazole group. Because of the reduced solvation energy, the hydrogen bonding interaction between the carboxyl group and the imidazole hydrogen in process (b) could dominate the equilibrium between the solvated and unsolvated species, leading to stabilization of the T quaternary form of Hb at high pH.

The ionization process suggested in (b) does permit a rationalization of the experimental results found by Huestis and Raftery. Further experimental and theoretical work is needed to test this interpretation.

## VII. Previous Models of the Electronic Structure of Oxyhemoglobin

There have been several formulations of the electronic structure of the Fe-O<sub>2</sub> bond. Pauling and Coryell were the first to suggest a description of the electronic structure of FeO<sub>2</sub> after they discovered the surprising fact that paramagnetic oxygen bound to paramagnetic hemoglobin gave a diamagnetic state of HbO<sub>2</sub>.<sup>33</sup> This spin-pairing of the reactant molecules has always been the dominant feature that any formulation of the electronic structure of HbO<sub>2</sub> must explain. Pauling and Coryell suggested the resonance forms for a linear Fe-O<sub>2</sub> bond shown in (28).

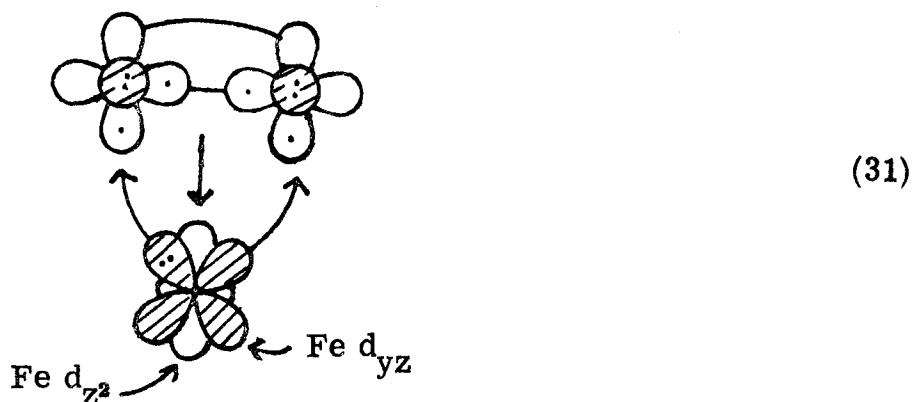
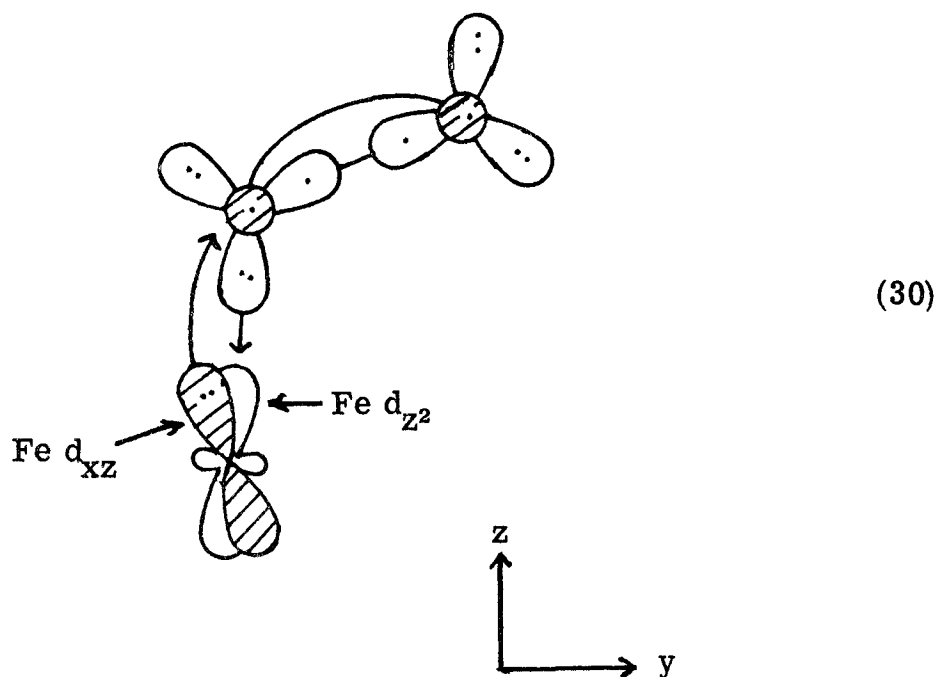


Pauling later suggested the bent end-on form of (29).<sup>77</sup>



He did not discuss the electronic structure of FeO<sub>2</sub> in terms of specific orbital occupations, but stated that in order to preserve charge neutrality on the Fe, a double bond is formed between Fe and O<sub>2</sub> in which two of the electrons involved in the bond originate on the Fe and two electrons originally belong to O<sub>2</sub>. Although the latter description qualitatively predicts the geometry of the FeO<sub>2</sub> moiety, it leads to unfavorable charge separation on the O<sub>2</sub> ligand.

In 1956, Griffith proposed the two structures shown in (30) and (31).<sup>78</sup>

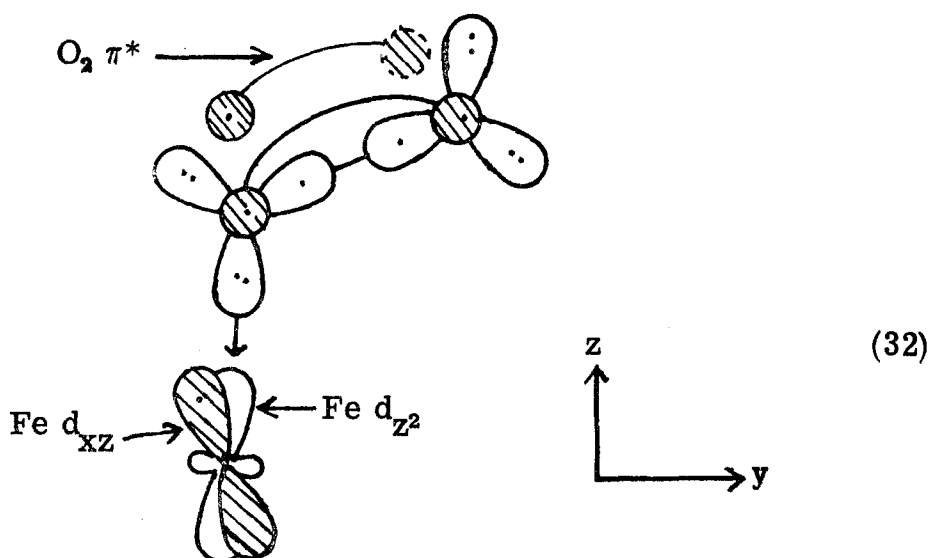


The crosshatched orbitals represent the  $t_{2g}$  orbitals of Fe and the  $O_2$   $\pi$  orbitals. The arrows indicate delocalization of occupied orbitals into unoccupied spaces. In the case of the Fe  $t_{2g}$  orbitals delocalizing onto the  $O_2$  ligand, the unoccupied spaces are the  $\pi^*$  orbitals of  $O_2$  that are not explicitly shown.

Griffith explained the bent end-on structure of Pauling (30) as arising from an  $sp^2$  hybrid orbital of  $O_2$  forming a dative bond to the  $t_{2g}^6$  state of Fe, with possible Fe d- $\pi$  back bonding to  $O_2$ . He also suggested

the perpendicular geometry (31) in which an  $O_2$   $\pi$  orbital makes a dative bond into the empty  $e_g$  space of Fe, and a  $t_{2g}$  doubly-occupied orbital donates electron density back into the  $\pi^*$  orbital of  $O_2$  lying in the  $FeO_2$  plane. From estimates of the ionization potential of the differently bound dioxygen molecules, he predicted structure (31) to be the ground state of  $FeO_2$ . A recent experimental determination of the geometry of  $FeO_2$ <sup>23</sup> indicates that structure (31) cannot correspond to the ground state of the system. In both (30) and (31), an excited singlet state of  $O_2$  is bonding to an excited singlet state of Fe (s state). There is no experimental evidence to indicate that either Hb or  $O_2$  is activated before the reaction occurs. Thus the reaction between ground state Hb and ground state  $O_2$  would involve a large energy of activation. This is not consistent with the fast, reversible nature of the reaction. Also, these formulations indicate that the properties arising from the electron structure of Fe, such as the Mössbauer effect and the electronic excitation spectrum, should be similar in the  $O_2$  and CO complexes, since Fe would be in the s state for both complexes. This is not the case, as discussed in Sec. VI, and thus both experimental and theoretical arguments indicate that neither (30) nor (31) is the proper description for the ground state of  $FeO_2$ .

The next structure to be suggested was that of Weiss (32),<sup>79</sup> where he describes the Fe as being in a ferric Fe(III)  $d^5$  electronic configuration, with  $O_2$  being bound as  $O_2^-$ , the superoxide anion. This corresponds to structure (30) where an Fe  $t_{2g}$  electron has been transferred completely to the  $\pi^*$  space of  $O_2$ . This  $\pi^*$  orbital is shown in (32) with the antibonding  $\pi^*$  character being indicated by a solid circle joined to a broken



circle. The unpaired electrons on the Fe(III) and the  $\text{O}_2^-$  ligand are assumed to be spin-paired to give the diamagnetic state of  $\text{FeO}_2$ . Weiss was led to this conclusion because the electronic absorption spectra of  $\text{HbO}_2$  resemble the spectra of the hydroxide adduct of Hb, and the heme-linked acid dissociation constants of  $\text{HbO}_2$  are more similar to metHb than deoxyHb.

The Weiss model and the ozone model of the  $\text{FeO}_2$  bond are similar in many respects. If charge separation is neutralized in the Weiss model by making the  $\text{sp}^2$  hybrid orbital on the center oxygen a covalent bond by delocalizing an electron into the  $\text{Fe } d_{z^2}$  orbital, both models become qualitatively the same. Our model gives an explicit description of the occupation of the  $\text{O}_2 \pi$  orbitals, whereas the Weiss model states that the electron giving rise to the  $\text{O}_2^-$  anion resides in the  $\pi^*$  orbital of  $\text{O}_2$ , but the character of this orbital is not explicitly indicated. The real difference between the two models is the amount of charge transferred onto the  $\text{O}_2$  ligand. Our calculations indicate only very small amounts of electron transfer ( $\sim 0.1$  a.u.), whereas the Weiss

model has been applied to other transition metal-O<sub>2</sub> complexes where almost a full electron is transferred onto the O<sub>2</sub> ligand.<sup>80</sup> At present, there are no experimental data that clearly indicate the amount of charge transfer in FeO<sub>2</sub> complexes. In the following section we will show how taking the Weiss model too literally will lead to erroneous conclusions about transition metal-O<sub>2</sub> complexes, and how using the ozone model can lead to a qualitatively consistent description of these molecules. Note that delocalization from the formal Weiss model must be in the  $\sigma$  system to obtain a structure similar to the ozone model. If charge neutralization occurs in the  $\pi$  system, the structure returns to one similar to Griffith's bent geometry model (30) and retains all the unfavorable characteristics of that description, as discussed above.

More recently, from studies on hemerythrin, Gray proposed an oxidative addition model of O<sub>2</sub> bonding to Hb,<sup>81</sup> as shown in (33),



In this model, a d<sup>4</sup> low-spin state of iron binds a formally peroxo ligand in a cyclic (possibly asymmetric) seven-coordinate geometry. This model has even higher amounts of formal charge separation than the Weiss model. It predicts an O-O stretching frequency similar to peroxo ligands ( $\sim 900 \text{ cm}^{-1}$ ), which is contrary to experimental evidence.<sup>28</sup>

Apparently McClure was the first to suggest that the FeO<sub>2</sub> bond in Hb should be formed with O<sub>2</sub> remaining essentially in its triplet ground state.<sup>82</sup> He indicated that the observed diamagnetic character of the complex could then be obtained by promoting deoxyHb to an excited

triplet state and coupling the triplet state of  $O_2$  with the triplet state of deoxyHb to give an overall singlet state. This idea was discussed in more detail by Harcourt in his formulation of the increased valence model of the  $FeO_2$  bond (34).<sup>83</sup>



In this idealized structure, two electrons on the Fe are spin-paired with two electrons on the closest oxygen, the remaining electron already having been spin-paired in the ground state of  $O_2$ . This model leads to charge separation in the  $O_2$  ligand concurrent with forming the  $Fe-O_2$  bond, due to orthogonality constraints between the electrons on the Fe involved in the  $Fe-O_2$  bond and the electrons forming the one-electron bonds in  $O_2$  (see Ref. 83). It does not have the problem of requiring a drastic change in the character of  $O_2$  upon bond formation encountered by all the earlier proposed models of the electronic structure of  $FeO_2$ .

## VIII. Bonding of O<sub>2</sub> to Other Transition Metal Complexes

Monomeric O<sub>2</sub> complexes are known to exist for porphyrin complexes of titanium (Ti),<sup>84</sup> chromium (Cr),<sup>85</sup> manganese (Mn),<sup>86</sup> iron (Fe),<sup>8,9</sup> and cobalt (Co).<sup>87,88</sup> Studies on these metal-O<sub>2</sub> complexes, particularly Fe and Co complexes, have been used to investigate the nature of reversible O<sub>2</sub> binding. In this section the work carried out on Co complexes will be discussed first. Following this discussion, various experiments performed on the other transition metal-O<sub>2</sub> complexes that pertain to the nature of O<sub>2</sub> bonding will be reviewed. In the last part of this section, a qualitative description of the energetics of high-spin transition metal-O<sub>2</sub> complexes is presented.

### A. CoO<sub>2</sub> Complexes

Co has an s<sup>2</sup>d<sup>7</sup> configuration. The ground state of Co is a quartet state with three unpaired d electrons. The lowest lying doublet state is ~ 46 kcal above the ground quartet state.<sup>10</sup> Two exchange terms are lost upon pairing up an electron in the quartet state, leading to an exchange term > 23 kcal. This is slightly larger than the 22 kcal exchange term found in Fe. Since the antibonding character of the d<sub>x<sup>2</sup>-y<sup>2</sup></sub> orbital of Co is expected to be similar to that found for Fe (> 40 kcal), Co-porphyrin complexes will have a strong tendency to be low-spin for small to moderately large porphyrin hole radii. Thus the ground state of Co-porphyrin will be a doublet state with a low-lying quartet excited state. The doublet configuration, which is important for discussing the bonding of O<sub>2</sub>, is

$$(d_{xy})^2(d_{xz})^2(d_{yz})^2(d_{z^2})^1. \quad (35)$$

This state is reached by adding an electron to the  $d_{xz}$  orbital of the t state of Fe. In this configuration the  $d_{z^2}$  orbital is still available to make a covalent bond with a 2p orbital of oxygen, but there is no longer a singly-occupied metal orbital to pair up with the  $\pi$  system of  $O_2$ .

Thus, a singly-occupied orbital in the  $\pi$  system of  $O_2$  will remain unpaired after  $O_2$  has bound to a five-coordinate Co-porphyrin complex. The ozone model for  $CoO_2$  predicts unpaired spin density on the  $O_2$  ligand without any charge separation occurring in the molecule. This unpaired electron has been detected in an EPR experiment and shown to have 90% of its spin density located on the  $O_2$  ligand.<sup>87</sup>

The Weiss model is used to describe  $CoO_2$  as  $Co(III)O_2^-$  with Co having a configuration of

$$(d_{xy})^2(d_{xz})^2(d_{yz})^2. \quad (36)$$

This model predicts that the unpaired spin density resides on the  $O_2^-$  ligand, as is found experimentally. This result has often been used as strong support for the Weiss model. But the ozone model of transition metal- $O_2$  complexes also predicts a doublet ground state of  $CoO_2$  with no unpaired spin density on the metal center. Therefore, the EPR studies of  $CoO_2$  cannot be used to distinguish between the Weiss model and the ozone model.

The geometry of a five-coordinate Co-porphyrin complex should be very similar to the t state of Fe, since neither metal has an electron in the  $d_{x^2-y^2}$  orbital. Our calculations predict an Fe out-of-plane displacement of 0.13 Å, whereas the experimental geometry for a five-coordinate Co-porphyrin complex has Co 0.14 Å out of the porphyrin plane.<sup>89</sup>

The  $\text{CoO}_2$  bond strength is found to be weaker than the  $\text{FeO}_2$  bond, with a  $\Delta H$  of 8-9 kcal.<sup>90, 91</sup> We can make a qualitative estimate of the  $\text{CoO}_2$  bond strength by comparing  $\text{CoO}_2$  with the planar t state of  $\text{FeO}_2$ . The bond strength of  $\text{FeO}_2$  was found to be  $\sim 34$  kcal. This must be corrected by (i) the gain of one-half of an Fe exchange term, +11 kcal, (ii) the loss of the  $\pi$  bonding due to the presence of the doubly-occupied  $d_{xz}$  orbital in  $\text{CoO}_2$ , -35 kcal, (iii) the energy required to pull Co back into the plane in the five-coordinate Co-porphyrin complex, -3 kcal, and (iv) the repulsive interaction between the doubly-occupied  $d_{xz}$  orbital on Co and the doubly-occupied central oxygen  $\pi$  orbital. We do not yet have a reliable estimate for the latter quantity, but a small interaction brings the estimated bond strength of  $\text{CoO}_2$  in line with the experimental numbers.

The Fe atom of Hb has been replaced by a Co atom and the  $\text{O}_2$  binding properties of this molecule, called coboglobin (CoHb), have been investigated. CoHb gives an oxygen equilibrium curve with a sigmoid shape characteristic of cooperative oxygen binding. Using the protein forces calculated for the T and R forms of Hb, and the force constant for the t state of the unconstrained five-coordinate Fe-porphyrin complex, 250 kcal/ $\text{\AA}^2$ , leads to the following parameters for CoHb:

$$\begin{aligned}\chi^u &= 0.13 \text{ \AA} \\ \chi^R &= 0.15 \text{ \AA} \\ \chi^T &= 0.18 \text{ \AA} \\ \Delta(\Delta H)^R &= 0.83 \text{ kcal} \\ \Delta(\Delta H)^T &= 2.23 \text{ kcal.}\end{aligned}\tag{37}$$

In this analysis the porphyrin was assumed to be domed by 0.03  $\text{\AA}$ .<sup>94</sup>

Again, we find very small movements of the metal center upon incorporation of the cobalt-substituted heme into the protein, and a slight additional movement when the subunits bind together to form the CoHb molecule. From these qualitative arguments we predict a reduction in the O<sub>2</sub> bond strength of CoMb of  $\sim 0.8$  when compared with an unconstrained five-coordinate Co-porphyrin complex, and a free energy of cooperativity ( $\Delta G_{\text{coop}}$ ) for CoHb of  $\sim 1.4$  kcal.

The  $\Delta G_{\text{coop}}$  for CoHb has recently been measured by Imai and Yonetani and found to be 1.6 kcal.<sup>97</sup> In this study they also found a slightly higher  $\Delta G_{\text{coop}}$  for Hb of 3.7 kcal, an effect 0.3 kcal larger than that reported in Ref. 57. The excellent agreement between our predicted cooperative energy for CoHb and the experimental value strongly supports the molecular description of the cooperative effect presented here.

The O<sub>2</sub> bond strength has been measured for a five-coordinate Co-porphyrin complex in the solid state and found to be 0.5 kcal larger than the O<sub>2</sub> bond strength in CoMb.<sup>9</sup> Again, our predicted value is in good agreement with experiment. If the above reaction is carried out in a toluene solution, the O<sub>2</sub> bond strength is found to be slightly less than that for CoMb. In an earlier study, an O<sub>2</sub> bond enhancement of  $\sim 1$  kcal due to the protein in CoMb was estimated because a five-coordinate Co-porphyrin complex in toluene solution gave a weaker O<sub>2</sub> bond strength than CoMb.<sup>95</sup> This difference in O<sub>2</sub> bond energies now appears to be caused by solvent effects and not by properties of the protein.

The Northwestern group has argued that lack of a metal spin state change upon O<sub>2</sub> binding in CoHb and a much smaller movement of the Co center as compared with the Fe center in Hb during O<sub>2</sub> bond formation

indicate that the Perutz "trigger" mechanism of cooperativity is incomplete.<sup>87</sup> Recent experimental evidence of the movement of Fe in Hb has tended to negate the latter argument.<sup>48</sup> As we mentioned before, the spin state change on Fe upon bonding O<sub>2</sub> is not promoted by a modified protein environment (i.e., a change in quaternary structure) but is due to the interaction between Fe-porphyrin and O<sub>2</sub> only. In our model, which is based to some extent upon the Perutz "trigger" mechanism of cooperativity, no change of spin state is expected upon O<sub>2</sub> binding for CoHb, and none is needed to explain the cooperative binding effect in CoHb. The 12.0 kcal/Å protein force for the T quaternary form of Hb coupled to the movement of the Co center of  $\sim 0.2$  Å gives rise to a  $\Delta G_{\text{coop}}$  in agreement with the measured value.

#### B. EPR Experiments on O<sub>2</sub> Complexes

EPR experiments provide experimental information regarding the unpaired spin density of transition metal-O<sub>2</sub> complexes. FeO<sub>2</sub> complexes, being diamagnetic, do not exhibit an EPR spectrum, but the EPR spectra of the odd electron systems of MnO<sub>2</sub><sup>86</sup> and CoO<sub>2</sub> are known.<sup>80</sup>

The analysis of the EPR spectra for CoO<sub>2</sub> indicates almost all of the unpaired spin density is on the O<sub>2</sub> ligand, in agreement with the Weiss model. For MnO<sub>2</sub>, using 50% <sup>17</sup>O enriched O<sub>2</sub> does not affect the EPR spectrum, indicating that none of the unpaired spin density resides on the O<sub>2</sub> ligand. This led the authors of this experiment to conclude that the MnO<sub>2</sub> does not have a structure of Mn(III)O<sub>2</sub><sup>-</sup> (i.e., does not follow the Weiss model), and they suggested a peroxo model Mn(IV) O<sub>2</sub><sup>2-</sup>.

Using the ozone model of O<sub>2</sub> binding, we have shown how the unpaired spin density will be on the O<sub>2</sub> ligand for CoO<sub>2</sub>, since the  $\pi$  system of O<sub>2</sub> can no longer spin pair with a Co  $d\pi$  singly-occupied orbital.

A different situation occurs for  $\text{MnO}_2$ , as we shall now discuss. For Mn, the number of exchange terms lost upon changing from the high-spin sextet state to the intermediate-spin quartet state is four. This amount of exchange energy is large compared with the antibonding character induced by a porphyrin ligand, so Mn will have a strong tendency to remain high-spin. Because of its smaller atomic number, its d orbital will also be larger than in Fe and lead to larger interaction with the porphyrin ligand, making it more difficult to move high-spin Mn back into the porphyrin plane than high-spin Fe. For these reasons Mn will be the least likely first-row transition metal to form six-coordinate complexes. This is the case for  $\text{O}_2$  binding, where  $\text{O}_2$  replaces the axial nitrogenous base of a five-coordinate Mn-porphyrin complex, rather than forming a six-coordinate complex.<sup>80</sup> When  $\text{O}_2$  binds to Mn to form a five-coordinate complex, the Mn is initially in a high-spin state. As in  $\text{FeO}_2$ , a singly-occupied Mn  $d_{z^2}$  and  $d\pi$  orbital spin pair with the  $\text{O}_2$  ligand, leaving no unpaired spins on the  $\text{O}_2$  ligand and three remaining singly-occupied d orbitals of the Mn. Thus the ozone model predicts a paramagnetic (quartet)  $\text{MnO}_2$  complex with the unpaired spin density residing in the Mn center, in complete agreement with the EPR data for  $\text{Mn}(\text{TPP})\text{O}_2$ .\*

In taking a closer look at the Weiss model for  $\text{MnO}_2$ , the qualitative results of the EPR experiment could be rationalized by postulating antiferromagnetic coupling between Mn(III) and the  $\text{O}_2^-$  ligand. The ozone model predicts the EPR results directly, but a quantitative analysis of the EPR data for  $\text{MnO}_2$  may be needed to clearly determine experimentally the amount of charge transfer in  $\text{MnO}_2$ .

---

\* TPP = tetraphenylporphyrin.

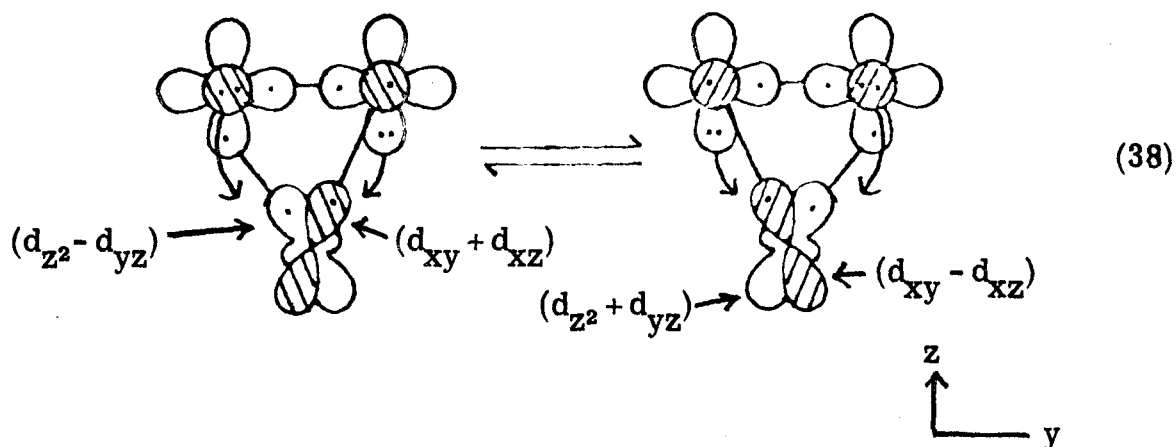
### C. Geometry and Magnetic Properties of O<sub>2</sub> Complexes

We have already discussed the bonding of O<sub>2</sub> to Mn, Fe, and Co. Nickel (Ni) is expected to have a low-spin d<sup>8</sup> configuration when it is complexed by a porphyrin ligand. The d<sub>x<sup>2</sup>-y<sup>2</sup></sub> orbital remains unoccupied and all the other d orbitals are doubly-occupied. There are no singly-occupied Ni d orbitals available for making covalent bonds to O<sub>2</sub>, and therefore Ni-porphyrin will not bind O<sub>2</sub>. For either s<sup>1</sup>d<sup>10</sup> or s<sup>2</sup>d<sup>9</sup> copper (Cu), a bonding mode analogous to that given for FeO<sub>2</sub> does not exist. Since O<sub>2</sub> is known to form complexes with Cu,<sup>98</sup> we believe it must involve bonds to the (4s, 4p, 4d) space of Cu. The lowest state of Cr-porphyrin has a high-spin d<sup>4</sup> electronic configuration.<sup>85</sup> The antibonding d<sub>x<sup>2</sup>-y<sup>2</sup></sub> orbital is not occupied, so even when the Cr center is centered in the porphyrin plane, the complex will remain high-spin. Cr has the singly-occupied d<sub>z<sup>2</sup></sub> and dπ orbitals needed to form an ozone-like bond with <sup>3</sup>O<sub>2</sub>. After pairing up two of its d electrons with O<sub>2</sub>, it has two remaining singly-occupied d orbitals, leading to a triplet ground state for the O<sub>2</sub> complex of five-coordinate Cr-porphyrin, as is found experimentally.<sup>85</sup> As in all the transition metal-O<sub>2</sub> complexes except Co, there is no unpaired spin density on the O<sub>2</sub> ligand.

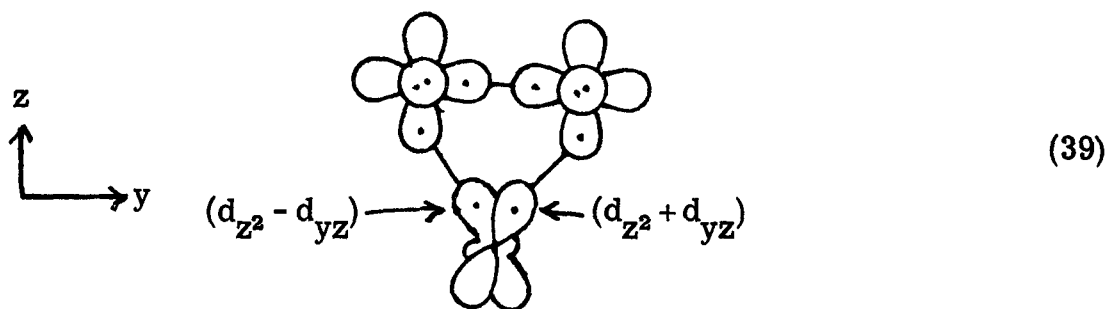
In Fe and Co there is a doubly-occupied d orbital (d<sub>yz</sub>) in the FeO<sub>2</sub> plane that interacts with the doubly-occupied 2pσ lone pair on the outer oxygen. Nonbonded repulsions between these two orbitals tend to increase the metal-O-O angle from the idealized value of 90°. In Cr and Mn this orbital is singly-occupied and a similar (although perhaps not as large) bond angle opening is expected. The ozone model predicts that the geometries of the O<sub>2</sub> complexes of Cr, Mn, Fe, and Co should

all be bent end-on modes of bonding. As mentioned earlier, the bond angles for  $\text{FeO}_2$  and  $\text{CoO}_2$  range from  $117^\circ$  to  $136^\circ$ . A determination of the structure of  $\text{CrO}_2$  and  $\text{MnO}_2$  complexes has not yet been done. The structure of the  $\text{MnO}_2$  complex has been previously predicted to be ring-like.<sup>86</sup>

In bonding  $^3\text{O}_2$  to the  $d^2$  and  $d^3$  high-spin states of Ti and V-porphyrin, respectively, it is not necessary to occupy the  $d_{yz}$  orbital. No repulsion is encountered by the outer oxygen that would tend to open up the metal O-O bond angle. In fact, the outer oxygen lone-pair orbital can make a dative bond to the metal center, which will tend to close up the metal-O-O bond angle. As this angle closes up, two modes of bonding become possible. A configuration in which a  $\sigma$  and a  $\pi$  bond is made to  $^3\text{O}_2$ , as in the ozone model, will give rise to two resonance forms, as shown in (38).



In this structure the d orbitals have been hybridized among themselves in order to give orbitals that will form stronger covalent bonds. Using these same hybrid orbitals, we could bond to  $^1\text{O}_2$ , breaking the  $^1\text{O}_2$   $\pi$  bond and forming two strong metal-O covalent  $\sigma$  bonds, (39), analogous to the ring state of ozone (10). Both bonding modes give rise to a



symmetrically bound  $O_2$ , as is found experimentally for  $TiO_2$ .<sup>84</sup> These hybridized orbitals would give rise to an unstrained O-Ti-O bond angle of  $45^\circ$ . The angle is found to be  $47^\circ$  from x-ray studies.

A 1:1  $VO_2$  complex has not yet been synthesized, but these ideas indicate that it should be stable and would probably form a symmetric bound complex as in  $TiO_2$ . Its EPR spectrum is predicted not to give any unpaired spin density on the  $O_2$  ligand.

A summary of the electronic configurations for the transition metal- $O_2$  complexes is given in Table III.

#### D. Vibrational Transitions

The O-O stretching frequency has been measured for a number of metal-porphyrin- $O_2$  complexes. These are given in Table IV together with the O-O stretching frequencies for some related molecules.

We analyzed the vibrational spectrum for  $FeO_2$  in Sec. III. For transition metal- $O_2$  complexes where  $O_2$  is bound in a bent end-on geometry, we expect two stretching frequencies involving the metal- $O_2$  unit. In analogy with ozone, we expect these two vibrational frequencies to occur between  $\sim 1000$  and  $1200\text{ cm}^{-1}$  and to be separated by  $\sim 60\text{ cm}^{-1}$ . For the symmetrically bound  $O_2$  ligands, we expect an O-O stretch similar to peroxy compounds and metal-O stretches of lower frequency.

Table III. Electronic configuration of Transition-Metal-O<sub>2</sub> complexes.<sup>a</sup>

Metal	d <sub>xy</sub>	d <sub>xz</sub>	d <sub>yz</sub>	d <sub>z<sup>2</sup></sub>	d <sub>x<sup>2</sup>-y<sup>2</sup></sub>	O <sub>c</sub> σ	O <sub>c</sub> π	O <sub>o</sub> σ	O <sub>o</sub> π	geometry	unpaired electrons
Ti( <sup>3</sup> O <sub>2</sub> ) <sup>b</sup>	0	<u>1</u>	0	<u>1</u>	0	<u>1</u>	2	2	<u>1</u>	bent	0
Ti( <sup>1</sup> O <sub>2</sub> ) <sup>b</sup>	0	0	<u>1</u>	<u>1</u>	0	<u>1</u>	2	<u>1</u>	<u>2</u>	ring	0
V( <sup>3</sup> O <sub>2</sub> ) <sup>b</sup>	1	<u>1</u>	0	<u>1</u>	0	<u>1</u>	2	2	<u>1</u>	bent	1
V( <sup>1</sup> O <sub>2</sub> ) <sup>b</sup>	1	0	<u>1</u>	<u>1</u>	0	<u>1</u>	2	<u>1</u>	<u>2</u>	ring	1
Cr	1	<u>1</u>	1	<u>1</u>	0	<u>1</u>	2	2	<u>1</u>	bent	2
Mn	1	<u>1</u>	1	<u>1</u>	1	<u>1</u>	2	2	<u>1</u>	bent	3
Fe	2	<u>1</u>	2	<u>1</u>	0	<u>1</u>	2	2	<u>1</u>	bent	0
Co	2	2	2	<u>1</u>	0	<u>1</u>	2	2	<u>1</u>	bent	1

<sup>a</sup> The underlined orbital occupation numbers indicate electrons involved in covalent bonding.

<sup>b</sup> The orbitals for these states are hybridized in pairs (d<sub>xy</sub>, d<sub>xz</sub>) and (d<sub>yz</sub>, d<sub>z<sup>2</sup></sub>).

Table IV. Stretching frequencies ( $\text{cm}^{-1}$ ) for complexed  $\text{O}_2$  molecules.

Metal	O-O Å	$\nu_{\text{oo}}$ ( $\text{cm}^{-1}$ )
Ti	1.46 <sup>a</sup>	898 <sup>a</sup>
Cr	'	1142 <sup>b</sup>
Fe	1.23, 1.26 <sup>c</sup>	~1100, 1163 <sup>d</sup>
Co	1.26 <sup>e</sup>	1080, 1155 <sup>d</sup> 1060, 1140 <sup>f</sup>
<hr/>		
$\text{O}_2$	1.21 <sup>g</sup>	1580 <sup>g</sup>
$\text{KO}_2$	1.28 <sup>h</sup>	1145 <sup>i</sup>
$\text{O}_3$	1.28 <sup>j</sup>	1042, 1103 <sup>k</sup>
$\text{HO}_2^\bullet$	1.34 <sup>l</sup>	1101 <sup>l</sup>
$\text{H}_2\text{O}_2$	1.49 <sup>h</sup>	877 <sup>k</sup>

<sup>a</sup> Ref. 84; <sup>b</sup> Ref. 85; <sup>c</sup> Ref. 23; <sup>d</sup> Ref. 28; <sup>e</sup> Ref. 25; <sup>f</sup> Ref. 99; <sup>g</sup> Ref. 27; <sup>h</sup> Ref. 100; <sup>i</sup> Ref. 101; <sup>j</sup> Ref. 102; <sup>k</sup> Ref. 103; <sup>l</sup> Ref. 26.

The fact that  $\text{CrO}_2$  has a stretching frequency similar to  $\text{FeO}_2$  and  $\text{CoO}_2$  indicates that it binds in a bent, end-on geometry.<sup>85</sup> The stretching frequencies for  $\text{MnO}_2$  have not yet been observed, but we expect them to also be in this region of the spectrum, which is characteristic for  $\text{O}_2$  ligands bound in a bent end-on manner.

In most instances only one stretching frequency has been assigned for transition metal- $\text{O}_2$  complexes, and this transition is thought to correspond to the O-O stretch. In general, the oscillator strength for the "symmetric" metal- $\text{O}_2$  stretch may be rather small, and this transition

may not be easily observed in porphyrin complexes where there is a large number of infrared bonds. For  $\text{CoO}_2$  there is some experimental indication for a second vibrational stretch involving  $\text{O}_2$ . The infrared spectrum of  $\text{Co}$  (3-methoxysalen) (pyridine) ( $\text{O}_2$ ) shows two bonds at 1060 and 1140 that have been tentatively assigned to frequencies involving the  $\text{O}_2$  ligand.<sup>99</sup> In the  $^{16}\text{O}_2$ - $^{18}\text{O}_2$  difference spectra reported for  $\text{Co}(\text{T}_{\text{piv}}^{\text{PP}})(\text{NTrIm})\text{O}_2$ ,\* there is an unassigned peak at  $1080\text{ cm}^{-1}$  that could be attributed to the second stretching frequency of  $\text{Co}^{16}\text{O}_2$  and a peak at  $1000\text{ cm}^{-1}$  that is consistent with an assignment of a  $\text{Co}^{18}\text{O}_2$  stretch.<sup>28</sup>

The frequencies reported for  $\text{TiO}$  are consistent with its formulation as a cyclic peroxo complex. The O-O stretching frequency for  $\text{TiO}_2$  is much closer to the O-O stretching frequency for  $\text{H}_2\text{O}_2$  than for  $\text{KO}_2$  or  $\text{FeO}_2$ . Relatively high energy  $\text{TiO}$  stretches ( $645$  and  $600\text{ cm}^{-1}$ ) have also been reported for this compound.

---

\*  $\text{T}_{\text{piv}}^{\text{PP}}$  = meso-tetra( $\alpha, \alpha, \alpha, \alpha$ -o-pivalamidophenyl)porphyrin.

### E. Energetics of High-Spin O<sub>2</sub> Complexes

The bonding of O<sub>2</sub> to high-spin complexes by spin-pairing singly-occupied orbitals of O<sub>2</sub> and singly-occupied metal d orbitals can result in the loss of a large number of favorable metal exchange interactions. For the high-spin state of Mn, spin-pairing two of its five singly-occupied orbitals to O<sub>2</sub> results in the loss of  $3\frac{1}{2}$  exchange terms on the metal center. From the energy separation of the lowest sextet and quartet states of Mn,  $\sim 72$  kcal,<sup>10</sup> we estimate an Mn exchange interaction to be larger than 18 kcal. Bonding <sup>3</sup>O<sub>2</sub> to ground state sextet Mn therefore results in the loss of  $\sim 63$  kcal in exchange energy. This large loss of exchange energy prevents the MnO<sub>2</sub> bond from forming in a manner analogous to FeO<sub>2</sub>. The ozone model for transition metal-O<sub>2</sub> bonds seems to be in disagreement with experiment on the bond strength of MnO<sub>2</sub>, since O<sub>2</sub> is known to bind reversibly to Mn(TPP).<sup>86</sup>

In bonding triplet O<sub>2</sub> to triplet Fe to form an overall singlet, we singlet-coupled Fe d<sub>z<sup>2</sup></sub> and O<sub>2</sub> σ orbitals, and singlet-coupled Fe dπ and O<sub>2</sub> π orbitals. Singlet coupling these four singly-occupied orbitals among themselves leads to an overall singlet state. In coupling the electron spins in this manner we have destroyed the local triplet character on both the O<sub>2</sub> and the Fe, and, as a result, destroyed some of their favorable exchange energy. Another manner in which these four singly-occupied orbitals could be coupled into an overall singlet would be to low-spin couple the triplet state of Fe to the triplet state of O<sub>2</sub>. This type of coupling preserves the local exchange interactions but sacrifices much of the bonding interaction between the two reacting molecules. In the case where the orbitals are not allowed to readjust,

using the coupling scheme that preserves local exchange interactions decreases the bond energy of the reacting molecules by  $1/N$ , where  $N$  is the number of unpaired electrons on the metal center.<sup>104</sup> In many instances a large number of exchange terms is lost upon bond formation when the first spin-coupling scheme is used. In this situation, a more favorable mode of bonding might be to use the latter spin-coupling scheme that preserves local exchange interactions. Molecules formed with the latter type of spin-coupling scheme will always lead to rather weak bonds.

In solving for the wavefunctions for the oxygenated model systems, we have allowed both types of spin coupling to mix into the final wavefunctions. Because of the large number of electronic configurations used in the final wavefunction, it is not easy to separate out the contributions from the different types of spin-coupling. In the following qualitative discussion we will assume that the final wavefunction for the  $t$  state of  $\text{HbO}_2$  involves only the first type of spin-coupling.

In order to estimate the bond energy for the different types of spin-coupling in  $\text{MnO}_2$ , we need to analyze the importance of the various bonding interactions in  $\text{FeO}_2$  in more detail.

In Sec. II, the 118 kcal of  $^3\text{O}_2$  bond energy was attributed to 47 kcal of O-O  $\sigma$  bond energy, and 71 kcal of  $\pi$  bonding and resonance energy. We also saw that a three-electron  $\pi$  bond was worth 14 kcal of energy. Six kcal of energy is lost upon destroying the triplet coupling of the two singly-occupied orbitals of  $^3\text{O}_2$ , so the remaining 37 kcal of energy we attribute to an interaction between the two resonance forms.

O-O $\sigma$ bond	47	
two three-electron $\pi$ bonds	28	
$\frac{1}{2}$ O <sub>2</sub> exchange term	6	(40)
<sup>3</sup> O <sub>2</sub> resonance energy	37	
	<hr/> 118 kcal	

The bond strength of O<sub>2</sub> to the t state of Fe in a planar five-coordinate Fe-porphyrin complex was given as 34 kcal in Sec. IV. In order to form the FeO<sub>2</sub> bond, one-half of an exchange term on both the Fe and O<sub>2</sub> is lost. In addition, the resonance energy of O<sub>2</sub> is lost and one of the three-electron O<sub>2</sub>  $\pi$  bonds is broken. The nonbonded repulsions between the O<sub>2</sub> and the porphyrin ligand must also be overcome. Since the Fe returns to the center of the porphyrin plane when the O<sub>2</sub> bonds,<sup>23</sup> we will assume that the nonbonded repulsions of the O<sub>2</sub> ligand are similar to those encountered by NH<sub>3</sub>, and estimate these interactions as decreasing the Fe-O<sub>2</sub> bond strength by ~15 kcal. Taking all these factors into account predicts a total energy of 117 kcal, which must be divided between an intrinsic Fe-O  $\sigma$  bond and an intrinsic Fe-O<sub>2</sub>  $\pi$  bond. We assume the  $\pi$  bond in FeO<sub>2</sub> to be similar in strength to the  $\pi$  interaction of O with O<sub>2</sub>, 35 kcal, which leads to an Fe-O  $\sigma$  bond strength of 82 kcal.

It remains to be determined how much of the resonance energy of O<sub>2</sub> is lost when the spin-coupling preserving local exchange interactions is used. We can use the calculated excitation energy between the t and q states of HbO<sub>2</sub> to estimate this number.

If we first assume that the first coupling scheme is used when O<sub>2</sub> bonds to the q state of Fe, we would estimate an O<sub>2</sub> bond strength of

$\sigma$ bond	+82	
$\pi$ bond	+35	
O <sub>2</sub> resonance	-37	
O <sub>2</sub> $\pi$ bond	-14	(41)
O <sub>2</sub> exchange term	- 6	
2 $\frac{1}{2}$ Fe exchange terms	-55	
O <sub>2</sub> nonbonded repulsions	-15	
	<hr/>	
	-10 kcal	

This is not consistent with the calculated O<sub>2</sub> bond strength of 8 kcal for the q state of Fe, and therefore the q state of Fe must bind O<sub>2</sub> while preserving some of its local exchange interaction. If we assume that the bonding uses the latter coupling scheme completely, we estimate a loss of O<sub>2</sub> resonance energy of 6 kcal due to local high-spin coupling.

$\frac{1}{4}$ $\sigma$ bond	+20	
$\frac{1}{4}$ $\pi$ bond	+ 9	
O <sub>2</sub> resonance	- 6	(42)
O <sub>2</sub> nonbonded repulsions	-15	
	<hr/>	
	8 kcal	

Using these bond energies for MnO<sub>2</sub>, for the spin-coupling scheme where local exchange interactions are destroyed, we estimate an O<sub>2</sub> bond energy of

$\sigma$ bond	+82
$\pi$ bond	+35
O <sub>2</sub> resonance	-37
O <sub>2</sub> $\pi$ bond	-14

O <sub>2</sub> exchange term	- 6	
3½ Mn exchange terms	-63	
O <sub>2</sub> nonbonded repulsions	- 7	
	<hr/>	
	-10 kcal	(43)

Using the local high-spin coupling scheme, the O<sub>2</sub> bond energy for Mn is estimated to be

1/5 σ bond	+16	
1/5 π bond	+ 7	
O <sub>2</sub> resonance	- 6	(44)
O <sub>2</sub> nonbonded repulsions	- 7	
	<hr/>	
	+10 kcal	

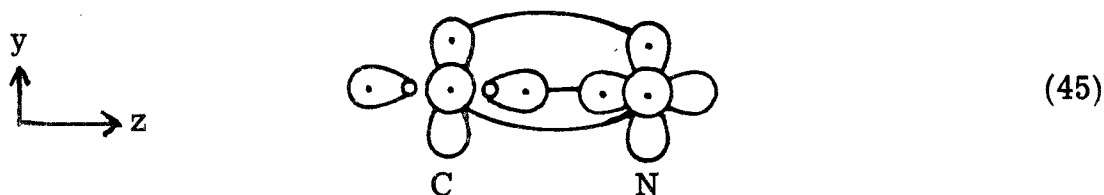
Thus, bonding O<sub>2</sub> to Mn probably involves a coupling scheme that does not destroy the large amount of exchange energy on the high-spin sextet Mn atom. Although a large number of assumptions was made in estimating the MnO<sub>2</sub> bond strength, these qualitative ideas about the bonding of ligands to high-spin metal atoms are important in understanding the chemistry of these complexes.

Using similar arguments, the bond strength of CrO<sub>2</sub> is estimated to be ~5-8 kcal for both spin-coupling schemes. Since O<sub>2</sub> makes an irreversible bond to Cr, these estimated bond strengths appear too low and a more quantitative analysis is needed to carry these ideas any further.

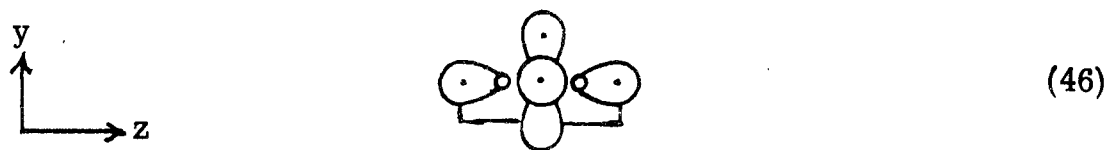
## IX. Bonding of Other Ligands to Fe-Porphyrin Complexes

We discussed the bonding of CO to a five-coordinate Fe-porphyrin complex in Sec. V. Other ligands that form dative bonds such as ammonia, pyridine, and other nitrogenous bases will also bind in a similar manner and need not be considered any further. The bonding of cyano (CN) and hydroxy (OH) ligands is similar in many respects to the bonding of  $O_2$ , and we will discuss these complexes in this section.

The valence bond diagram for CN is shown in (45).



The electronic structure about the carbon atom (C) is different from any we have discussed before. The ground state of C is  $1s^2 2s^2 2p^2$ . One 2p orbital is unoccupied and can be used to correlate the motion of the 2s pair of electrons, tending to move them to different sides of the atom. By mixing the 2s and empty 2p orbital and allowing each electron in the 2s pair to have its own orbital\* we reach a configuration about C as in (46),



where the  $(2s, 2p_z)$  lobe orbitals are singlet-coupled. In situations of

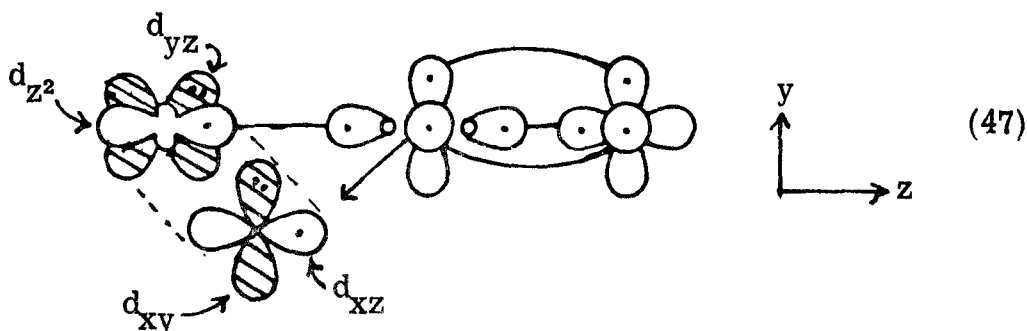
---

\* This removes the Hartree-Fock restriction. This method, involving a less restricted wavefunction, is referred to as the generalized valence bond (GVB) method.

strong covalent bonding, this singlet coupling can be broken and the electrons in this pair can be used to form two covalent bonds.

After forming a triple bond between C and N, one remaining electron in a lobe orbital on C is available for covalent bonding. In bonding CN to a five-coordinate Fe-porphyrin complex, this lobe orbital can pair up with the singly-occupied  $d_{z^2}$  orbital in either the q or the t state of Fe. An additional exchange term is lost upon bonding CN to the q state as compared with bonding CN to the t state. This loss of exchange energy can cause the q and t states to cross, as in the bonding of  $O_2$  to Fe (see Fig. 13). If this happens, the q state of FeCN is expected to be only slightly higher in energy.

Bonding CN to the t state of Fe is depicted in (47).



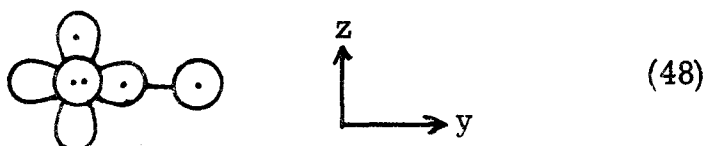
The Fe  $d_{z^2}$  orbital and a C lobe orbital are paired in a covalent bond with the Fe  $d_{xz}$  orbital remaining singly-occupied, giving rise to a doublet ground state of FeCN.

This spin state is in agreement with a value of 2.47 B.M. found for the magnetic moment of HbCN.<sup>105</sup> CN is known to bind very strongly to Hb, being very difficult to remove once it has been bound.<sup>106</sup> We expect the CN bond energy to be large because formation of the HbCN bond does not cause a destabilizing effect on the CN ligand similar to

that which occurs in  $^3\text{O}_2$  when it forms a covalent bond.

The chemistry of the OH adduct of Hb is less well understood. This complex has a magnetic moment of 4.4 B.M.<sup>105</sup> This value was originally interpreted as arising from a molecule with three unpaired electrons,<sup>105</sup> but later a thermal equilibrium between a high-spin state and a low-spin state was suggested to explain its intermediate value.<sup>78</sup> The temperature dependence on the absorption spectrum for HbOH is extremely small<sup>107</sup> and this fact casts doubt upon the suggestion of a thermal equilibrium between different spin states. Although the magnetic moment for HbOH is large, the OH adduct of another heme protein, horseradish peroxidase, is only 2.66 B.M., indicating a doublet ground state.<sup>108</sup>

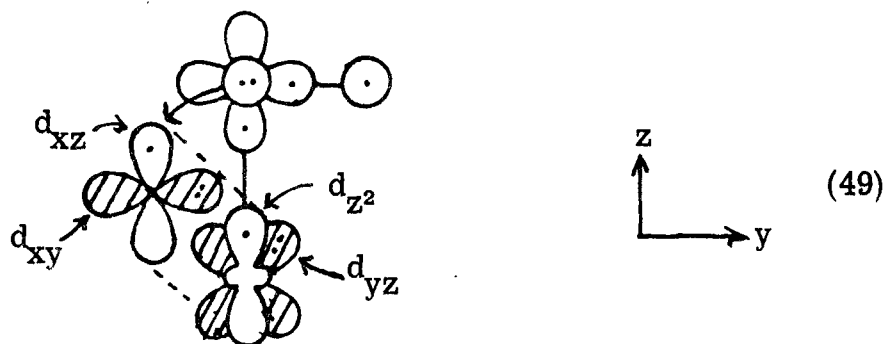
Bonding a hydrogen atom to the ground state of O atom leaves one singly-occupied 2p orbital available for covalent bonding (48),



As in  $\text{O}_2$  and CN, OH can form a covalent bond with the singly-occupied Fe  $d_{z^2}$  of both the q and t states of Fe. Bonding to the q state instead of the t state results in the loss of one additional exchange term. Since the q state is  $\sim 18$  kcal lower than the t state, and the Fe exchange term is  $\sim 22$  kcal, bonding to either the q or the t state results in approximately the same bond energy. At this level of description we cannot predict with certainty either a quartet or doublet ground state of HbOH. Because the protein affects, to some extent, the separation between the q and t states, the protein can cause OH (or CN) to bind preferentially to either

the q or the t state. From the observed magnetic moments, we suggest that HbCN and horseradish peroxidase-OH involve bonding to the t state of Fe, and the q state of Fe forms the bond to OH in Hb. With the ideas presented here, a thermal equilibrium is not needed to explain the magnetic moments of these complexes.

The bonding of OH to the t state of Fe is shown in (49).



In addition to making the covalent bond between the O  $2p_{\sigma}$  orbital and the Fe  $d_{z^2}$  orbital, the doubly-occupied O  $\pi$  orbital and the singly-occupied Fe  $d_{xz}$  orbital can form a three-electron  $\pi$  bond. From (13) and (49) we see that the bonding interaction between the Fe and O in HbOH is identical to the interaction between Fe and the central O atom in HbO<sub>2</sub>. Thus any properties involving the Fe center should be very similar in the HbO<sub>2</sub> and HbOH molecules. The correspondence between the ultraviolet-visible spectrum of HbO<sub>2</sub>, HbOH, and HbCN was one of the facts upon which Weiss based his model. The ozone model also clearly predicts these similarities.

Notice that we formed FeOH from neutral reactants. We could also have formed the same complex from a ferric  $d^5$  Fe and a hydroxy anion, OH<sup>-</sup>, with a substantial amount of delocalization of the doubly-occupied oxygen  $2p_z$  orbital of the Fe(III) center. The end result of

either description is equivalent, but since the actual charge separation in this complex is only a fraction of an electron (0.26), the neutral reactants correspond more closely to the final electronic structure. For this reason, we choose to idealize the reactants as neutral species. The alternative view in which the hydroxy complex is described as  $\text{Fe(III)OH}^-$  is consistent with the description of the  $\text{O}_2$  complex as  $\text{Fe(III)O}_2^-$ . However, it must be remembered that this description is really a formal one, and that there is not a whole electron transferred from the Fe  $d_{z^2}$  orbital onto the  $\text{O}_2$  ligand. What this formalism does do is associate a particular bonding state of Fe (the t state of Fe, in this case) and a particular bonding mode (covalent in this case) with the Fe(III) formal oxidation state. It is not correct to view Fe(III) as having a  $d^5$  configuration, or superoxide ion as having an additional electron.

The ultraviolet-visible spectra for a number of Hb complexes are listed in Table V. The electronic spectrum of hemoglobin is not particularly sensitive to various ligands. Only the high-spin complexes (F,  $\text{H}_2\text{O}$ ) clearly stand out. The spectrum for HbCO is surprisingly similar to  $\text{HbO}_2$ , HbOH, and HbCN.\* It has been suggested that the two different types of spectra indicate the population of the  $d_{x^2-y^2}$  orbital.<sup>52</sup> Only the suggested high-spin form of HbOH seems to violate this rule.

---

\* On the basis of resonance Raman studies, FeCO has been formulated as  $\text{Fe(III)CO}^-$ .<sup>110</sup>

Table V. Spectral Characteristics of Hb Complexes.<sup>109</sup>

Ligand	Visible		Soret
	$\alpha$ -band	$\beta$ -band	$\gamma$ -band
None		555	430
O <sub>2</sub>	577	541	415
OH	575	540	410
CN	(560)	540	419
N <sub>3</sub>	575	540	417
Nitrosobenzene	562	542	420
alkyl-ICN	560	530	428
CO	569	540	419
H <sub>2</sub> O	631	500	405
F	605	483	403
actetate	620	496	404

X. Properties Involving the Electronic States of Fe

A. Electronic Spectra of Hb Complexes

In the past it has been very difficult to see electronic transitions between different states of the Fe coordination sphere because intense transitions involving porphyrin  $\pi \rightarrow \pi^*$  excitations occur throughout the visible and ultraviolet spectra. There are two characteristics of porphyrin spectra that do allow some information to be gained about the excited states of the metal coordination sphere. Free-base porphyrins do not absorb below  $12,000 \text{ cm}^{-1}$  so that any near-infrared bands observed must correspond to excitation involving metal orbitals.<sup>111</sup> More importantly, the porphyrin  $\pi \rightarrow \pi^*$  spectrum is plane (x,y) polarized.<sup>112</sup> Any z-polarized transitions in this region then indicate excitations involving the metal center. Through the use of single crystal measurements, the relatively weak z-polarized spectrum can be separated from the porphyrin  $\pi \rightarrow \pi^*$  transitions. These experiments have been carried out for single crystals of  $\text{HbO}_2$ ,  $\text{HbCO}$ ,  $\text{MbO}_2$ ,  $\text{MbCO}$ , and  $\text{MbCN}$ .<sup>112,113</sup> The spectra of the related molecules,  $\text{HbO}_2$  and  $\text{MnO}_2$   $\text{HbCO}$  and  $\text{MbCO}$ , are essentially identical. It is not clear from the experiments in what manner the cyanide molecule is complexed to myoglobin. The complex is described as a cyanide ion complex of ferrous iron. An analogous complex has been reported to be unstable for hemoglobin.<sup>114</sup> Because of the strong similarity between the spectra of the  $\text{MbO}_2$  and  $\text{MbCN}$  molecules reported in the single crystal studies, and the similarity between the solutions spectrum for  $\text{MbCN}$  from the above mentioned study and the solution spectrum given in the literature,<sup>115</sup> we assume that the cyanide complex of myoglobin in the single crystal

studies corresponds mainly to metMbCN. The z-polarized transitions for MbO<sub>2</sub>, MbCN, and MbCO are given in Table VI. The x,y-polarized band in the near infrared is also listed for MbO<sub>2</sub> and MbCN.

Table VI. Electronic transitions involving the Fe center in Mb complexes (cm<sup>-1</sup>).

MbO <sub>2</sub>	10, 800	15, 500	21, 000	31, 500
MbCN	8, 500	16, 000	21, 000	31, 500
MbCO	None			

In assigning the above transitions of MbO<sub>2</sub> and MbCN, we first eliminate any transitions of the type porphyrin  $\rightarrow d_{z^2}$ ,  $d_{x^2-y^2}$ , since, if they were to occur, we would also expect similar transitions to occur for MbCO. Also, since CO and CN have similar electronic structures after they have been bound to iron, we do not expect any of the transitions in MbCN to correspond to excitations to the  $\pi^*$  orbitals of CN.

As we discussed earlier, we expect both O<sub>2</sub> and CN to bind to the t state of iron. This state has one t<sub>2g</sub> orbital (Fe d<sub>xz</sub>) singly-occupied, so that we expect low-lying transitions involving excitations into this orbital. Since the CO molecule binds to the s state of iron, where all the t<sub>2g</sub> orbitals are filled, we would not expect any corresponding transitions to occur in MbCO. Excitation from a porphyrin  $\pi$  orbital to a d<sub>xz</sub> Fe orbital would be x,y-polarized, so we assign the near-infrared transition to this type of transition. Support for the assignment comes from the near-infrared transitions observed in deoxyHb and other

Fe(III) complexes such as  $\text{Fe(III)OH}^-$ ,<sup>52</sup> all of which would be expected to have a singly-occupied  $t_{2g}$  orbital. The assignment has previously been made by Eaton and co-workers for the near-infrared transitions in the ferric complexes.<sup>116</sup> There is also the possibility of d-d transitions involving the singly-occupied  $d_{xz}$  orbital. In our calculations, we find an excited state around  $14,000\text{ cm}^{-1}$  (z-polarized) that corresponds to exciting the Fe atom to the s state ( $d_{z^2} \rightarrow d_{xz}$ ) while simultaneously exciting an outer oxygen  $2p_z$  electron to the singly-occupied  $2p_x$  orbital of the outer oxygen. This double-excitation process transforms the ground state into a Griffith-like state where singlet  $\text{O}_2$  binds to the s state of Fe. We assign the transition at  $16,000\text{ cm}^{-1}$  in  $\text{MbO}_2$  to this state. In  $\text{MbCN}$  the  $d_{z^2} \rightarrow d_{xz}$  excitation will have a z-polarized component occurring at around the same energy, but the readjustments on the cyanide ligand will be less than those occurring for  $\text{O}_2$ , so the transition will have more d-d character than in  $\text{MbO}_2$ , and, as a result, should be less intense. Intensities of the transitions for  $\text{MbCN}$  have not yet been determined experimentally. The intensities of the z-polarized transitions have been obtained for  $\text{MbO}_2$  by fitting the singly-crystal polarizability data. The broad  $16,000\text{ cm}^{-1}$  transition has a maximum extinction coefficient of  $\sim 10^1,^3$  which is consistent with this excitation involving a significant amount of d-d character.<sup>112</sup> We tentatively assign the remaining transitions at  $21,000$  and  $31,500\text{ cm}^{-1}$  as involving  $d_{z^2} \rightarrow \text{porphyrin } \pi$  character. The intense  $\pi \rightarrow \pi^*$  spectrum of porphyrin molecule is thought to arise from transitions occurring between the two highest occupied  $\pi$  molecular orbitals and the two lowest unoccupied  $\pi$  molecular orbitals. Significant configuration interaction between the

states made up from different occupations of these four molecular orbitals is needed in order to explain the relative intensities of the Soret and visible transitions.<sup>117</sup> The splitting between these two transitions is  $\sim 15,000 \text{ cm}^{-1}$  for the  $\pi \rightarrow \pi^*$  state of porphyrin. For  $d_{z^2} \rightarrow \text{porphyrin } \pi^*$ -type transitions, we might expect the splitting to be less since only one donor level is involved.

Spectra have been taken of various metalloporphyrin complexes below 700 nm ( $\sim 14,000 \text{ cm}^{-1}$ ).<sup>118</sup> Of the first-row transition metals, Cu, Ni, and Co have been investigated. Cu and Ni do not show a transition in this region, as expected, because they do not have any singly-occupied  $t_{2g}$  orbitals available for porphyrin  $\rightarrow$  metal charge transfer. Co(TPP) does show a transition around  $13,000 \text{ cm}^{-1}$ . In four-coordinate Co complexes, the  $d_{z^2}$  orbital is not destabilized by axial ligands, and the ground state is expected to be

$$(d_{z^2})^2(t_{2g})^5. \quad (50)$$

For this configuration the porphyrin  $\rightarrow t_{2g}$  transition can occur. In a five-coordinate cobalt complex, the destabilization of the  $d_{z^2}$  orbital favors a ground state of the configuration

$$(t_{2g})^6(d_{z^2})^1. \quad (51)$$

Thus, for five- and six-coordinate Co-porphyrin complexes, the near-infrared transition should not be seen. Near-infrared transitions are observed in Cr(TPP)Cl, Mn(TPP)Cl, and Fe(TPP)Cl, as expected.

More information is needed to make any assignments of these spectra more concrete. The above discussion does suggest further experimental studies that could be made in order to test the assignments made.

Analogous 10,500 and 16,000  $\text{cm}^{-1}$  transitions would not be expected to be found in  $\text{CoMbO}_2$ , since there are no singly-occupied  $t_{2g}$  orbitals in this molecule. Substitution of a different macrocycle, as in the octaaza [14]annulene model Fe oxygen carrier, would test the sensitivity of the transitions to the Fe environment. From our assignments, we would predict very little change in the 16,000  $\text{cm}^{-1}$  band, but possible large changes in the other three transitions.

Since it is possible to explain the z-polarized spectra of  $\text{MbO}_2$ ,  $\text{MbCN}$ , and  $\text{MbCO}$  by considering transitions involving the metal d orbitals, we have not needed to consider transitions involving the excitation of the electrons in the covalent Fe-porphyrin bonds. The presence of singly-occupied orbitals on the ligands indicates the possibility of covalent bonds being formed between the axial ligands and the (4s, 4p, 4d) space of Fe in some of the excited states of Fe-porphyrin complexes. Since this involves basically atomic transitions on the Fe atom, they would be expected to be rather weak transitions. Also, large changes in geometry might be expected that would further reduce the intensity of these possible transitions.

#### B. Mössbauer Experiments on Fe-Porphyrin Complexes

Mössbauer spectroscopy directly yields information about the charge distribution of the molecule near the Fe nucleus. The quadrupole splitting in Mössbauer spectra is related to the electric field gradient (EFG) of the molecule at the Fe center by the relationship

$$\Delta E = \frac{1}{2}e^2Qq(1 + \frac{1}{3}\eta^2)^{\frac{1}{2}}, \quad (52)$$

with  $eq = V_{zz}$  and  $\eta = (V_{zz} - V_{yy})/V_{zz}$ .  $V_{xx}$ ,  $V_{yy}$ , and  $V_{zz}$  are the

principal components of the EFG.<sup>7</sup> The component with the largest magnitude is defined to be  $V_{zz}$ . Since the sum of the principal components is zero, only two independent parameters are needed to define the EFG and normally  $q$  and  $\eta$  are used. From (52) we see that large asymmetries,  $\eta \approx 1$ , only change  $\Delta E$  by  $\sim 15\%$ , so we will be concerned mainly with the magnitude and sign of  $q$ . The sign of  $q$  cannot be obtained from (52), but in the presence of a magnetic field, hyperfine interactions produce asymmetric spectra that allow its determination.<sup>119</sup> In some cases, curve fitting or directional information obtainable from single crystal studies have also yielded the orientation of the EFG with respect to the molecular axis.<sup>120</sup>

In transition-metal complexes, contributions to the EFG are normally analyzed as arising from either the  $d$  orbitals (valence contributions) or the ligand orbitals.<sup>7</sup> The EFG has a  $1/r^3$  dependence, where  $r$  is the average distance between the electronic density and the Fe center. Since  $d$  electrons are obviously much closer to the Fe center than are ligand electrons, they give rise to much larger individual contributions. In our calculations we find that the  $d$  orbitals give rise to  $\sim 80\%$  of the calculated EFG. Therefore, to a first approximation, we can estimate the EFG by considering only the Fe  $d$  orbitals.

In comparing the Mössbauer data for a few Fe-porphyrin complexes, it becomes obvious that a simple explanation of Mössbauer parameters cannot always be found.  $\Delta E$  is measured to be  $+0.58$  for Fe(OTBP) and  $+0.68$  for Fe(OTBP)(pyridine)<sub>2</sub>.<sup>92</sup> In the latter compound a small  $\Delta E$  is expected because the molecule is diamagnetic with a  $(t_{2g})^6$  configuration about the Fe. For this configuration there will be

very little d orbital asymmetry, which explains its small  $\Delta E$ . In the four-coordinate Fe(OTBP) complex, the magnetic moment indicates a high-spin state. For  $s^2d^6$  Fe this state has only one of its d orbitals doubly-occupied. This configuration will give rise to large d orbital asymmetry, and a large  $\Delta E$  is expected, contrary to what is observed. There is no temperature dependence for  $\Delta E$ , and it appears that a thermal equilibrium between different states cannot be invoked to explain the small observed  $\Delta E$ . In both complexes  $\eta$  is  $\approx 0$  and the sign of  $V_{zz}$  is positive, indicating that for both compounds there is greater electron density in the plane of the porphyrin ligand than in the axial positions. Since the ligand electron density must give rise to the  $\Delta E$  in the six-coordinate Fe(OTBP)(pyridine)<sub>2</sub> complex, it should only increase the  $\Delta E$  for the four-coordinate Fe(OTBP) complex.

The Mössbauer spectrum of Fe(TPP) should be similar to either the high-spin Fe(OTBP) spectrum or the intermediate-spin Fe (octaaza [14]-annulene) spectrum. Its reported  $\Delta E$  of 1.32<sup>122</sup> and 1.51<sup>45</sup> lies close to neither, with the Fe octaaza[14] annulene complex having a  $\Delta E$  of 4.04.<sup>46</sup> Unless the ground state of Fe(TPP) involves a strong interaction between the high-spin and intermediate-spin states, no trend can be found in the Mössbauer data for these planar four-coordinate Fe complexes. Another molecule that has an anomalous Mössbauer spectrum is the diamagnetic Fe(phthalocyanine)(pyridine)<sub>2</sub> complex. This molecule has a relatively large  $\Delta E$  of 1.96,<sup>123</sup> while very little EFG asymmetry is expected.

Another problem in using Mössbauer data to probe the electronic structure of Fe complexes is that the sign of the nuclear quadrupole

moment has not been determined conclusively. Its determination can only be made after the EFG for some reference compound has been calculated theoretically. The present value for the magnitude and sign of the nuclear quadrupole moment of Fe rests on crystal field<sup>124</sup> and iterative extended Hückel calculations.<sup>125</sup>

The  $\Delta E$  of Fe(OTBP) and Fe(OTBP)(pyridine)<sub>2</sub> can be explained if the sign of the nuclear quadrupole moment is assumed to be wrong. A negative  $V_{zz}$  with an  $\eta \approx 0$  would indicate that the ground state of Fe(OTBP) had either a doubly-occupied  $d_{z^2}$  orbital or had the doubly-occupied orbital shared between the degenerate  $d\pi$  orbitals. In both of these cases, contributions from the porphyrin lone pairs would tend to reduce the  $\Delta E$  of these states. In the Fe(OTBP)(pyridine)<sub>2</sub> complex, lone pairs on the pyridine would have to cause greater electron density to be along the axis perpendicular to the porphyrin plane than in the porphyrin plane in order to give a consistent sign of  $V_{zz}$  for this molecule.

In our calculations we found that changing the porphyrin ring radius from 1.85 Å to 2.01 Å has a small effect on the EFG of all the low-lying states of Fe-porphyrin, typically changing them by  $\sim 10\%$ . Thus, variations in geometry cannot account for the differences in  $\Delta E$  found in the four-coordinate Fe complexes.

In light of the problems associated with a qualitative description of Mössbauer parameters, we will discuss the Mössbauer data for Hb, HbO<sub>2</sub>, and HbCO. These data are summarized in Table VII.

We begin first by analyzing the parameters for HbCO. The lack of temperature-dependence on  $\Delta E$  indicates that only one state is

Table VII. Mössbauer data for selected Hb complexes.<sup>126</sup>

Molecule	Temperature	$\Delta E$	Sign of $V_{zz}$	Direction of $V_{zz}$
Hb	4.2	2.4	+	(in heme plane)
	175	$\sim 1.9$		
HbO <sub>2</sub>	4.2	2.2	-	?
	195	1.9		
HbCO	4.2	0.36	+	z
	195	0.36		

thermally accessible. For HbCO, the ground state is the s state ( $t_{2g}$ ), which, because of its nearly spherically symmetric charge distribution, is expected to give rise to a small quadrupole splitting. The small observed  $\Delta E$  could be due to a nonspherical charge distribution on the ligands, or due to  $t_{2g}$  orbitals of slightly different spatial extent. From our earlier discussion of the electronic structure of HbCO, we suggested the possibility of low-lying excited states. In the Mössbauer spectrum of MbCO, two small peaks with a quadrupole splitting of  $\sim 2.4$  nm/sec have been attributed to impurities of MbO<sub>2</sub>, but could also possibly be due to excited states of MbCO whose relaxation rate is slow compared with the time scale of the Mössbauer experiment. The relaxation rate of these excited states is expected to be slow due to changes in the spins of these states.

For the q state of deoxyHb, the asymmetry in the Fe d orbital space resulting from the doubly-occupied  $d_{yz}$  orbital gives a large contribution to the EFG. This contribution has a positive major

component lying in the porphyrin plane, in agreement with the observed parameters. The strong temperature dependence indicates that the states in which the doubly-occupied orbital is either the  $d_{xy}$  or  $d_{xz}$  orbital are thermally accessible, and that the relaxation rate between these states is fast on the Mössbauer time scale.

A convincing explanation of the sign of the EFG for  $\text{HbO}_2$  has, as yet, not been given. Semi-empirical wavefunctions that give EFG tensors in reasonable agreement with observed values involve large amounts of asymmetric ligand-orbital delocalization into the d space of Fe.<sup>121,127</sup> Our ab initio calculations indicate that the ligand orbitals remain highly localized on their respective centers.

From our wavefunction we calculate an EFG for  $\text{HbO}_2$  that has a positive major component and lies in the porphyrin plane. If, following Lang and co-workers,<sup>96</sup> we assume that the  $\text{O}_2$  is free to rotate about the Fe-O axis, and that this rotation is fast on the Mössbauer time scale, the average of the two possible geometrical conformers will give a negative major component normal to the porphyrin plane. The sign of this averaged EFG is in agreement with experiment. The direction of  $V_{zz}$  for  $\text{HbO}_2$  has not yet been determined experimentally. This model does not lead to the temperature dependence of the quadrupole splitting that is observed in  $\text{HbO}_2$ .

Several factors need to be considered in comparing our calculated results against the experimental parameters. For ease of calculation we have chosen the  $\text{FeO}_2$  plane to lie along one of the iron-(porphyrin) nitrogen axes, rather than bisecting the porphyrin nitrogens, as has been shown experimentally.<sup>23</sup> Rotating our  $\text{FeO}_2$  plane  $45^\circ$  would allow

different interactions of the doubly-occupied d orbitals with the d orbitals involved in bonds to the O<sub>2</sub> ligand, which could have noticeable effects on the EFG. Also, in these calculations we have had to restrict ourselves to calculations that included only one of the two possible porphyrin resonance structures. Because of this limitation, the x and y directions in the porphyrin plane are substantially different. In the six-coordinate O<sub>2</sub> complex, the resonance in the porphyrin plane could be greatly reduced, but we have not yet done the calculations to verify this assumption.

The presence of an asymmetric coordination sphere about Fe also removes the degeneracy in the iron "e<sub>g</sub>" space, and the d orbitals may not correspond to d<sub>z<sup>2</sup></sub> or d<sub>x<sup>2</sup>-y<sup>2</sup></sub> orbitals. The form of the porphyrin resonance structure could greatly affect which combination of "e<sub>g</sub>" orbitals would be used in forming the FeO<sub>2</sub> covalent sigma bond. In our present calculations, the d orbital involved in the sigma bond corresponds more to a d<sub>z<sup>2</sup>-y<sup>2</sup></sub> orbital than to a d<sub>z<sup>2</sup></sub> (2z<sup>2</sup> - x<sup>2</sup> - y<sup>2</sup>) orbital.

Finally, there still remains some ambiguity on the sign of the <sup>57</sup>Fe nuclear quadrupole moment. If this sign was found to be incorrect, our calculations would be in agreement with the Mössbauer data for HbO<sub>2</sub>, but not in obvious agreement with the Mössbauer data for Hb.

## XI. Summary

We have discussed the bonding of  $O_2$  to Hb at the molecular level. The bond between Fe and  $O_2$  is formed by coupling a triplet state of Fe to the triplet ground state of  $O_2$ . The electronic structure of the  $FeO_2$  moiety is analogous to that of ozone. We have shown how the ozone model is in agreement with the EPR data for  $MnO_2$  and  $CoO_2$ , predicting unpaired spin density on the Mn for the former molecule, and unpaired spin density on the  $O_2$  ligand in  $CoO_2$ . Our calculations lead to a bound molecule with very little transfer of electron density onto the  $O_2$  ligand. Valence bond ideas also indicate the similarity between  $HbO_2$  and the formal Fe(III) complexes of  $HbOH$  and  $HbCN$ .

The heme plane and axial imidazole ligand are seen to play a key role in promoting reversible  $O_2$  binding. The effective size of high-spin Fe is found not to play a major role in the  $O_2$  binding process. The Fe remains in the heme plane for four-coordinate molecules, regardless of the local spin state about the Fe. The Fe moves out of the heme plane for five-coordinate complexes in order to keep a strong dative bond to the axial ligand while reducing the nonbonded repulsions between the heme plane and the axial ligand. The spin state change on Fe is found to occur, not because the Fe moves into the plane of the porphyrin, but because the formation of the  $FeO_2$  bond reduces the number of local exchange interactions that stabilize the high-spin state. The role of the coordination sphere of Fe pertaining to the chemistry of the Hb molecule is to reduce the energy separation between the atomic states. It makes an intermediate-spin state accessible for bond formation and thereby provides a mechanism by which an  $O_2$  molecule

can easily and reversibly bind to Hb. Neither the diamagnetic ( $t_{2g}$ )<sup>6</sup> excited state of Fe nor the excited singlet state of O<sub>2</sub> play a role in the formation of the FeO<sub>2</sub> bond.

We have shown how movement of the proximal imidazole, long thought to initiate the change in quaternary structure of Hb, is also responsible for the reduced O<sub>2</sub> affinity in the T quaternary form of Hb. Assuming that protein forces hinder the movement of the axial ligand leads to the calculation of protein forces in the T and R quaternary forms, and a prediction of the movement of Fe upon a change in the quaternary structure. This movement of the Fe center is found to be on the order of 0.05 Å. Based upon the structural studies of Perutz and co-workers, we have shown how the different protein forces in the T and R quaternary forms can be traced to a small number of hydrogen bonds and salt bridges. This allows us to present a model that displays the molecular origin for the cooperative binding effect. Transferring these protein forces to the coboglobin molecule allows us to calculate the magnitude of the cooperative effect in this metal-substituted Hb. The predicted cooperative effect is found to be in excellent agreement with the experimentally determined value.

The ozone model of transition-metal O<sub>2</sub> binding leads to the prediction of a second metal-O<sub>2</sub> stretching band between 1000-1200 cm<sup>-1</sup>. It has also been used to tentatively assign the near-infrared and z-polarized ultraviolet-visible spectra of HbO<sub>2</sub>, HbCN, and HbCO.

## XII. Conclusions

We feel that these theoretical studies have made a contribution to the understanding of the inorganic chemistry of metalloporphyrins and transition metal-O<sub>2</sub> complexes. This knowledge has been used to further elucidate the molecular description of the biological function of oxygen transport and storage.

These calculations show the feasibility of applying valence bond ideas to the description of inorganic chemistry. The importance of metal exchange interactions has been stressed throughout this discussion. The consideration of modifications in exchange terms due to bonding processes is essential for a qualitative understanding of the chemistry of inorganic systems.

Ab initio theory has the advantage that it can be designed to test any idea concerning the electronic structure of molecules, at least to some level of approximation. With the advent of more powerful computational abilities, useful approximations can now be made to test ideas concerning the molecular description of biological functions, tests that sometimes cannot easily be carried out experimentally due to the complexity of biological molecules. Coupled with the design and characterization of model enzyme systems, theoretical calculations will be an increasingly useful tool in the field of biochemistry.

The biological functions of other heme proteins such as cytochrome-c and cytochrome P-450 are not nearly as well understood as those of Hb. The theoretical studies carried out here will be of use in designing calculations to explore the chemistry of these protein systems.

The description given here has been qualitative in nature. Much work remains to be done in order to obtain quantitatively accurate results for  $\text{FeO}_2$ , particularly with respect to bond energies. Calculations on  $\text{HbCO}$  and other Hb complexes need to be done to verify some of the qualitative results discussed above. And finally, additional effort is needed to resolve the remaining discrepancies between the calculated and observed Mössbauer parameters for Hb and  $\text{HbO}_2$ .

In conclusion, hemoglobin is a rather special molecule. It has been so intensely studied that present studies reveal very little new information about its physical and chemical properties. Yet much remains to be learned about how and why these properties arise. We hope that the studies discussed here have helped to further the understanding of the chemistry of hemoglobin.

### XIII. References

1. J. Haldane and J. Lorrain Smith, J. Physiol. 20, 497 (1896).
2. G. S. Adair, J. Biol. Chem. 63, 529 (1925).
3. J. Monod, J. Wyman, and J. P. Changeux, J. Mol. Biol. 12, 88 (1965).
4. D. E. Koshland, G. Nemethy, and D. Filmer, Biochem. 5, 365 (1966).
5. J. C. Kendrew, Science 139, 1259 (1963).
6. M. F. Perutz, Science 140, 863 (1963).
7. M. Weissbluth, Struct. Bonding 2, 1 (1967).
8. J. P. Collman, Acc. Chem. Res. 10, 265 (1977).
9. C. K. Chang and T. G. Traylor, Proc. Nat. Acad. Sci. USA 72, 1166 (1975).
10. C. Moore, Atomic Energy Levels (National Bureau of Standards, 1952), Vol. II.
11. W. A. Goddard III in Lecture Notes, School on the Fundamental Chemical Basis of Reactions in the Polluted Atmosphere, C. W. Kern, Ed. (Battelle Research Center, Seattle, Washington, 1973), p. 254.
12. P. J. Hay, T. H. Dunning, Jr., and W. A. Goddard III, J. Chem. Phys. 62, 3912 (1975).
13. L. B. Harding and W. A. Goddard III, J. Am. Chem. Soc., submitted for publication.
14. W. R. Wadt and W. A. Goddard III, J. Am. Chem. Soc. 97, 3004 (1975).
15. W. R. Wadt, Ph.D. Thesis, California Institute of Technology,

1974.

16. N. W. Winter, W. A. Goddard III, and C. F. Bender, Chem. Phys. Lett. 33, 25 (1975).
17. B. J. Moss and W. A. Goddard III, J. Chem. Phys. 63, 3523 (1975).
18. P. Krupenie, J. Phys. Chem. Ref. Data 1, 423 (1972).
19. W. A. Goddard III, unpublished results.
20. S. W. Benson in Thermochemical Kinetics (John Wiley and Sons, Inc., New York, 1976).
21. L. Pauling, J. Chem. Soc. 1461 (1948).
22. L. B. Harding and W. A. Goddard III, J. Am. Chem. Soc., in press.
23. J. P. Collman, R. R. Gagné, C. A. Reed, W. T. Robinson, and G. A. Rodley, Proc. Nat. Acad. Sci. USA 71, 1326 (1974).
24. R. S. Gall, J. F. Rodgers, W. P. Schaefer, and G. G. Christoph, J. Am. Chem. Soc. 98, 5135 (1976).
25. G. A. Rodley and W. T. Robinson, Nature 238, 438 (1972).
26. D. E. Milligan and M. E. Jacox, J. Mol. Spectrosc. 42, 495 (1972).
27. G. Herzberg in Molecular Spectra and Molecular Structure (D. Van Nostrand Co., Inc., Princeton, New Jersey, 1950), Vol. I, p. 560.
28. J. P. Collman, J. I. Brauman, T. R. Halbert, and K. S. Suslick, Proc. Nat. Acad. Sci. USA 73, 3333 (1976).
29. J. P. Collman, private communication.
30. H. Bürger in Porphyrins and Metalloporphyrins, K. M. Smith, Ed.

(Elsevier Scientific Publishing Co., Amsterdam, The Netherlands, 1975).

31. J. C. Maxwell, J. A. Volpe, C. H. Barlow, and W. S. Caughey, *Biochem. Biophys. Res. Commun.* 58, 166 (1974).
32. C. H. Barlow, J. C. Maxwell, W. J. Wallace, and W. S. Caughey, *Biochem. Biophys. Res. Commun.* 55, 91 (1973).
33. L. Pauling and C. D. Coryell, *Proc. Nat. Acad. Sci. USA* 22, 210 (1936).
34. M. Cerdonio, A. Congiu-Castellano, F. Mogno, B. Pispisa, G. L. Romani, and S. Vitale, *Proc. Nat. Acad. Sci. USA* 74, 398 (1977).
35. W. Karger, *Ber. Bunsenges. Phys. Chem.* 68, 793 (1963).
36. M. Makenin and W. A. Eaton, *Ann. N. Y. Acad. Sci.* 206, 210 (1973).
37. J. C. Cheng, G. A. Osborne, P. J. Stephens, and W. A. Eaton, *Nature* 241, 193 (1973).
38. C. K. Chang, *J. Am. Chem. Soc.* 99, 2819 (1977).
39. C. K. Chang, private communication.
40. L. E. Webb and E. B. Fleischer, *J. Chem. Phys.* 43, 3100 (1965).
41. L. Pauling in Nature of the Chemical Bond (Cornell University Press, Ithaca, New York, 1960), 3rd Ed.
42. J. L. Hoard, *Science* 174, 1295 (1971).
43. J. E. Baldwin and J. Huff, *J. Am. Chem. Soc.* 95, 5757 (1973).
44. R. G. Little, J. A. Ibers, and J. E. Baldwin, *J. Am. Chem. Soc.* 97, 7049 (1975).

45. W. M. Reiff, H. Wong, J. E. Baldwin, and J. Huff, *Inorg. Chim. Acta* 25, 91 (1977).
46. J. P. Collman, J. L. Hoard, N. Kim, G. Lang, and C. A. Reed, *J. Am. Chem. Soc.* 97, 2676 (1975).
47. L. J. Radonovich and J. L. Hoard, unpublished. Quoted in J. L. Hoard and W. R. Scheidt, *Proc. Nat. Acad. Sci. USA* 70, 3919 (1973).
48. T. Takano, *J. Mol. Biol.* 110, 569 (1977).
49. J. P. Collman, R. R. Gagné, C. A. Reed, T. R. Halbert, G. Lang, and W. T. Robinson, *J. Am. Chem. Soc.* 97, 1427 (1975).
50. S. Peng and J. A. Ibers, *J. Am. Chem. Soc.* 98, 8032 (1976).
51. J. C. Norvell, A. C. Nunes, and B. P. Schoenborn, *Science* 190, 568 (1975).
52. E. Antonini and M. Brunori in Hemoglobin and Myoglobin in Their Reactions with Ligands (North-Holland Publishing, Co., Amsterdam, 1971).
53. C. K. Chang and D. Dolphin, *Proc. Nat. Acad. Sci. USA* 73, 3338 (1976).
54. U. Gonser, R. W. Grant, and J. Kregdze, *Science* 143, 680 (1964).
55. R. H. Austin, K. W. Beeson, L. Eisenstein, H. Frauenfelder, and I. C. Gunsalus, *Biochem.* 14, 5355 (1975).
56. M. F. Perutz, *Br. Med. Bull.* 32, 195 (1976).
57. I. Tyuma, K. Imai, and K. Shimizu, *Biochem.* 12, 1491 (1973).
58. M. F. Perutz, *Nature* 228, 726 (1970).
59. J. L. Hoard in Hemes and Hemoproteins, B. Chance, R. W.

- Estabrook, and T. Yonetani, Eds. (Academic Press, New York, 1966).
60. R. G. Shulman, S. Ogawa, K. Wuthrich, T. Yamane, J. Peisach, and W. E. Blumberg, *Science* 165, 251 (1969).
  61. J. J. Hopfield, *J. Mol. Biol.* 77, 207 (1973).
  62. J. P. Collman, J. I. Brauman, and K. S. Suslick, *J. Am. Chem. Soc.* 97, 7185 (1975).
  63. Ref. 52, p. 221.
  64. J. M. Baldwin, *Prog. Biophys. Mol. Biol.* 209, 225 (1975).
  65. G. Fermi, *J. Mol. Biol.* 97, 237 (1975).
  66. Figure taken from Ref. 58.
  67. G. H. F. Diercksen, *Theoret. Chim. Acta (Berl.)* 21, 335 (1971).
  68. Figure taken from Ref. 65.
  69. W. Bolton and M. F. Perutz, *Nature* 228, 551 (1970).
  70. Q. H. Gibson, *Proc. Nat. Acad. Sci. USA* 70, 1 (1973).
  71. R. C. Ladner, E. J. Heidner, and M. F. Perutz, *J. Mol. Biol.* 114, 385 (1977).
  72. E. J. Heidner, R. C. Ladner, and M. F. Perutz, *J. Mol. Biol.* 104, 707 (1976).
  73. M. W. Makinen and W. A. Eaton, *Nature* 247, 62 (1974).
  74. L. Anderson, *J. Mol. Biol.* 79, 4956 (1973).
  75. J. A. Ibers, J. W. Lauher, and R. G. Little, *Acta Crystallogr. B* 30, 268 (1974).
  76. B. R. Gelin and M. Karplus, *Proc. Nat. Acad. Sci. USA* 74, 801 (1977).
  77. L. Pauling in Haemoglobin, F. J. W. Roughton and J. C. Kendrew,

Eds. (Butterworths Scientific Publications, New York, 1949).

78. J. S. Griffith, Proc. Roy. Soc. A 235, 23 (1956).
79. J. J. Weiss, Nature 202, 83 (1964).
80. B. M. Hoffman, D. L. Diemente, and F. Basolo, J. Am. Chem. Soc. 92, 61 (1970).
81. H. B. Gray, Adv. Chem. Ser. 100, 365 (1971).
82. D. S. McClure, Radiat. Res. Suppl. 2, 218 (1960).
83. R. D. Harcourt, Int. J. Quantum Chem. 5, 479 (1971).
84. R. Guillard, M. Fontesse, P. Fournari, C. Lecomte, and J. Protas, J. Chem. Soc. Chem. Commun. 161 (1976).
85. S. K. Cheung, C. J. Grimes, J. Wong, and C. A. Reed, J. Am. Chem. Soc. 98, 5028 (1976).
86. C. J. Weschler, B. M. Hoffman, and F. Basolo, J. Am. Chem. Soc. 97, 5278 (1975).
87. F. Basolo, B. M. Hoffman, and J. A. Ibers, Acc. Chem. Res. 8, 384 (1975).
88. J. P. Collman, R. R. Gagné, J. Kouba, and H. Ljusberg-Wahren, J. Am. Chem. Soc. 96, 6800 (1974).
89. W. R. Scheidt, J. Am. Chem. Soc. 96, 90 (1974).
90. D. V. Stynes, H. C. Stynes, J. A. Ibers, and B. R. James, J. Am. Chem. Soc. 95, 1142 (1973).
91. T. J. Beugelsdijk and R. S. Drago, J. Am. Chem. Soc. 97, 6466 (1975).
92. J. R. Sams and T. B. Tsin, Chem. Phys. Lett. 25, 599 (1974).
93. B. M. Hoffman and D. H. Petering, Proc. Nat. Acad. Sci. USA 67, 637 (1970).

94. R. G. Little and J. A. Ibers, J. Am. Chem. Soc. 96, 4452 (1974).
95. B. M. Hoffman, C. A. Spilburg, and D. H. Petering, Cold Spring Harbor Symposium on Quantum Biology, 36, 343 (1971).
96. K. Spartalian, G. Lang, J. P. Collman, R. R. Gagné, and C. A. Reed, J. Chem. Phys. 63, 5375 (1975).
97. Unpublished results, quoted in Ref. 56.
98. J. Peisach, P. Aisen, and W. E. Blumberg in The Biochemistry of Copper (Academic Press, New York, 1966).
99. C. Floriani and F. Calderazzo, J. Chem. Soc. A 946 (1969).
100. J. Valentine, Chem. Rev. 73, 235 (1973).
101. E. Lee-Ruff, Chem. Soc. Rev. 6, 195 (1977).
102. G. Herzberg in Molecular Spectra and Molecular Structure (D. Van Nostrand Co., Inc., Princeton, New Jersey, 1966), Vol. III, p. 604.
103. T. Shimanouchi, J. Phys. Chem. Ref. Data 6, 993 (1977).
104. W. A. Goddard III, Ph.D. Thesis, California Institute of Technology, 1965.
105. C. D. Coryell, F. Stitt, and L. Pauling, J. Am. Chem. Soc. 59, 633 (1937).
106. Ref. 52, p. 46.
107. P. George, J. Beetlestone, and J. S. Griffith in Haematin Enzymes, J. E. Falk, R. Lemberg, and R. K. Morton, Eds. (Pergamon Press, Ltd., London, 1961).
108. H. Theorell, Ark. Kemi Min. Geol. 16A, 1 (1942).

109. Compiled from Ref. 52.
110. T. G. Spiro and T. C. Strekas, J. Am. Chem. Soc. 96, 338 (1974).
111. G. D. Dorough, J. R. Miller, and F. M. Huennekens, J. Am. Chem. Soc. 73, 4315 (1951).
112. W. A. Eaton and E. Charney, J. Chem. Phys. 51, 4502 (1969).
113. A. K. Chung and M. W. Makinen, J. Chem. Phys. 68, 1913 (1978).
114. Ref. 52, p. 33.
115. Ref. 52, p. 59.
116. J. C. Cheng, G. A. Osborne, P. J. Stephens, and W. A. Eaton, Nature 241, 193 (1973).
117. M. Gouterman, G. H. Wagniere, and L. C. Snyder, J. Mol. Spectrosc. 11, 108 (1963).
118. L. Edwards, D. H. Dolphin, M. Gouterman, and A. D. Adler, J. Mol. Spectrosc. 38, 16 (1971).
119. R. L. Collins, J. Chem. Phys. 42, 1072 (1965).
120. P. Zory, Phys. Rev. A 140, 1401 (1965).
121. B. H. Huynh, D. A. Case, and M. Karplus, J. Am. Chem. Soc. 99, 6103 (1977).
122. H. Kobayashi, Y. Maeda, and Y. Yanagawa, Bull. Chem. Soc. Japan 43, 2342 (1970).
123. B. W. Dale, R. J. P. Williams, P. R. Edwards, and C. E. Johnson, Trans. Faraday Soc. 64, 3011 (1968).
124. R. Ingalls, Phys. Rev. A 133, A787 (1964).
125. A. Trautwein and F. E. Harris, Phys. Rev. B 7, 4755 (1973).

- 126. A. Trautwein, Structure and Bonding 20, 101 (1974).
- 127. G. H. Loew and R. F. Kirchner, J. Am. Chem. Soc. 97, 7388 (1975).
- 128. A. Warshel, Proc. Nat. Acad. Sci. USA 74, 1789 (1977).
- 129. J. S. Olson and Q. H. Gibson, J. Biol. Chem. 247, 1713 (1972).
- 130. W. H. Huestis and M. A. Raftery, Biochem. 14, 1886 (1975).
- 131. W. H. Huestis and M. A. Raftery, Proc. Nat. Acad. Sci. USA 69, 1887 (1972).
- 132. T. Lee, W. H. Huestis, and M. A. Raftery, Biochem. 12, 2535 (1973).
- 133. G. Yagil, Tetrahedron 23, 2855 (1967).
- 134. See Proposition I, this thesis.

## PROPOSITIONS

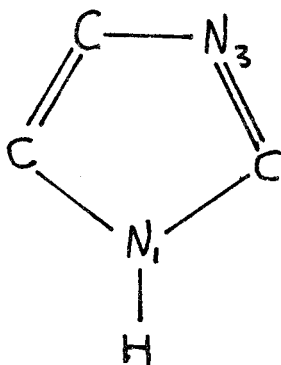
**Proposition I**

Proposition: A second complexing form of imidazole is proposed, and reinterpretation of experimental evidence is given to support this idea.

The chemistry of imidazole plays a very important role in the chemistry of biological systems. For example, as the end group of a histidine amino acid, it is present in the active site of hemoglobin, cytochromes, serine proteases, copper proteins and oxidation-reduction enzymes.

It is believed to act as a nitrogenous base in its interaction with metals, but not all of its chemistry can be easily rationalized if this is the case. This is the main topic of this proposition, but a necessary first step is the determination of the structure of free imidazole.

Imidazole is a five-membered heterocyclic compound containing two nitrogen atoms. The resonance form for this molecule is shown below.



In this resonance form N<sub>1</sub> and N<sub>3</sub> are not equivalent nitrogens, and they are commonly referred to as the "pyrrole" and the "pyridine" nitrogens

of imidazole, respectively. In a protic solvent the exchange of hydrogen atoms is very fast, and in solution the two nitrogens of imidazole can appear to be equivalent.<sup>15</sup> Even in the solid state, because of the strong hydrogen bonding which is possible between two imidazoles, the nitrogens appear almost equivalent.<sup>1</sup> Neutron diffraction data on imidazole in the solid state indicate a structure in which the bonds to the two nitrogens are very similar, and lie between expected C-N single and C-N double bond lengths.<sup>2</sup> This is not unexpected, but the fact that electron diffraction data of imidazole in the vapor phase<sup>3</sup> also give a structure very similar to that found for imidazole in the solid state is quite surprising. Contrary to this, the analysis of the quadrupole hyperfine structure of the rotational spectrum of two isotopic forms of imidazole has led to much different nuclear quadrupole coupling constants for the nitrogens of imidazole, in the gaseous state<sup>4</sup> when compared to the coupling constants obtained from NQR experiments of imidazole in the solid state.<sup>5</sup> Only a preliminary report of the electron diffraction data was presented in 1972, and as of this date no further information has been given.

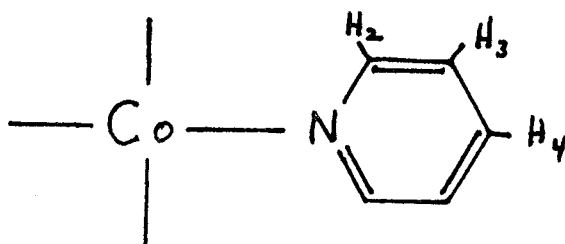
Present day theoretical techniques could easily determine whether the equivalent nitrogen or the non-equivalent nitrogen form of imidazole is the most stable one. These calculations or further electron diffraction work should be done in order to determine the structure of free imidazole. The rest of this proposition is written with the assumption that the non-equivalent-nitrogen form of imidazole would indeed be shown to be the more correct description of gaseous

imidazole if further studies were made.

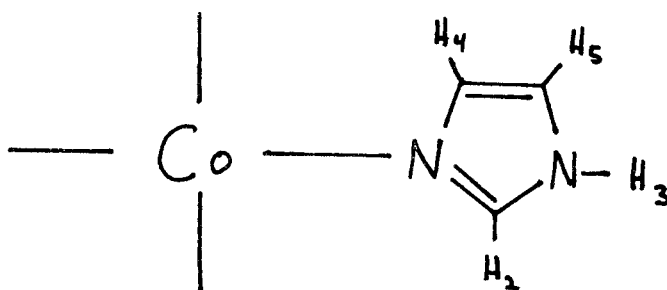
Imidazole is known in many cases to react with metal ions in the same manner as a class of compounds referred to as nitrogenous bases, i.e., ammonia, amines, pyridine, pyrimidine, etc. The nitrogenous bases are viewed to interact through a lone pair of electrons on nitrogen making a dative bond with the metal. Almost invariably, the complexing properties of imidazole are rationalized according to its properties as a nitrogenous base. Furthermore, since the doubly occupied pair of electrons on the "pyrrole" nitrogen are part of the aromatic system, they do not make strong dative bonds. Only the "pyridine" nitrogen of imidazole has an unhindered doubly occupied orbital, and can easily make dative bonds in imidazole-metal complexes. In a recent article, Pujari and Dash state,<sup>6</sup> "In all the known complexes of imidazole, the imidazole group coordinates via the pyridine nitrogen of the five-membered heterocyclic ring rather than the pyrrole nitrogen."

There are two experimental facts which are not easily explained assuming imidazole always complexes as a nitrogenous base. An NMR study of pyridine and imidazole complexed to Co given the following results:<sup>7</sup>

- a) With pyridine, three resonances can be assigned to pyridine hydrogens.



- b) With imidazole, only three resonances attributed to imidazole hydrogens appear to be resolved. The resonances for H<sub>4</sub> and H<sub>5</sub> were assigned to the same peak.



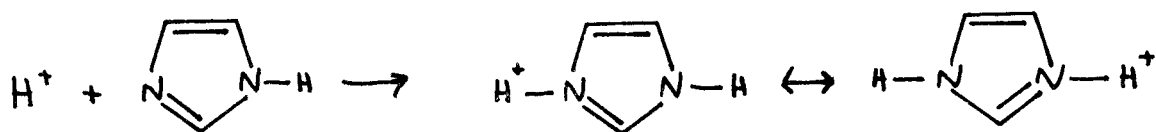
- c) The imidazole ligand forms hexakis complexes, whereas using pyridine as a ligand led to tetrakis complexes, the other two coordination sites being occupied by perchlorate.

The tendency for imidazole to form hexakis complexes with divalent metal ions has been observed by others.<sup>8, 9</sup> Two arguments have been given concerning the above point. The first, in which the different steric constraints of the two ligands are considered, has been largely

discounted.<sup>10</sup> The second argument given<sup>8</sup> is that the  $\pi$  accepting ability of imidazole is much less than that of pyridine, leading to charge buildup on the metal ion and preventing negatively charged ions from entering the first coordination sphere.

It is proposed here that the above experimental facts can be explained with a second form of complexed imidazole involving the "pyrrole" nitrogen. In this liganded form the hydrogen atom is displaced and a covalent link with the metal ion is formed. Other bonding modes for imidazole involving the "pyrrole" nitrogen have been suggested,<sup>11,12</sup> but these involve a dative type bond similar to other nitrogeneous bases.

In imidazole the "pyrrole" proton is bound very tightly, having a  $pK_a \sim 14$ ,<sup>13</sup> but complexing a strong acid to the "pyridine" nitrogen can change this bond strength greatly. When  $H^+$  is bound to the "pyridine" nitrogen, the "pyrrole" hydrogen is activated due to a second possible resonance form.

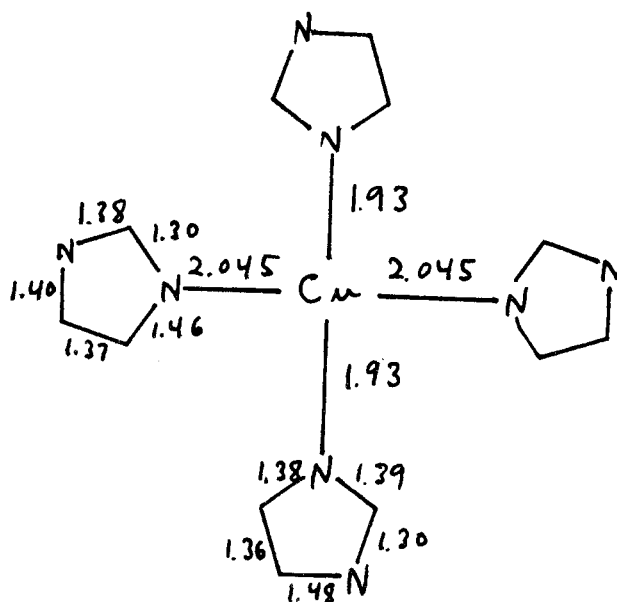


The  $pK_a$  for  $\text{Im}H^+$  is 7.1.<sup>10</sup> In a similar situation when imidazole is complexed to a metal instead of  $H^+$ , to whatever extent the resonance structure on the right is important, a lessening of the "pyrrole" proton bond strength occurs. If the "pyrrole" proton were to leave completely

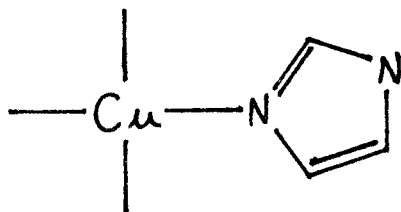
it would leave a complexed form of imidazole where it appears a hydrogen atom has been replaced by a metal ion at the "pyrrole" nitrogen, and a covalent bond has been formed between the metal and the ligand. Because of the presence of the two nitrogens in imidazole it is possible to effectively substitute a group at the "pyrrole" nitrogen without attacking it directly.

There are two basic ways the resonance structure involving the metal-nitrogen covalent bond can be stabilized. Any changes in the other ligands complexed to the metal center which cause electron charge to be donated to the metal will stabilize the covalent complex, since this form can remove electrons from the metal. Also any strong base which can deprotonate the "pyrrole" nitrogen will stabilize the covalently linked complex.

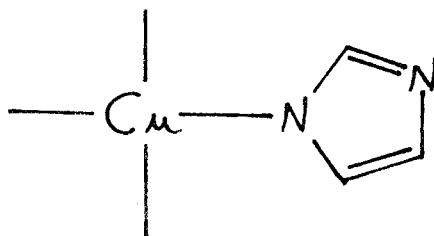
Strong evidence for the covalently complexed form of imidazole comes from the X-ray crystal structure of bis(methoxyacetato)tetrakis-(imidazole)copper(II).<sup>14</sup> In this molecule the four imidazole ligands are arranged as two trans-oriented pairs. One pair of imidazoles has a normal Cu-N bond length of 2.045 Å, while the other pair has a very short bond length of 1.913 Å. They also have much different ring geometries as shown below.



The imidazole which complexes with a long bond length appears to have a resonance form



which corresponds to complexing to the metal with a dative bond on the "pyridine" nitrogen, while the other imidazole has the form



which corresponds to a covalent metal-nitrogen bond at the "pyrrole" nitrogen. Another interesting aspect of the crystal structure is the exceedingly long bond length between Cu and the complexing oxygen of the methoxyacetato group. The structure of the methoxyacetato ligand was also significantly different from that found in other methoxyacetato complexes. There appears to be strong hydrogen bonding between the uncomplexed nitrogens in the imidazole rings and the three oxygens of the methoxyacetato ligand. Also the different pairs of imidazole ligands have different geometries with respect to the methoxyacetato ligands. Unfortunately, due to the small X-ray scattering power of hydrogen atoms, their position could not be located. It is possible that the tightly bonded imidazoles may have replaced the methoxyacetato ligand in neutralizing the charge on the metal center, subsequently transferring their "pyrrole" protons to the methoxyacetato ligands. Similar ideas were explored by the authors of the crystal structure.

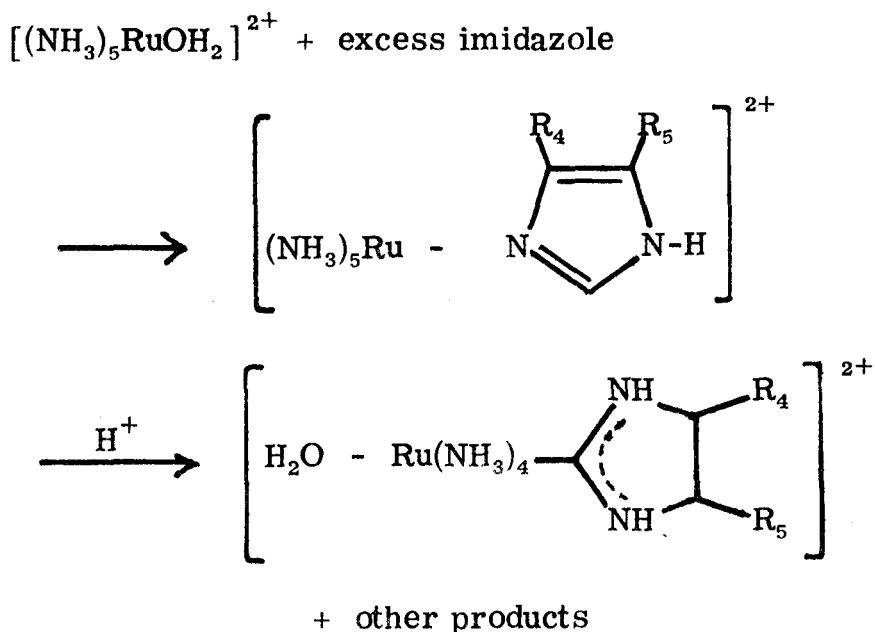
Assuming that a second bonding process involving imidazole is possible, it now becomes easy to rationalize why imidazole complexes can have six imidazole molecules in the coordination sphere whereas only four pyridine ligands enter the coordination sphere of analogous complexes. Four of the ligands complex as nitrogenous bases. The remaining two ligands are needed to neutralize the charge on the metal. Imidazole can serve this purpose when they are covalently bonded through the "pyrrole" nitrogen to the metal. Since no similar nitrogen is available in pyridine, pyridines cannot totally fill the coordination sphere and neutralize the charge on the metal at the same time.

If the coordination sphere of the Co-imidazole complex consists of four datively bound imidazoles and two covalently bound imidazoles we would expect to see seven separate hydrogen resonances attributable to imidazole nitrogens in an NMR experiment. But since the imidazole nitrogens are accessible to solvent, we might expect the differently complexed imidazoles to tautomerize through hydrogen exchange with the solvent, and the peaks for the two different types of imidazole will become averaged. In this case the  $H_4$  and  $H_5$  proton resonances will become equivalent and the experimental NMR spectrum can be explained.

Further tests are possible which could support the idea that imidazole can form covalent complexes. A neutron diffraction study of the bis(methoxyacetato)tetrakis(imidazole)Cu(II) complex to locate the positions of the protons originally bound to the "pyrrole" nitrogens would support the above ideas if the protons were found to be mainly associated with the methoxyacetato ligands. A reinvestigation of the above mentioned NMR experiment might indicate how many protons are included in the peak assigned to the "pyrrole" hydrogen. The original study was done to investigate the number of imidazole ligands coordinated to Co. Low temperature studies were needed to separate the coordinated imidazole peaks from the bulk imidazole peaks. Of the seven spectra reported for the imidazole complex at temperatures  $\leq -30^\circ \text{C}$ , six were in the range of 5.4 to 5.7 coordinated imidazoles and one spectrum gave 6.3 coordinated imidazoles. The number of imidazoles was obtained by integrating the area underneath the

resonance attributed to complexed imidazole hydrogens. If we assumed two of the complexed imidazoles were missing a "pyrrole" hydrogen the average number of complexed imidazoles found in the first six spectra would be 6.1. It might also be possible to go to even lower temperatures in the NMR experiment such that "pyrrole" hydrogen exchange might be slow enough on the NMR time scale to resolve the hydrogen peaks from the differently coordinated imidazoles.

Another form of complexed imidazole ligand has been described by Sundberg et al., in which the imidazole ligand is bound to the metal center through the C-2 carbon.<sup>16</sup> It is formed as a minor product in the following reaction,



The largest yield, 20-30%, of the C-2 bound complex was obtained when R<sub>4</sub> and R<sub>5</sub> were methyl groups. The presence of hydrogens at these

sites made this mode of ligation much harder to obtain. The bond between the metal center and the C-2 carbon of imidazole has been verified from its x-ray structure.<sup>16</sup>

This mode of ligation is not likely to explain the results of the Co NMR experiments because it does not appear to act in a manner that would neutralize the charge on the metal center. Two forms of experimental evidence support this contention. The geometry of the ruthenium complex indicates an  $sp^2$  hybridized lone pair datively bound to the metal center,<sup>16</sup> and conductivity measurements also indicate that the charge on the metal center remains after the imidazole-metal bond has been formed.

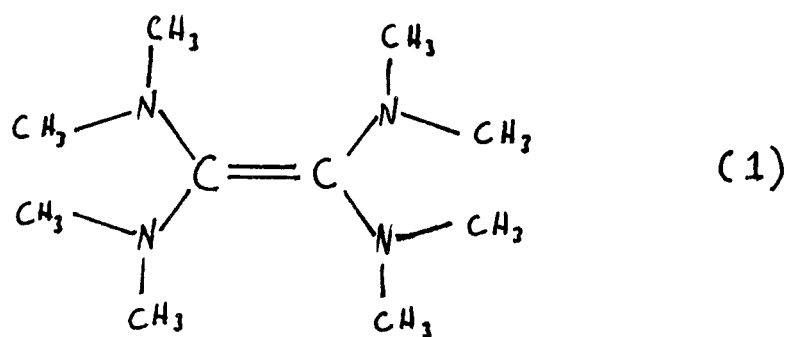
## References

1. B. M. Craven, R. K. McMullan, J. P. Bell and H. C. Freeman, *Acta Cryst.* B33, 2585 (1977).
2. International Tables for X-Ray Crystallography, Vol. III, C. MacGillavry and G. D. Rieck, Ed., (The Kynoch Press, Birmingham, Eng., 1952).
3. J. F. Chiang and M. J. Kratus, *Acta Cryst.* 28A, S206 (1972).
4. G. L. Blackman, R. D. Brown, F. R. Burden and F. R. Elsum, *J. Mol. Spec.* 60, 63 (1976).
5. J. Koo and Y. -N. Hsieh, *Chem. Phys. Lett.* 9, 238 (1971).
6. P. Pujari and K. Dash, *J. Inorg. Nuc. Chem.* 38, 2183 (1976).
7. A. Fratiello, R. E. Schuster, and G. Bartolini, *J. Am. Chem. Soc.* 92, 2304 (1970).
8. W. J. Eilbeck, F. Holmes, and A. E. Underhill, *J. Chem. Soc. A*, 757 (1967).
9. C. D. Burbridge and D. M. L. Goodgame, *Inorg. Chem. Acta* 4, 231 (1970).
10. R. J. Sundberg and R. B. Martin, *Chem. Rev.* 74, 471 (1974).
11. L. G. Marzilli and P. A. Marzilli, *Inorg. Chem.* 11, 457 (1972).
12. G. R. Lenz and A. E. Martell, *Biochem.* 3, 750 (1964).
13. G. Yagil, *Tetrahedron* 23, 2855 (1967).
14. C. K. Prout, G. B. Allison and F. J. C. Rossotti, *J. Chem. Soc. A*, 3331 (1971).
15. L. A. Paquette in Modern Heterocyclic Chemistry (W. A. Benjamin, Inc., New York, 1968).
16. R. J. Sundberg, R. F. Bryan, I. F. Taylor, Jr., and H. Taube, *J. Am. Chem. Soc.* 96, 381 (1974).

**Proposition II**

**Proposition:** The ionization potential of tetrakis-dimethylamino-ethylene (TMAE) and related compounds is discussed from the viewpoint of their electronic structure. Simple experimental and calculation tests are proposed to verify this analysis.

The extremely low ionization potential of TMAE(1)



has long been a mystery to chemists. Its value of  $\leq 5.36$  eV is probably the lowest ionization potential for any organic molecule.<sup>1</sup> This proposition tries to explain the ionization potential of TMAE and similar compounds by comparing ionization potentials of related, less complex molecules. The design of other organic molecules with low ionization potentials is also considered. Although TMAE has a low ionization potential, it has a rather weak capability for making charge transfer-type interactions<sup>2</sup> and this is thought to be due to steric interactions caused by the relatively bulky methyl groups.<sup>2</sup> An under-

standing of the ionization potentials of organic molecules might be useful for the design of effective organic reducing agents, and it would also be useful in the study of charge-transfer complexes.

The reason that TMAE has such a low ionization potential is proposed to be due to the fact that it has two centers of rather low ionization potential connected by a carbon-carbon double bond. Although only one center is initially ionized, a recoupling of the pi system of the ionic form of the molecule allows the stabilization of the ionic forms of both centers to contribute additively to the stabilization of the ionic form of the molecule. As will be shown below, this is not equivalent to the interaction of two resonating forms of the ionic state. Any molecule which has two ionization centers connected by a suitable pi system should show additive stabilization effects in the ionization potential of the molecule.

The factors affecting a molecule's ionization potential will be grouped into four categories

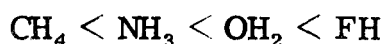
- 1) effective nuclear charge
- 2) orthogonality constraints
- 3) bond formation or electron recoupling effects
- 4) relaxation effects.

By analyzing these factors for simple organic molecules we will see how they naturally lead to the design of easily ionized organic molecules which are very similar to TMAE. Only molecules made up of C, N, O, F and H will be considered.

We begin first by noting the ionization potential of simple hydrides which can be formed with the above atoms.

<u>Molecule</u>	<u>IP(eV)</u>
CH <sub>4</sub>	12.70
NH <sub>3</sub>	10.19
OH <sub>2</sub>	12.61
FH	15.77

If we consider only the effective nuclear charge, we would expect the ionization potentials of these hydrides to increase in the order of



because of less effective nuclear shielding by the additional valence electrons. CH<sub>4</sub> does not follow this sequence because all of its valence electrons are involved in bonds. From their ionization potentials we see that valence electrons involved in bonds are relatively hard to ionize, and we conclude that easily ionized electrons must come from lone pair or radical orbitals.

It is also instructive to consider the ionization potentials of the simple fluorides.<sup>3</sup>

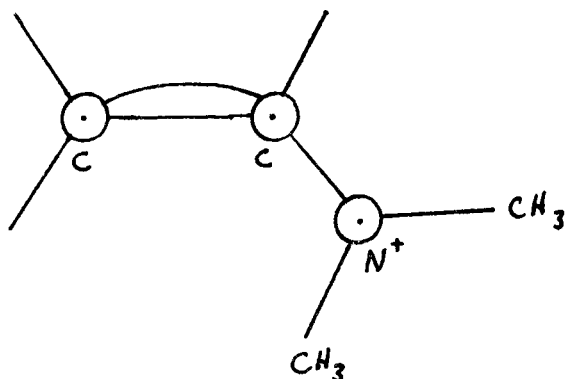
<u>Molecule</u>	<u>IP(eV)</u>
CF <sub>4</sub>	14.36
NF <sub>3</sub>	13.2
OF <sub>2</sub>	13.54
F <sub>2</sub>	15.7

The greater electronegativity of fluorine<sup>4</sup> has the effect of increasing the effective nuclear charge on nitrogen such that ionization from the nitrogen lone pair orbital has increased by three eV. Since hydrogen is the least electronegative of the elements we are considering,<sup>4</sup>  $\text{NH}_3$  appears to be a suitable starting point for designing a molecule with a low ionization potential. In  $\text{NH}_3$  the lone pair orbital is relatively unhindered by orthogonality effects. In the independent particle approximation of electronic structure, i.e., each electron is defined by its independent spatial coordinates, the experimentally observed rule that all suitable wavefunctions describing a molecule must be anti-symmetric upon interchange of any two electrons is equivalent to stating that all particles must be orthogonal. In the event that two electrons have the same spin, they must be represented by spatial orbitals which have zero overlap. This constraint leads to increased kinetic energy for these electrons and a lessened ionization potential. Adding methyl groups to  $\text{NH}_3$  increases the orthogonality constraints of the nitrogen lone pair and decreases its ionization potential,<sup>3</sup> as shown below.

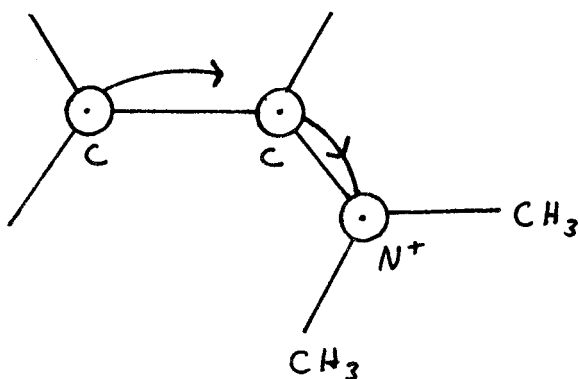
<u>Molecule</u>	<u>IP(eV)</u>	
$\text{NH}_3$	10.19	$\left. \begin{array}{l} > 1.22 \\ > 0.61 \\ > 0.24 \end{array} \right\}$
$\text{NH}_2\text{CH}_3$	8.97	
$\text{NH}(\text{CH}_3)_2$	8.36	
$\text{N}(\text{CH}_3)_3$	8.12	

The first methyl group has the largest effect, and additional groups have decreasing effectiveness in lowering the nitrogen lone pair ionization potential. By replacing hydrogen atoms with methyl groups, since hydrogen and carbon have very similar electronegativities,<sup>4</sup> to a first approximation, we should not be changing the effective nuclear charge of the nitrogen atom. In organic chemistry it is known that reactions which go through carbonium ion intermediates are stabilized by attaching methyl groups to the formally ionized carbon.<sup>5</sup> This effect has been explained by arguing that methyl groups can donate electron density to the carbonium center and thereby stabilize the ionized state. From the above considerations, a more likely argument is that the methyl groups tend to destabilize the parent molecule through orthogonality constraints, thereby making the transition state easier to attain.

So far we have looked at ways of raising the energy of an orbital to be ionized. If the orbital were initially doubly occupied, we have, after ionization, a radical electron in a highly destabilized orbital. We would like to find some means to stabilize this orbital, without stabilizing the parent molecule. Clearly this is impossible if the electronic structure of the remainder of the molecule is unchanged in both the parent and ionized molecule. Consider what would happen if we had a carbon-carbon double bond adjacent to a nitrogen lone pair orbital. In the ionized state we could draw a valence bond structure for the pi system as below.

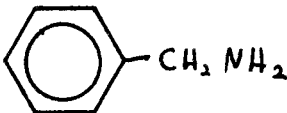
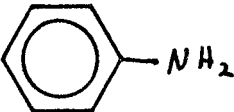
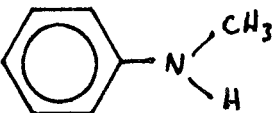
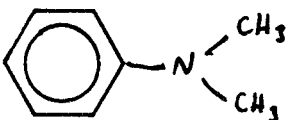
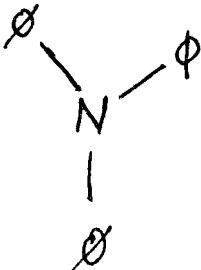


This configuration would correspond to a vertical ionization of this molecule. If this state of the molecule were allowed to relax, a lower energy form would result corresponding to the valence bond structure

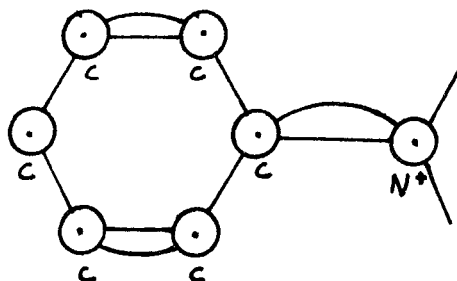


since a  $C=N^+$  double bond is expected to be substantially stronger than a normal  $C=C$  double bond. There will also be a strong polarity in the pi system as indicated. This recoupling of the electrons in the pi system allows the center which was originally ionized to be transferred to another part of the molecule, and it now becomes possible to stabilize the ionic radical orbital, without stabilizing the orbital which was originally ionized. We can estimate the energy lowering in the molecule caused by the recoupling of the electrons in the pi system by

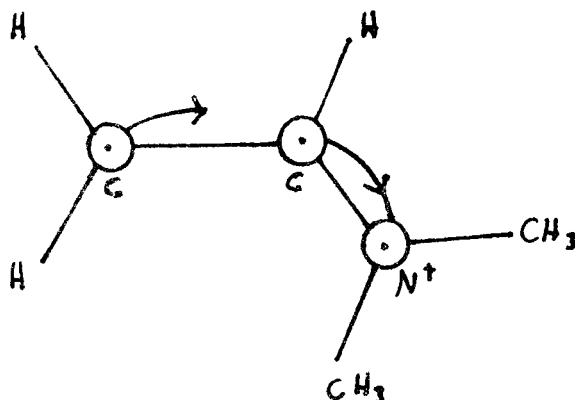
comparing the ionization potential of the following molecules.<sup>3</sup>

<u>Molecule</u>	<u>IP</u>	<u>Molecule</u>	<u>IP</u>
	9.03		
	7.69	$\text{CH}_3\text{NH}_2$	8.97
	7.34	$(\text{CH}_3)_2\text{NH}$	8.36
	7.14	$(\text{CH}_3)_3\text{N}$	8.12
	6.86		

The ionization potential of the first molecule is very close to that of  $\text{CH}_3\text{NH}_2$  as expected. In the other molecules where a nitrogen atom is adjacent to the benzene pi system there is a much lower ionization potential due to the valence bond structure for the ionized state of these molecules shown below



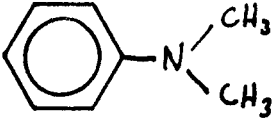
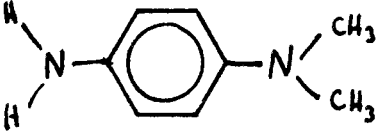
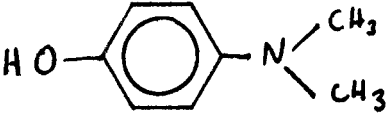
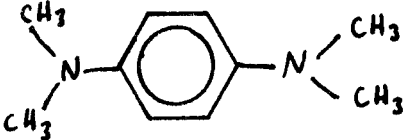
Adding additional methyl groups to the nitrogen of aniline, the second molecule in the above list, gives relative lowerings similar to their corresponding methyl amines, indicating that the orthogonality constraints for phenyl substituents are similar to those caused by methyl groups. From these ionization potentials we estimate that the recoupling of the pi system for an ethylene substituted tertiary amine leads to a decrease of about one eV in the ionization potential of the molecule. We also note that additional phenyl groups lead to successively smaller decreases in the ionization potential. The recoupling of the pi system should be relatively energetically more favorable when ethylene is a substituent as opposed to phenyl groups, since the orthogonality constraints for the carbon radical orbital will be smaller in the ethylene substituted amine due to greater bond polarity in the adjacent  $C=N^+$  pi bond. At this point we have constructed a molecule which is expected to have an ionization potential lower than seven eV.



We can further lower the ionization potential of this molecule by stabilizing the ionic forms of the molecule shown above. Since the pi system is highly polarized due to the formal  $N^+$  center, the carbon radical orbital will have a tendency to move its electron density unto its neighboring carbon atom. Since this delocalization is similar in character to the ionization of this orbital, those factors which would have contributed to a low ionization potential for this orbital will also contribute towards stabilizing the delocalized radical orbital.

<u>Molecule</u>	<u>IP</u>
$CH_3\dot{C}$	9.84
$CH_3CH_2\dot{C}$	8.4
$NH_2CH_2\dot{C}$	6.13
$OHCH_2\dot{C}$	8.00

From the above ionization potentials<sup>3</sup> it appears that amino groups would be the most effective in stabilizing the carbon radical orbital.  $NH_2$  groups would cause the largest orthogonality constraints for the radical orbital of the three groups considered,  $CH_3$ ,  $NH_2$  and  $OH$ , and  $NH_2$  would be intermediate in its deshielding of the carbon radical nucleus through sigma withdrawing effects. These ideas are consistent with the experimental ionization potentials of the following substituted anilines.

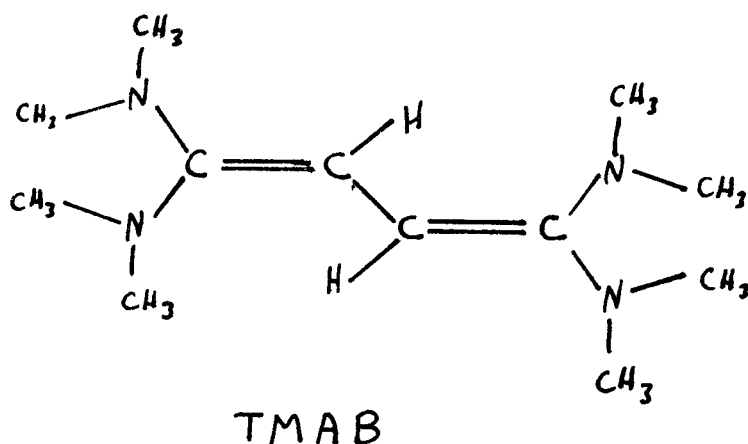
<u>Molecule</u>	<u>IP</u>
	7.14
	$\lesssim 6.46$
	$\lesssim 6.75$
	$\lesssim 6.20$

Here we see that  $\text{NH}_2$  is a better stabilizing group than OH towards the ionization of N,N-dimethylaniline, and that additional methyl groups on the amino nitrogen further lower the ionization potential as expected.

With the above ideas it should be quite easy to explain the low ionization potential of TMAE. Starting out with ammonia, which has an ionization potential of 10.19 eV, adding three methyl groups lowers its ionization potential to 8.12 eV. Recoupling the pi system of ionized TMAE should further lower its ionization potential to  $\leq 7.1$  eV.

Adding one trans dimethyl amino group should result in a lowering of the ionization potential by  $\sim 0.9$  eV to  $\leq 6.2$  eV, due to stabilization of the carbon radical orbital. We can also estimate the additional energy lowering due to increased polarization in the ethylene system as compared to the phenyl systems if we assume the polarization

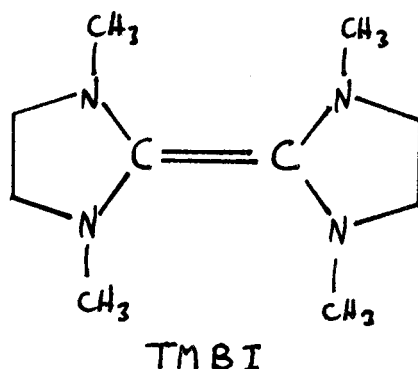
effects in TMAB are similar to those in phenyl substituted molecules since they involve the same number of carbon-carbon double bonds between the initially ionized center and the radical center of the ionized molecule.



TMAB has an ionization potential<sup>6</sup> 0.25 eV higher than TMAE. This would lead to a corrected predicted ionization potential of TMAE of 5.95 eV. We have not yet taken into account the two other dimethyl-amino groups of TMAE. They must lead to the additional stabilization in the ionized molecule and a further decrease of the ionization potential to the experimental value of  $\leq 5.36$  eV.

One other fact to be considered is the position of the nitrogen lone pairs in relation to the carbon pi system in the parent and ionized form of TMAE. NMR experiments indicate that in TMAE the nitrogen lone pairs lie in the sigma system<sup>7</sup> and our arguments clearly indicate that for  $\text{TMAE}^+$  the nitrogen lone pairs are in the pi system. The fact that in a related molecule, TMBI, where the nitrogen lone pairs are forced to be much more parallel to the carbon pi system in the un-

ionized form, the ionization potential increases by only 0.05 eV.<sup>1</sup> This indicates that the position of the nitrogen lone pairs is not very critical in determining the ionization potential of TMAE. The barrier to



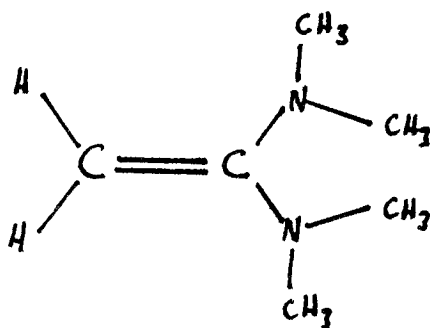
rotation about the C-N single bond must be rather small, and the nitrogen lone pairs have no large stabilizing or destabilizing effect on the parent molecule. This is further evidence for the idea that the low ionization potential of TMAE results from stabilization of the carbon radical orbital in the ionized molecule.

Most of these ideas can easily be tested with theoretical calculations. A study of  $\text{CH}_2=\text{CHNH}_2$ ,  $\text{CH}_2=\text{C}(\text{NH}_2)_2$  and  $\text{CH}(\text{NH}_2)=\text{CH}(\text{NH}_2)$  would indicate whether recoupling of the pi system is critical to explaining the low ionization potentials of TMAE. From the above discussion we would predict the following.

<u>Molecule</u>	<u>Predicted IP(eV)</u>
$\text{CH}_2=\text{CHNH}_2$	7.5
$\text{CH}_2=\text{C}(\text{NH}_2)_2$	7.2-7.3
$\text{CH}(\text{NH}_2)=\text{CH}(\text{NH}_2)$	6.5

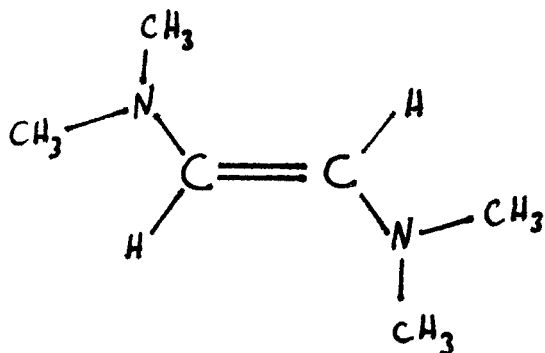
Because of the large change in the character of the ionized molecule, Koopman's theorem ionization potentials would be expected to be much higher than the experimental values. A separate, consistent calculation for the ionized molecule is necessary. That large readjustments in the molecule are taking place upon ionization is indicated by the fact that the vertical ionization potentials of TMAE is 0.75 EV higher than the adiabatic ionization potential.<sup>1</sup>

None of the ionization potentials of the three simple amino ethylenes discussed above has been determined experimentally. Vinylamine,  $\text{CH}_2=\text{CHNH}_2$  has been isolated<sup>8</sup> at low temperatures from a pyrolysis experiment and its structure determined from its rotational spectrum. These molecules may be hard to synthesize because of tautomerism to the imine form, although thermochemical evidence<sup>9</sup> indicates that vinylamine is more stable than  $\text{CH}_3\text{CH}=\text{NH}$ .

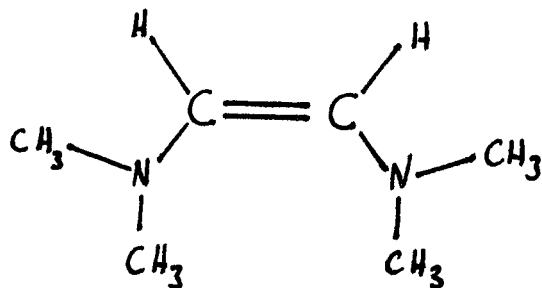


The methylated diamino ethylene shown above has a measured ionization potential of 6.8 eV.<sup>10</sup> This is approximately the ionization potential that would have been predicted from the above ideas. It has been suggested that the low ionization potential of TMAE occurs because of a strong interaction between nitrogen lone pairs,<sup>11</sup> but this would seem to indicate a similar low ionization potential for the above molecule and

this does not occur. Our ideas indicate that



or



should have a low ionization potential (below six eV), and an experimental confirmation of the predicted ionization potential of either of the above molecule would be a strong test of these ideas.

## References

1. Y. Nakato, M. Ozaki, A. Egawa and H. Tsubomura, Chem. Phys. Lett. 9, 615 (1971).
2. M. Hori, K. Kimura and H. Tsubomura, Spectrochimica Acta 24A, 1397 (1968).
3. J. L. Franklin, J. G. Dillard, H. M. Rosenstock, J. T. Herron, K. Draxl and F. H. Field, Ionization Potentials, Appearance Potentials, and Heats of Formation of Gaseous Positive Ions, Nat. Stand. Ref. Data Ser. (1969).
4. L. Pauling, Nature of the Chemical Bond (Cornell University Press, Ithaca, New York, 1939).
5. J. March, Advanced Organic Chemistry: Reactions, Mechanisms, and Structure, (McGraw-Hill, Inc., New York, 1968).
6. Y. Nakato, T. Chiyoda and H. Tsubomura, Bull. Chem. Soc. Jap. 47, 3001 (1974).
7. N. Wiberg and J. W. Buchler, Angew. Chem. 74, 490 (1962).
8. F. J. Lovas and F. O. Clark, J. Chem. Phys. 62, 1925 (1975).
9. Reference 3 and references therein.
10. H. Bock, G. Wagner, K. Wittel, J. Sauer and D. Seebach, Chem. Ber. 107, 1869 (1974).
11. M. B. Robin, Higher Excited States of Polyatomic Molecules (Academic Press, Inc., New York, 1975).

Proposition III

Proposition: Ab initio calculations on the low lying states of  $\text{FeCl}_2 \cdot 4\text{H}_2\text{O}$  are proposed in order to determine the value of the nuclear quadrupole moment of the 14.4 keV excited state of  $^{57}\text{Fe}$  in conjunction with Moessbauer spectra.

Much of what is known about the electronic structure of complex molecules containing iron has been obtained from the analysis of  $^{57}\text{Fe}$  Moessbauer spectra.<sup>1</sup> From these spectra it is possible to determine the magnitude, sign and orientation of the electric field gradient (EFG) about the iron center.<sup>2</sup> The EFG is highly sensitive to various electronic configurations, particularly those involving different occupations among the iron 3d orbitals. Experimental knowledge of the EFG can therefore tell us a great deal about the electronic environment of the iron center.

Unfortunately the EFG cannot be determined unambiguously by experiment alone. It is obtained from Moessbauer spectra by measuring the quadrupole splitting ( $\Delta E$ ), which is related to the EFG by the following relationship<sup>2</sup> for  $^{57}\text{Fe}$

$$\Delta = \frac{1}{2}e^2qQ(1+\frac{1}{3}\eta^2)^{\frac{1}{2}}$$

where  $-e$  is the charge of an electron,  $Q$  is the nuclear quadrupole moment of the 14.4 keV excited state of  $^{57}\text{Fe}$ ,  $eq$  is the major component of the EFG ( $eq = V_{zz}$ ), and  $\eta$  is the asymmetry of the EFG ( $\eta = (V_{xx} - V_{yy})/V_{zz}$ ).

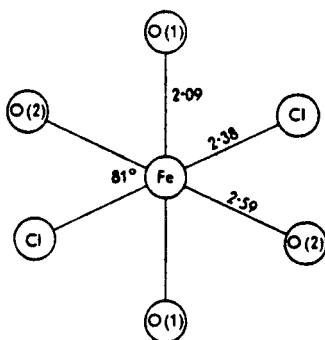
Neither the value of  $q$  nor  $Q$  has been determined experi-

mentally, but only their product  $qQ$ . The value of  $q$  or  $Q$  can only be obtained when one of them has been determined theoretically. Given a proper wavefunction for a molecule, it is not difficult to evaluate its EFG, and by using the above relationship the value of  $Q$  can be found. Once  $Q$  is known, the EFG of any molecule which exhibits an  $^{57}\text{Fe}$  Moessbauer spectrum can be measured, but we must remember that this experimentally determined EFG is no more accurate than the theoretically calculated EFG that was used to find the value of  $Q$ .

To date all determinations of the value of  $Q$  have been from the EFG of wavefunctions generated from semi-empirical theories. In general these methods determine the ordering of states involving different iron 3d orbital occupations with ligand field arguments, estimate their energy splittings by fitting the temperature dependence of the quadrupole splitting, and use large and often unrealistic corrections to the EFG due to lattice effects.<sup>3</sup> Since these calculations do not appear to be conclusive in determining the EFG of any molecule for which the  $^{57}\text{Fe}$  Moessbauer spectrum is known, it is proposed that an ab initio study be carried out to check the validity of these semi-empirical calculations.

The crystal structure of  $\text{FeCl}_2 \cdot 4\text{H}_2\text{O}$  has been determined by x-ray crystallography.<sup>4</sup> The structure consists of packed distorted octahedral complexes of iron. Each Cl atom and  $\text{H}_2\text{O}$  molecule is associated with only one iron, and the  $\text{FeCl}_2 \cdot 4\text{H}_2\text{O}$  units are held together by hydrogen bonds. Since the  $\text{FeCl}_2 \cdot 4\text{H}_2\text{O}$  units appear to be isolated from each other as far as dative or

covalent bonds are concerned, and since each octahedral unit carries no overall electric charge, we expect that the electronic structure of the  $\text{FeCl}_2 \cdot 4\text{H}_2\text{O}$  units is essentially unaffected by lattice contributions. Because of its structure, its relatively small size, and the amount of published experimental information about its properties,  $\text{FeCl}_2 \cdot 4\text{H}_2\text{O}$  would be the best system to treat with ab initio studies in order to determine the value of  $Q$ . The geometry of the  $\text{FeCl}_2 \cdot 4\text{H}_2\text{O}$  unit is shown below.



We see from the  $\text{Fe}-\text{H}_2\text{O}$  bond distances that two water molecules are strongly datively bonded to the iron. The other two waters are only weakly bound to the iron, if at all, and their major bonding interactions probably involve hydrogen bonds with chlorines in adjacent octahedra.

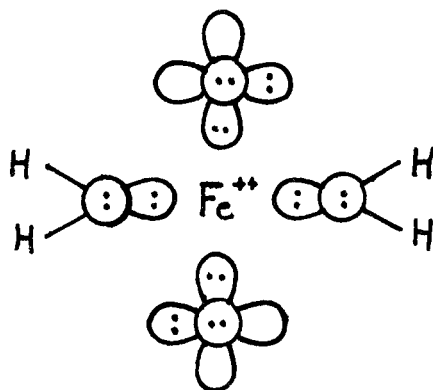
Single crystal Moessbauer spectra were taken of this complex in order to determine the magnitude, sign, orientation and asymmetry of its EFG about the iron center.<sup>2</sup> Using the accepted value of  $Q$ ,  $+0.209$  barns,<sup>5</sup> the EFG was found to have its major

axis aligned along the Cl-Fe-Cl axis and the sign of this component was positive.

The two major contributors to the EFG of this complex will be the localization of the iron bonding electrons along the Cl-Fe-Cl axis, and the asymmetry of the d orbitals. The first effect will lead to a major component of the EFG along the Cl-Fe-Cl axis, in agreement with experiment, but the sign of this component will be negative. If this effect dominates the EFG, we see that the accepted sign of Q is incorrect. Magnetic susceptibility experiments indicate that  $\text{FeCl}_2 \cdot 4\text{H}_2\text{O}$  has four unpaired electrons<sup>6</sup> ( $\mu_{\text{eff}} = 5.39$ ), leading to a quintet ground state. For  $d^6$  iron this implies that one d orbital will be doubly occupied. If d orbital asymmetry dominates the EFG, there are two states which will give the correct orientation of the EFG. If the doubly occupied orbital is a  $d_{z^2}$  type orbital along the Cl-Fe-Cl axis, the orientation of the EFG is in agreement with experiment, but the sign would again be negative. If the doubly occupied d orbital is a  $t_{2g}$  type orbital perpendicular to the Cl-Fe-Cl axis, both orientation and sign would agree with the present interpretation of the Moessbauer spectra. From our work on Fe-porphyrins, we expect that neither of these electronic configurations is the ground state for  $\text{FeCl}_2 \cdot 4\text{H}_2\text{O}$ , as we now explain.

If we ignore the two weakly bound waters, we have a chemical environment about the iron center which is similar to Fe-porphyrin. If we idealize the Fe-Cl bonds as being totally ionic, we can represent the molecule as four planar lone pairs directed

towards an  $\text{Fe}^{++}$  center.



For our Fe-porphyrin model, we found the lowest lying quintet state to be a  $d_x^2$  orbital (x is now the direction out of the plane of the molecule,  $d_x^2 = 2x^2 - y^2 - z^2$ ) doubly occupied. The next lowest-lying quintet state for Fe-porphyrin had the  $d_{yz}$  orbital doubly occupied. The splitting between these states was 2 kcal/mole for Fe-porphyrin. For  $\text{FeCl}_2 \cdot 4\text{H}_2\text{O}$  the presence of the two weakly bound waters would tend to decrease this splitting and probably would invert these two states. The states with the  $d_{xy}$  and  $d_{xz}$  orbitals doubly occupied were 5 kcal/mole above the  $d_{yz}$  doubly occupied state for Fe-porphyrin and the presence of the two weakly bound waters should increase this splitting for  $\text{FeCl}_2 \cdot 4\text{H}_2\text{O}$ . Thus the two  $d^6$  configurations which would give the proper orientation of the EFG,  $d_{xy}$  doubly occupied, or  $d_x^2$  doubly occupied,

do not appear to be the ground state of the  $\text{FeCl}_2 \cdot 4\text{H}_2\text{O}$  complex.

The experimental estimates of the asymmetry of the EFG vary from  $0.1^7$  to  $0.4 \pm 0.15^2$ , the most recent result being the largest one. If the large asymmetry is correct, it indicates that the EFG cannot be easily explained by assuming either the d orbital asymmetry or the iron bonding electrons heavily dominate one another in making up the EFG. The large asymmetry can only occur if both effects contribute significantly. The proper orientation is obtained only when the Fe-Cl bonding contribution is larger than the d orbital asymmetry. As an illustration, suppose we approximate the two iron electrons involved in the bonding to the chlorines as having a spatial extent similar to an iron 4p electron. This is reasonable since an iron 4p orbital has a maximum amplitude in the same region as a chlorine lone pair orbital when the Fe-Cl bond distance is similar to that found in  $\text{FeCl}_2 \cdot 4\text{H}_2\text{O}$ . These electrons would have an EFG<sup>8</sup> of

$$\begin{aligned} V_{xx} &= 4/5 (r^{-3})_{4p} \\ V_{yy} &= 4/5 (r^{-3})_{4p} \\ V_{zz} &= -8/5 (r^{-3})_{4p} \end{aligned}$$

where  $(r^{-3})_{4p}$  is the average value of  $r^{-3}$  integrated over the iron 4p orbital. The expected ground state d asymmetry would lead to an EFG<sup>8</sup> of

$$\begin{aligned} V_{xx} &= 4/7 (r^{-3})_{3d} \\ V_{yy} &= -2/7 (r^{-3})_{3d} \\ V_{zz} &= -2/7 (r^{-3})_{3d} \end{aligned}$$

Using  $(r^{-3})_{4p} = 2.04$  a.u. and  $(r^{-3})_{3d} = 5.00$  a.u.,<sup>9</sup> combining these two effects gives a resultant EFG of

$$V_{xx} = 4.49 \text{ a.u.}$$

$$V_{yy} = 0.20 \text{ a.u.}$$

$$V_{zz} = -4.69 \text{ a.u.}$$

Although the asymmetry of this EFG is much larger than the experimental value, it illustrates how different effects can combine to give an EFG with the proper orientation and a large asymmetry. It clearly shows that the most likely sign for the major component of the EFG in  $\text{FeCl}_2 \cdot 4\text{H}_2\text{O}$  is negative, leading to a negative sign for Q. Since the knowledge of Q is crucial for rationalizing the electronic structure of many iron containing complexes, its value must be unambiguously determined by further theoretical studies.

## References

1. R. Greatrex, Spect. Prop. Inorg. Organomet. Comp. 6, 494 (1973), and references therein.
2. T.C. Gibb, Chem. Phys. 7, 449 (1975).
3. R. Ingalls, Phys. Rev 133, A787 (1964).
4. B.R. Penfold and J.A. Grigor, Acta Cryst. 12, 850 (1959).
5. J. G. Stevens and B.D. Dunlap, J. Phys. Chem. Ref. Data 5, 1093 (1976).
6. R.D. Pierce and S.A. Friedberg, J. Appl. Phys. 32, 66S (1961).
7. P. Zory, Phys. Rev. 140, A1401 (1965).
8. R.L. Collins, J. Chem. Phys. 42, 1072 (1965).
9. R.E. Kirchner and G.H. Loew, J. Am. Chem. Soc. 99, 4639 (1977).

**Proposition IV**

**Proposition:** A study of the hydrogen bonding interactions in water dimer for a number of different orientations over a range of short and long interaction distances is proposed in order to better understand the chemistry of hydrogen bonding in constrained environments.

The chemistry of hydrogen bonded species is still actively being investigated, even though the basic nature of hydrogen bonds appears to be well understood.<sup>1</sup> It is generally believed that the hydrogen bond is most stable when the hydrogen atom lies along the axis connecting the donor atom and the acceptor atom. This spatial configuration, referred to as a linear hydrogen bond, has been shown both theoretically<sup>2</sup> and experimentally<sup>3</sup> to be the most favorable orientation for unconstrained hydrogen bonded species such as gaseous water dimer. It is also the case that in constrained environments such as waters of hydration in crystals, it is believed that the most stable orientation of the water should be the one that deviates least from the linear hydrogen bond.<sup>4</sup> However, not all hydrogen bonded species seem to follow this rule. From the neutron diffraction of perdeuterated violuric acid monohydrate (Fig. 1), it is found that the water occupies a position which has a high degree of hydrogen bond strain. It also has one very short hydrogen bond length. It appears that there is a configuration accessible to the water molecule which would relax both these seemingly unfavorable interactions. It might at first be thought that the orientation of D(W2) having its O-D bond axis point between

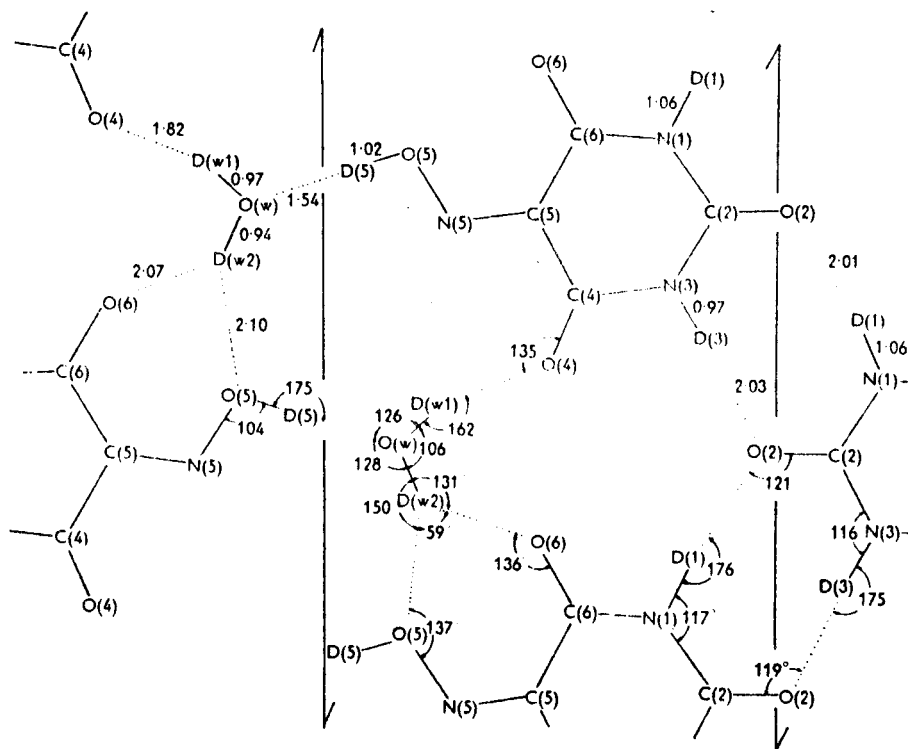
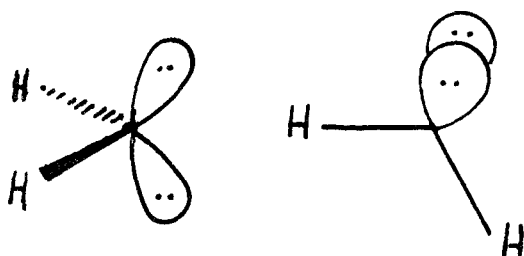


Figure 1

O(5) and O(6) would lead to a stronger hydrogen bond, but it has been found from studies on water dimer that this orientation is less stable than a linear hydrogen bond.<sup>2</sup> It has also been found from neutron diffraction studies of ice II, a high-pressure polymorph of ice, that the hydrogen bond angles that give the least amount of hydrogen bond strain are not the hydrogen bonds actually formed.

We suggest two lines of study which may help to explain deviations from the normal hydrogen bonding situation. First, a more comprehensive study of the stability of various hydrogen bond configurations should be carried out over a wide range of bond lengths. The theoretical studies to date have differentiated between different bonding situations close to the energy minimum found for unconstrained molecules,<sup>7</sup> but very little work has been done on short interaction distances which could be forced on a hydrogen bonded species by crystal packing forces or rigid molecular conformations. For example, the proper orientation of the water molecule in perdeuterated violuric acid monohydrate may depend only on the very short interaction between O(W) and O(5) and may depend very little on the orientation of the other hydrogen bonds. For such a short distance, we might expect the orientation of the oxygen lone pairs involved in this bond to be as



The most stable orientation of these lone pairs may determine the orientation of the hydrated water molecule. A second line of study would involve consideration of next nearest neighbor orientations and the relative stability of various configurations at longer than normal

hydrogen bond lengths. This information is necessary in order to correctly assess the deviations from linear hydrogen bonds in crystals where all the molecules are involved in extensive hydrogen bonding, such as the polymorphs of ice.

To indicate how studies of this type might be of use in understanding hydrogen bonds, we have chosen a non-standard hydrogen bond geometry and calculated its stability with respect to a linear hydrogen bond over a range of distances.

We can graphically depict a water molecule as a tetrahedron with two positively charged points representing hydrogens and two negatively charged points representing oxygen lone pairs. To form a linear bond we simply join two oppositely charged points from different tetrahedra. Another possible favorable orientation of two water molecules might be to join two oppositely charged edges of different tetrahedra. This is somewhat analogous to Pauling's original description of a carbon-carbon double bond.<sup>8</sup> In this configuration two strained hydrogen bonds are formed rather than a single optimal hydrogen bond. This orientation has been found to be  $\sim 0.7$  kcal/mole less stable than the linear hydrogen bond at their respective equilibrium separations, but for O-O separations less than  $2.78 \text{ \AA}$ , the linear hydrogen bond is less stable than a hydrogen double bond.<sup>2</sup>

Taking it one step further we could form a hydrogen triple bond by joining two oppositely charged faces of different tetrahedra. No calculations have been published which give the relative stability of this configuration so we performed calculations on this geometry for

a few selected bond lengths. The basis set used was a double zeta quality basis augmented with a set of d polarization functions on the oxygen and p polarization functions on the hydrogens.<sup>9</sup> The hydrogen bond pairs were correlated left-right and the lone pairs were correlated radially. The occupied and correlating orbitals were used in extensive CI calculations. The dominant correlation effects occurred between electrons on the same water molecule. Correlation between electrons involved in hydrogen bonds which are associated with different molecules was extremely small. As a result the hydrogen bond can be viewed as basically electrostatic in nature. A similar conclusion about linear hydrogen bonds has also been reached by others.<sup>10</sup> The CI potential surface for the linear configuration and the triple bond configuration is shown in Fig. 2. At distances less than 2.74 Å, the triple hydrogen bond is more stable than the linear hydrogen bond. Another thing to note is that the potential surfaces are very flat, especially the hydrogen triple bond surface. The total strength of an equilibrium hydrogen bond is  $\sim 5$  kcal/mole,<sup>1</sup> so we see that large variations in hydrogen bond lengths are accessible to hydrated water.

We would like to be able to make direct comparison from these calculations on two water molecules to the structure of ice polymorphs, but there is a problem. For normal atmospheric ice, the O-O bond separation is 2.76 Å<sup>11</sup> and not the 2.98 Å<sup>3</sup> found for water dimer. It also appears from neutron diffraction studies that linear hydrogen bonds are present in normal ice, but proton disorder makes the

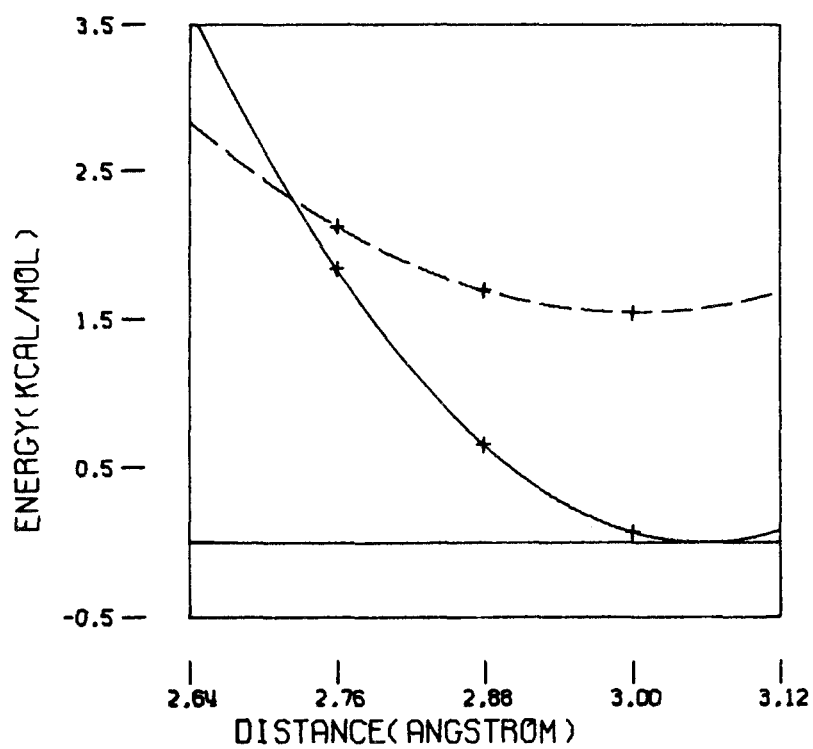


Figure 2. Relative energies as a function of distance for a linear hydrogen bond and a triple (face) hydrogen bond in water dimer.

analysis somewhat difficult. The linear hydrogen bonded structure did give the best agreement of those considered, but the agreement was not as good as one would normally expect.<sup>11</sup> Because of the indicated additive effects on the geometry of water dimer caused by bonding additional waters, it is not clear how to adjust the potential surfaces of the different geometries of water dimer to correspond to the ice polymorphs. However, studies on water dimer do indicate the possibility of non-linear hydrogen bonds being accessible in certain crystalline environments. From the above calculations we suggest that the triple hydrogen bond configuration may play a role in the structure of ice II and ice VII. Ice VII is the densest form of ice known, having a density almost twice that of normal ice (ice I). It is much denser than ice I despite the fact that its nearest neighbor distances are longer than in ice I. It is a general trend in all the high pressure forms of ice that nearest neighbor distances are longer than in ice I, but that next-nearest neighbor distances decrease drastically.<sup>12</sup> In fact, for ice VII the four next-nearest neighbor distances have decreased to the point that they are identical to the normal four nearest neighbor distances, i.e., the oxygens in ice VII have eight nearest neighbors, rather than the four nearest neighbors found for the other forms of ice.<sup>13</sup>

The structure of ice VII has been partially determined by X-ray crystallography. The oxygen centers have been found to form a body-centered cubic structure where the closest O-O distances are at 2.86 Å for the pressure at which ice VII is stable (~20 kbar) and to

have an O-O separation of 2.96 Å in its metastable form at normal atmospheric pressure. It is also estimated that at atmospheric pressure ice VII is ~1 kcal/mole less stable than ice I.

The positions of the hydrogens have not yet been determined by neutron diffraction studies. The oxygen atoms are believed to form two ice I lattices which are intermeshed, the oxygen atoms from one ice I type lattice filling the empty spaces of the other lattice. It has been suggested that the hydrogen atoms are used to form linear hydrogen bonds as in ice I. The hydrogen bonds connect only the oxygens of one of the lattices, and the two ice I lattices in ice VII are thought to be non-interacting except for a small repulsive effect.<sup>13</sup>

We find the suggestion that four of the eight nearest neighbors of an oxygen atom in ice VII are essentially non-interacting to be unlikely due to the short O-O separation. For the distances encountered we might expect repulsive interactions of ~3 kcal/mole between two non-hydrogen bonded oxygens. These large repulsive effects could clearly not be tolerated in the crystal where the stability of ice VII is estimated to be only 1 kcal/mole higher than ice I.

One structure which would allow eight bonding interactions with each water would be to form four linear hydrogen bonds and to also form four triple hydrogen bonds to each water molecule, since access to the face of a water tetrahedron is relatively unhindered by the linear hydrogen bonds. This type of local structure about a water molecule could be extended in three dimensions if there were some reorientation of the water molecules such that two tetrahedrons involved in a triple

hydrogen bond directed their linearly hydrogen bonded waters to different regions of space. The strain caused by this reorientation could be lessened by making the linear hydrogen bonds slightly non-linear. The non-linearity in the two sets of hydrogen bonds and the misorientation of the two faces must make up a total of 60 degrees. In this type of structure the two lattices are very strongly interacting, with the water molecule of one lattice always paired up with a water molecule of the other lattice. The protons of one of the lattices can be disordered with a subsequent parallel disorder in the other lattice, giving an overall disordered proton structure, as is observed experimentally.<sup>13</sup>

For another ice polymorph, ice II, it appears that a similar next nearest neighbor hydrogen triple bond exists. In this polymorph the positions of the hydrogen atoms are known<sup>14</sup> and they form an ordered structure. The next nearest neighbors in ice II are only 3.3 Å apart, compared to a next nearest neighbor distance of 4.5 Å in ice I.<sup>12</sup> The four nearest neighbors are used in forming strained linear hydrogen bonds where the least strained angles available for linear hydrogen bonding are not used. The angles which are used are those which give rise to a hydrogen triple bond of next nearest neighbors, as shown in Fig. 3. Atoms labeled I and II are next nearest neighbors.

Much remains to be learned about hydrogen bonds in constrained environments. Inferred positions of hydrogen atoms involved in hydrogen bonds are often indicators of local electronic structure in crystals and can be very useful in determining the electronic structure

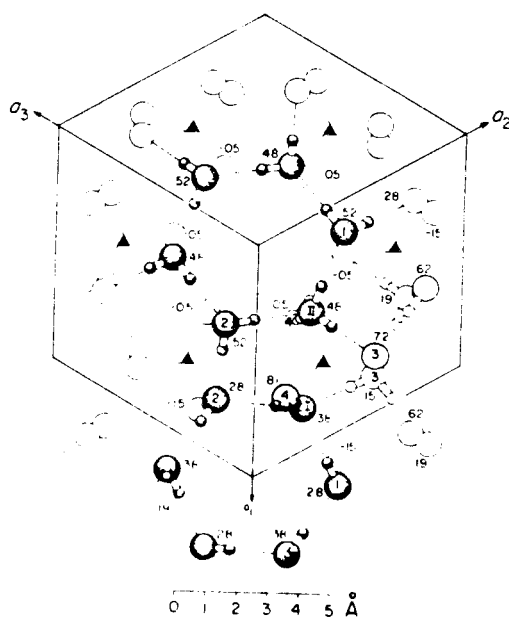


Fig. 3

of molecules in the crystalline state. Hydrogen bonded lattices may also serve as prototype systems for a better understanding of the packing forces in crystals. Next nearest neighbor considerations are certainly important in explaining the structure of the ice polymorphs. Finally, a better understanding of hydrogen bonds in the ice polymorphs should contribute a great deal to the theory of liquid water. The transformation of ice I to a denser state upon melting indicates that local bonding situations analogous to the denser forms of ice are thermally accessible to water even at low temperatures. For these reasons we

think that different water dimer orientations will serve as useful models for gaining a better understanding of constrained hydrogen bonds.

## References

1. G. C. Pimentel and A. L. McClellan, The Hydrogen Bond, (W. H. Freeman and Co., San Francisco, 1960).
2. O. Matsuoka, E. Clementi and M. Yoshimine, J. Chem. Phys. 64, 1351 (1976).
3. T. R. Dyke, K. M. Mack and J. S. Muentner, J. Chem. Phys. 66, 498 (1977).
4. W. C. Hamilton and J. A. Ibers, Hydrogen Bonding Solids, (W. A. Benjamin, Inc., New York, 1968).
5. B. M. Craven and W. J. Takei, Acta Cryst. 17, 415 (1964).
6. B. Kamb, Acta Cryst. 17, 1437 (1964).
7. H. Popkie, H. Kistenmacher and E. Clementi, J. Chem. Phys. 59, 1325 (1973) and references therein; reference 2 and references therein.
8. L. Pauling, J. Am. Chem. Soc. 53, 1367 (1931).
9. Dunning (9s5p)/(3s2p) for oxygen; (4s)/(2s) for hydrogen;  
 $\alpha(O_d) = 0.85$ ,  $\alpha(H_p) = 1.0$ .
10. G. H. F. Diercksen, W. P. Kraemer and B. O. Roos, Theoret. Chim. Acta (Berl.) 36, 249 (1975).
11. S. W. Peterson and H. A. Levy, Acta Cryst. 10, 70 (1957).
12. B. Kamb in Structural Chemistry and Molecular Biology, A. Rich and N. Davidson, Eds. (W. H. Freeman and Co., San Francisco, 1968).
13. B. Kamb and B. L. Davis, Proc. Nat. Acad. Sci. 52, 1433 (1964).
14. B. Kamb, Acta Cryst. 17, 1437 (1964).

**Proposition V**

Proposition: A "state-of-the-art" calculation on  $\text{FeCl}_2$  is proposed in order to assess the ability of present-day theoretical techniques to provide quantitative agreement with experimental results for transition metal complexes.

Today's theoretician working with small molecules made up of first- and second-row atoms can reliably reproduce or predict experimentally obtainable properties such as geometries, electronic excitation energies, thermochemical properties and vibrational frequencies.<sup>1</sup> In the case of transient species theoretical estimates are often more precise than experimental values.<sup>1</sup>

In order to get quantitatively accurate results, extended basis sets augmented with polarization functions, and sometimes diffuse basis functions, must be used in correlated SCF calculations which then form the basis for extensive CI calculations. To our knowledge no such type of calculation has been performed on a molecule containing a transition metal. We propose to test the ability of calculations of this type to give quantitatively accurate results for transition metal complexes.

The advent of low-temperature matrix isolation techniques has given experimentalists the ability to isolate small transition metal complexes which are too reactive to be studied in solution. Various forms of spectroscopy can be performed on these molecules in their matrix-isolated state. As a result of these experiments the feasibility of studying transition metal chemistry theoretically is greatly increased

because the experimental information necessary to provide checks on the theory are available for small transition metal complexes, and complicating solution effects do not have to be included in the theoretical treatment.

$\text{FeCl}_2$  is an excellent system to use as a test case both from an experimental and theoretical point of view. Its geometry has recently been determined by electron diffraction.<sup>2</sup> It is found to have an average Fe-Cl distance of 2.159 Å and appears to be linear. Its absorption spectrum has been measured from 4,000 to 50,000  $\text{cm}^{-1}$  and the following assignments have been made<sup>3</sup>

d-d transitions	4,600 $\text{cm}^{-1}$	( $^5\Pi \leftarrow ^5\Delta$ )
	7,100	( $^5\epsilon \leftarrow ^5\Delta$ )
spin-forbidden transition	19,500	(weak)
charge transfer transitions	37,500	
	39,800	
	41,600	
	44,100	
	47,600	

The vibrational frequencies have also been assigned<sup>4</sup>

$\nu_1 = 330 \text{ cm}^{-1}$	(symmetric stretch)
$\nu_2 = 88 \text{ cm}^{-1}$	(bend)
$\nu_3 = 490 \text{ cm}^{-1}$	(asymmetric stretch)

$\text{FeCl}_2$  appears a priori to have a relatively simple electronic structure when compared to most other transition metal complexes. We expect only the Fe 4s electrons to be involved in covalent bonds to the chlorine atoms, perhaps with a large degree of ionic character. No direct bonding effects should occur in the Fe 3d space as might be expected for metals with higher formal oxidation states. The  $d^6$  quintet configuration involves the interaction of one electron antisymmetrically coupled to a half-filled spherical shell of five d electrons. Because of strong interactions between tightly bound d electrons, this more symmetrical  $d^6$  system should be easier to treat theoretically than a  $d^2$ ,  $d^3$ ,  $d^7$  or  $d^8$ -type metal. Because of these theoretical considerations and the amount of experimental information available for  $\text{FeCl}_2$ , we choose this molecule as a test case for a "state-of-the-art" calculation.

We now describe the details of the calculations. A single linear combination of gaussian basis functions should adequately describe the core electrons of Fe and Cl. Two such contracted basis functions are needed for the valence electrons (Fe 3d, 4s, 4p and Cl 3s, 3p) in order to describe readjustments in the shape of the atomic-like orbitals. Additional polarization functions of d-like symmetry are needed on both the Fe and Cl to allow for further readjustments due to molecule formation. This is referred to as a valence double-zeta basis with polarization functions. For  $\text{FeCl}_2$  a basis of this type will include 73 basis functions.

Proper correlation of the valence electrons will have to be

included in the SCF calculation. The bond pairs should include four major types of intra-pair correlation; left-right, radial and two angular correlations. The Cl 3p lone pairs should be correlated radially and angularly and the Fe 3d doubly-occupied orbitals should be correlated radially. These correlating orbitals along with the remaining "radial" correlating orbital for the Fe 3d singly occupied orbitals, a total of 36 orbitals, constitute the valence space. They should be appropriate for describing all the major electronic correlation effects for this molecule.

CI calculation would be carried out in the following manner. First, all  $d^6$  configurations of the appropriate spin and space symmetry would be generated in the occupied valence space. The occupied valence space contains the dominant orbital for each electron pair and all the singly occupied orbitals. Then from these configurations, all configurations up to double excitations would be generated where only vertical excitations are allowed to occur. A vertical excitation is defined here to be the excitation from an occupied valence orbital into one of its correlating orbitals. This type of CI calculation will include all the SCF configurations and all the dominant intra-pair correlation effects. The inter-pair correlation effects can be included by allowing all vertical doubles within an electron pair with all vertical doubles in an adjoining electron pair. These configurations will not include any inter-pair correlation between electrons on different centers, unless they are involved in covalent bonds. This reduces the size of the calculation without excluding any major correlation effects. In addition

all single excitations from the dominant configuration within the valence space should be included to allow major shape readjustments in the dominant configuration which might occur when other correlation effects are also included. For all the configurations in this list the Fe d orbitals will have to be high spin coupled to all other singly occupied orbitals in order to reduce the size of the calculation. If the covalent bonds of transition metals are similar in nature to those formed by first- and second-row atoms, this level of CI would be expected to give a good potential surface for the ground state of  $\text{FeCl}_2$  and good d-d excitation energies. In order to properly describe the charge-transfer type transitions, the dominant configuration for the excited state (for example  $\text{Cl } 3p_x \rightarrow \text{Fe } d_{xz}$ ) should be correlated in the same manner as the d-d transitions, and both configuration lists included in the CI to insure proper orthogonality of the charge-transfer states to the lower states of the same symmetry.

A calculation of this type approaches the limits of standard ab initio theoretical treatments. If it did successfully reproduce experimental measurements it would tell us a great deal about the nature of transition metal bonds and charge-transfer states. In particular the electron density of charge-transfer states and the degree of covalent character in transition metal bonds are properties which have not yet been quantitatively determined. At worst these calculations will provide a starting point for developing better calculational methods for treatment of transition metal complexes.

## References

1. L. B. Harding and W. A. Goddard III, J. Chem. Phys. 67, 1777 (1977).
2. E. Vajda, J. Tremmel and I. Hargittai, J. Mol. Struct. 44, 101 (1978).
3. C. W. DeKock and D. M. Gruen, J. Chem. Phys. 49, 4521 (1968).
4. R. A. Frey, R. D. Werder and Hs. H. Gunthard, J. Mol. Spect. 35, 260 (1970).